Resolving the molecular mechanisms for bacterial selenium nanoparticle production

Submitted by

Claire Louise Brimilcombe

To the University of Exeter as a thesis for the degree of Masters by Research in Biological Sciences, October 2016.

I certify that all material in this thesis which is not my own work has been identified and that no material has previously been submitted and approved for the award of a degree by this or any other University.

Claire Louise Brimilcombe

Acknowledgements

I would like to thank Clive Butler for the opportunity to carry out this work and for all his help and support during my time at Exeter. I would also like to thank everyone who has given me support and answered my questions in the Biocatalysis Centre at the University of Exeter, particularly Mirella Vivoli, Will Finnigan, and Alice Cross.

I would like to thank the two third year project students Sophie Davies and Louise Larwood for help with preliminary experiments. I would also like to thank Karen Moore and Audrey Farbos for all their help and advice with mRNA extraction and analysis protocols.

Finally I would like to thank Joe Beadle for his support, suggestions and for being a great friend throughout my project, as well as my parents and sister for all their love and encouragement during these two years.

Abstract

Thauera selenatis is a bacterium that can respire using selenate as the sole electron acceptor and produce elemental selenium in the form of nanospheres. Analysis of the secreted protein profile from *T. selenatis* that was respiring using selenate, identified the selenium export factor protein, SefA. SefA was associated with the selenium nanospheres and is thought to stabilise the assembly of the nanospheres in *T. selenatis*. The N-terminus of SefA shows similarity to the N-terminal regions of other *mineralin* family proteins and is therefore speculated to be involved with SefA-selenium interactions. It has been suggested that other proteins may also play a role in the assembly of the selenium nanospheres and their exportation out of the *T. selenatis* cell, and they could interact with SefA.

SefA has been expressed in *Escherichia coli* and two His-tagged recombinant forms of the protein (His-SefA-His and His-SefA) have been purified. A SefA construct was also produced, which had an exposed N-terminal region, by proteolytic cleavage of the His-tag from the N-terminus of His-SefA-His using thrombin. Interactions between the N-terminal of SefA and soluble proteins from *T. selenatis* grown in selenate were investigated and three potentially interacting proteins were identified using pull-down experiments. MALDI-MS analysis identified peptide sequences of fragments from each of the three proteins and BLASTp analysis found that the closest matches for these proteins were threonyl-tRNA synthetase, glucosamine-fructose-6 phosphate aminotransferase, and the DNA protection during starvation proteins. Whilst attempts to crystallise the His-SefA-His protein were unsuccessful, the His-SefA-His protein was determined to be a tetramer and stabilising conditions for the His-SefA-His protein were determined for use in future crystallisation trials. A transcriptome analysis of *T. selenatis* grown with or without selenite was undertaken and this identified some interesting differentially expressed genes, but also indicated that the culture was in fact a mixed culture of *T. selenatis* and *Enterobacter cloacae*.

Table of Contents

List of Figures

List of tables

Abbreviations

BSA	Bovine serum albumin
CAPS	3-(Cyclohexylamino)-1-propanesulfonic acid
E. cloacae	*Enterobacter cloacae*
E. coli	*Escherichia coli*
EDTA	Ethylenediaminetetraacetic acid
GSH	Glutathione
GS-Se-SG	Selenodiglutathione
HEPES	N-(2-Hydroxyethyl)piperazine-N'-(2-ethanesulphonic acid)
His-tag	Poly histidine tag
IPTG	Isopropyl-1-thio-β-D-galactopyranoside
LB	Luria-Bertani medium
MALDI-MS	Matrix-assisted Laser Desorption/Ionization Mass Spectrometry
MOPS	3-propanesulphonic acid
MPD	2-Methyl-2,4-pentanediol
SDS	Sodium dodecyl sulpfate
SefA	Selenium export factor A
SeNPs	Selenium nanoparticles
T1SS	Type 1 secretion system
T6SS	Type 6 secretion system
TAE	Tris-acetate-EDTA
TAT	Twin-arginine-translocation
TE	Tris-ethylenediaminetetraacetic acid
TEM	Transmission electron microscopy
Tris-HCl	Tris(hydroxymethyl)aminomethane
T. selenatis	*Thauera selenatis*

1. Introduction

1.1 Introduction to biologically produced nanomaterials

Nanomaterials can be engineered using biological methods. Research into biologically produced nanomaterials is emerging due to their wide range of applications, as well as their potential to reduce energy and toxic chemical usage, allowing for greener manufacturing (Pearce *et al*., 2008). Bacteria from all biological systems can produce metal and metal oxide nanoparticles which have a wide range of sizes, compositions, and morphologies (Dobias *et al*., 2011). The enhanced or novel properties of these nanoparticles means that they can be used for a growing number of applications including areas within biomedicine, drug delivery, and catalysis (Liang *et al*., 2008). The mechanism for the formation and control of biologically produced nanoparticles is still not fully understood. If it was, these nanoparticles could be produced on a large scale using bacterial nano-manufacturing, and therefore, a full understanding of these bacterial processes is necessary (Dobias *et al*., 2011). A large number of bacteria are able to produce selenium nanoparticles (SeNPs) (Nancharaiah *et al*., 2015). SeNPs have a wide variety of applications in multiple areas of interest including medicine, therapeutics, and environmental remediation (Wadhwani *et al*., 2016).

1.2 Selenium

The element selenium, discovered by Jöns Jacob Berzelius in 1817, has a wide range of oxidation states, from -II to +VI. It belongs to the group 16 family of chalcogens and is semi-metallic (Boyd, 2011). Two oxidised forms of selenium are selenate (SeO_4^{2-}) and selenite (SeO_3^{2-}) which, under the reducing conditions of anoxic or anaerobic environments, are predicted to form elemental selenium (Se^0). The oxidation states of selenium during the biogeochemical cycle can be seen in Figure 1.1. Selenate and selenite are mostly located in oxygenated environments and have a high bioavailability, as well as toxicity

(Minaev *et al.*, 2005; Buchs *et al*., 2013). Elemental selenium can be further reduced to selenide Se(-II) under particularly reducing conditions. Selenide can then attach to organics or metals which results in the formation of organoselenides or metal selenides. The electrolytic refining of copper is the main source of selenium on Earth, where it is produced at the anode, and subsequently isolated from the surrounding mud that forms there. The most common use of selenium is as a dopant during the manufacturing of glass, due to its ability to form bright red and pink colours (Boyd, 2011). Elemental selenium and metal selenides have limited solubility and mobility in the natural environment, however, selenium oxyanions are highly soluble and stable as well as having the potential to be mobile (Nancharaiah *et al.*, 2015). It is essential that selenium is present in the human diet as it is a constituent of enzymes that contain selenocysteine, as well as being required for at least 25 human selenoproteins (Zhang *et al.*, 2011). Three well characterised types of selenoproteins are thioredoxin reductases (TrxR), glutathione peroxidases (GPx) and thyroid hormone deiodinases (DIO). These play a role in the redox regulation of multiple processes including intracellular signalling, redox homeostasis and thyroid hormone metabolism (Papp *et al.*, 2007). Metabolic functions including assimilation, methylation, detoxification, and anaerobic respiration are just some of the processes in which selenium is required in bacteria and archaea (Stolz *et al.*, 1999; Stolz *et al.*, 2002; Stolz *et al.*, 2006).

Selenium is present in most soils, with a range of 0.01 to 2 mg kg^{-1}, but selenium concentrations as high as 1200 mg kg^{-1} have been found (Fordyce *et al.*, 2013). Selenium concentrations in natural waters are in the range of <0.1 to 100 µg $litre^{-1}$, although concentrations of up to 2000 µg $litre^{-1}$ have been reported (Fordyce, 2013). Selenium contamination in both soils and groundwater can be a result of natural weathering of rocks containing selenium, as well as from volcanic eruptions. However, anthropogenic selenium contamination also contributes to selenium levels in the environment. Fossil fuel combustion, mining, agricultural processes, nuclear fuel production are some of the industrial processes that contribute to selenium contamination (Nancharaiah *et al.*, 2015). One example of selenium contamination due to human activity was seen at the Kesterton National Wildlife Reservoir in California, U.S.A.

where phosphate mining in the Blackfoot River Watershed, Idaho, was the origin of the toxic levels of selenium that affected wildlife at Kesterton (Myers, 2013). Elemental selenium can be present in the environment in varying allotrophic forms (crystalline, metallic and amorphous). Elemental selenium can also be present in the environment in the form of selenium nanoparticles (SeNPs) (Nancharaiah *et al*., 2015).

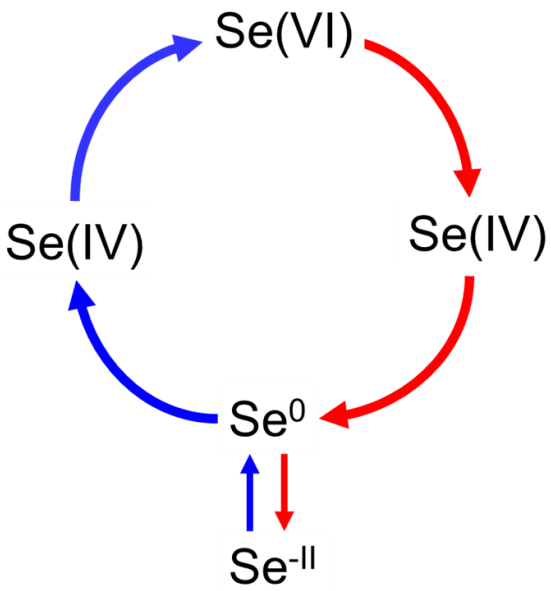

Figure 1.1: The oxidation states of selenium during the biogeochemical selenium cycle. Elemental selenium, Se^0, can be oxidized to form Se^{4+} and then further oxidized to form Se^{6+}. Se^{6+} can then be reduced back to Se^{4+} and then further to Se^0. Under highly reducing conditions, Se^0 can also be reduced to Se^{2-} which can also be oxidized back to Se^0. Blue arrows represent oxidation and red arrows represent reduction.

1.3 Applications of SeNPs

Selenium exhibits good semiconducting and photoconducting properties. Selenium can be used in solar cells, photographic exposure meters and xerography, and SeNPs in particular are being increasingly valued for use in electronics and optics (Wadhwani *et al*., 2016). SeNPs have low cytotoxicity unlike other selenium compounds and have a growing presence in medicinal applications due to their anticancer and therapeutic properties (Forootanfara *et al.*, 2013). Multiple medical applications of SeNPs have been investigated, including their antimicrobial properties. It has been found that biologically synthesized SeNPs have a significant antimicrobial effect on fungi, yeast, and

bacteria (Hariharan *et al.*, 2012). SeNPs are able to inhibit growth of *Staphylococcus aureus* (Tran *et al.*, 2011). SeNPs inhibit not only bacterial growth but also DNA integrity. This was identified when the amplified *zntR* gene was complexed with SeNPs and as a result had a 23% decreased melting temperature compared to a complex with the control nanoparticle (Chudobova *et al.*, 2014). Inhibiting growth of *S. aureus* is of particular interest due to its resistance to many commonly used antibiotics as well as its ability to form biofilms on medical devices such as urinary catheters and prosthetic heart valves (Singh *et al.*, 2009). The potential for SeNPs to be used to prevent biofilm formation has been investigated further using SeNPs from *Bacillus licheniformis* JS2. *S. aureus* growth on a glass and a catheter surface was inhibited by more than 60% using a concentration of 5 mg Se/ml, which offers an alternative potential treatment for preventing *S. aureus* biofilm growth (Sonkusre *et al.*, 2015). SeNPs also have antioxidant activity as they scavenge reactive oxygen species such as the superoxide anion ($O_2^{\cdot-}$) (Forootanfara *et al*., 2013).

SeNPs can be used as chemopreventative and chemotherapeutic agents and they have been shown to be active against multiple types of cancers, including kidney, breast, lung and osetosarcoma (Ali *et al.*, 2013; Gao *et al*., 2011; Ramamurthy *et al*., 2013; Shakibaie *et al*., 2010; Yang *et al*., 2012; Yazdi *et al*., 2013; Wadhwani *et al.*, 2016). SeNPs can be conjugated with organic molecules and drugs to enhance the anticancer properties of these substances. For example SeNPs have been linked to *Spirulina* polysaccharides. This combination was found to induce apoptosis which resulted in inhibited tumour growth, as well as aiding with targeted delivery of nanoparticles to cancerous cells due to its ability to interact with substrates found on the cell surface. An increase in cancer cell death from 20 % to 50 % was achieved when the antibiotic doxorubicin was conjugated to SeNPs due to the nanoparticles aiding in the uptake of doxorubicin by cancerous cells (Yang *et al*., 2012). SeNPs can also lessen or completely prevent toxic side effects associated with anticancer drugs. For example, the breast cancer treatment, Anastrozole, can cause osteoporosis and bone fractures. However, these side effects are completely absent when SeNPs are conjugated to anastrozole (Vekariya *et al*, 2013).

1.4 Abiotic SeNP formation and the protein corona

Abiotic synthesis of SeNPs has been widely investigated. Both physical and chemical methods can be used to synthesize SeNPs. Liquid Phase - Pulsed Laser Ablation (LP-PLA) can be used to synthesize SeNPs which have a diameter of ~60 nm (Overschelde *et al.*, 2013). A chemical hydrothermal method can also be used to synthesize SeNPs. However, chemical synthesis of SeNPs can involve the use of acid decomposition, sulfur dioxide, and sodium dodecyl sulfate among other chemicals. Methods used for synthesis can demand for high temperatures and highly acidic pH. These processes may result in the SeNPs produced being unsuitable for biomedical applications (Iranifam *et al.*, 2013). It has been found that spectroscopic properties of elemental SeNPs formed by microorganisms are significantly different from selenium nanospheres formed chemically. Oremland *et al*. (2004) found that microorganisms were able to assemble nanospheres in a way that chemical synthetic processes could not achieve. Multiple studies have found that proteins may play a key role in the formation and stabilization of selenium nanoparticles (Debieux *et al*., 2011; Lenz *et al*., 2011; Dobias *et al*., 2011).

Nanoparticles produced in microorganisms can be competitively bound by biomolecules, including proteins and lipids. This surface coating is called the protein corona and the exact composition of a nanoparticle's corona can be influenced by multiple conditions including its charge, size and stability (Prapainop *et al*., 2012; Gebauer *et al*., 2012; Del Pino *et al*, 2013). The protein corona can either be classified as 'hard', when it contains proteins of high affinity, or 'soft', when it contains proteins of low affinity (Fleischer *et al*., 2014). Forces involved in protein adsorption onto nanoparticle surfaces include hydrogen bonding, Van der Waals forces, hydrophobic interactions, and pi-stacking interactions (Saptarshi *et al*., 2013; Wolfram *et al*., 2014). Proteins are able to displace other molecules on the surface of nanoparticles in a similar way to ligands. Therefore protein adsorption onto the surface of nanoparticles has been likened to binding ligands to the nanoparticles (Del Pino *et al*., 2013). For each nanoparticle, the exact nature of the protein corona varies due to 3 main factors; the binding affinities and equilibrium constants for adsorbed proteins,

the differing association and dissociation rates of the proteins with the nanoparticle's surface, and the variations in the protein profile within biological liquids (Cuicui *et al.*, 2015).

Large proteins are able to fold into self-assembled complex structures to form cage-like particles which can be used for the delivery of drugs to a specific location without undesirable interactions ocurring before the target has been reached (Agapakis *et al.*, 2012). Alteration of the nanoparticle surface by the addition of a protein corona can allow this targeting of the nanoparticles to specific cells. Nanoparticles may not be able to enter the cell via cell-specific uptake but on addition of a protein corona which contains molecules specific to proteins in the target corona, misfolding of the target proteins can occur. This can then allow the nanoparticles to enter the target cell and the desired interaction of the nanoparticles with the cell can follow (Yang *et al*., 2012; Prapainop *et al*, 2012). It has been suggested that nanoparticles which possessed a surface entirely coated with peptides could have their physicochemical properties specifically tuned to their delivery pathway (Dittrich *et al*., 2012). However, the interaction between nanoparticles and proteins could result in conformational changes in the protein, exposing epitopes that could initiate undesirable signalling pathways. Consequently, it is important to monitor the conformation of proteins adsorbed onto nanoparticles during alterations of the protein corona, and this can be achieved using techniques including nuclear magnetic resonance (NMR), X-ray crystallography, Raman spectroscopy, circular dichroism, and fourier transformed infra-red spectroscopy (Cuicui *et al*., 2015). There is now increasing interest in the biotic production of nanoparticles and investigating natural nanoparticle protein coronas due to their enhanced properties compared to abiotically produced nanoparticles, and their potential applications in medical and biological therapeutics.

1.5 Bacterial selenate reduction

Reduction of selenate (SeO_4^{2-}, Se(VI)) can be carried out by multiple organisms both under aerobic and anaerobic conditions. Under anaerobic conditions, a number of microorganisms have developed the ability to use selenate as a terminal electron acceptor. In anaerobic conditions, selenate is first reduced to selenite (SeO_3^{2-}, Se(IV)), and then selenite is reduced to elemental selenium Se^0. The reduction of selenate to ultimately form elemental selenium, results in the formation of selenium precipitates which may be a burden to the cells due to the need for exportation of the precipitates to the external environment. Enzymes involved in selenate respiration have been studied primarily in three bacteria; *Thauera selenatis*, *Enterobacter cloacae* SLD1a-1, and *Bacillus selenatarsenatis* SF-1 (Nancharaiah *et al*., 2015).

Bacillus selenatarsenatis SF-1 is a Gram-positive bacterium, able to use lactate as the electron donor and selenate as the electron acceptor during selenate reduction. It was first isolated from the effluent sediments of a glass manufacturing plant (Fujita *et al*., 1997; Yamamura *et al*, 2007). The membrane-bound selenate reductase in *B. selenatarsenatis* SF-1 is a molybdoenzyme consisting of three subunits with the active site facing outside of the cell. Electrons originating from the quinol pool (QH_2) are transferred by SrdC and SrdB (an iron-sulfur protein) to the catalytic subunit, SrdA, which then donates electrons to SeO_4^{2-} via the molybdenum cofactor. Elemental selenium nanospheres are produced as a result of selenate/selenite reduction in *B. selenatarsenatis* SF-1 and these are released into the extracellular medium (Kuroda *et al*., 2011).

In 1997 a Gram-negative, rod-shaped bacterium capable of selenate reduction was isolated from the San Luis Drain. This *E. cloacae* strain was assigned the name *E. cloacae* SLD1a-1 and was found to reduce selenate and selenite, resulting in the precipitation of elemental selenium, in both aerobic and anaerobic growth conditions (Losi *et al*., 1997). *E. cloacae* SLD1a-1 can respire using selenate to produce elemental selenium under anaerobic conditions when glucose is used as the sole carbon source. However anaerobic growth cannot

be supported in *E. cloacae* SLD1a-1 with selenate as the sole electron acceptor and a non-fermentable carbon source (Watts *et al.*, 2003). The two electron reduction of selenate to selenite is catalysed by a membrane-bound molybdoenzyme which is exported from the cytoplasm through the twin-arginine translocase apparatus, and consists of three subunits (Ma *et al.*, 2007). This heterotrimeric complex's active site faces the periplasmic compartment and is located in the cytoplasmic membrane. The association of this enzyme with the cytoplasmic membrane suggests that the transfer of electrons from the Q-pool occurs via a core subunit (Ma *et al*, 2009). It has an apparent molecular mass of ~600 kDa and is thought to have an $\alpha_3\beta_3\gamma_3$ subunit composition. The α subunit is ~100 kDa, the β subunit is ~55 kDa, and the γ subunit is ~36 kDa. The *E. cloacae* SLD1a-1 selenate reductase contains the prosthetic constituents molybdenum, heme, and non-heme iron (Watts *et al.*, 2003; Ridley *et al.*, 2006). The genes that encode this selenate reductase have not been identified. However, *E. coli* has a molybdoenzyme, YnfE, which has been shown to act as a selenate reductase and this enzyme has multiple similar characteristics to the selenate reductase from *E. cloacae* SLD1a-1 (Guymer *et al.*, 2009). *E. cloacae* SLD1a-1 then reduces selenite to elemental selenium. The model proposed for the reduction of selenate to elemental selenium can be seen in Figure 1.2 (A). Selenium deposits have been detected in *E. cloacae* SLD1a-1 both intracellularly and extracellularly (Losi *et al.*, 1997). Figure 1.2 (B) shows an SEM micrograph of extracellular selenium deposits on the surface of *E. cloacae* SLD1a-1 cells. However, selenium particles associated with the cell surface are not able to be separated from cells during filtration (Butler *et al.*, 2012).

Selenite reduction to form elemental selenium occurs in a wide variety of microorganisms. Selenite reduction in microorganisms can be a detoxification strategy which can occur using various mechanisms including Painter-type reactions, the thioredoxin reductase system, as well as sulfide-mediated reduction. Some bacteria are able to respire using selenite although only a few have been isolated (Stolz *et al*., 2006). *Shewanella oneidensis* MR-1 is thought to have the ability to respire using selenite. It is believed that the CymA channels electrons from the quinol pool to FccA which then catalyses the reduction of selenite to elemental selenium, in the periplasm. However, it is not

clear whether selenite reduction does support growth or whether it is carried out for detoxification (Li *et al*., 2014).

Although the selenate reductases have been investigated in both *E. cloacae* SLD1a-1 and *B. selenatarsenatis* SF-1, the selenate reductases and the formation of elemental selenium nanospheres has been investigated most thoroughly in the β-proteobacterium, *Thauera selenatis*.

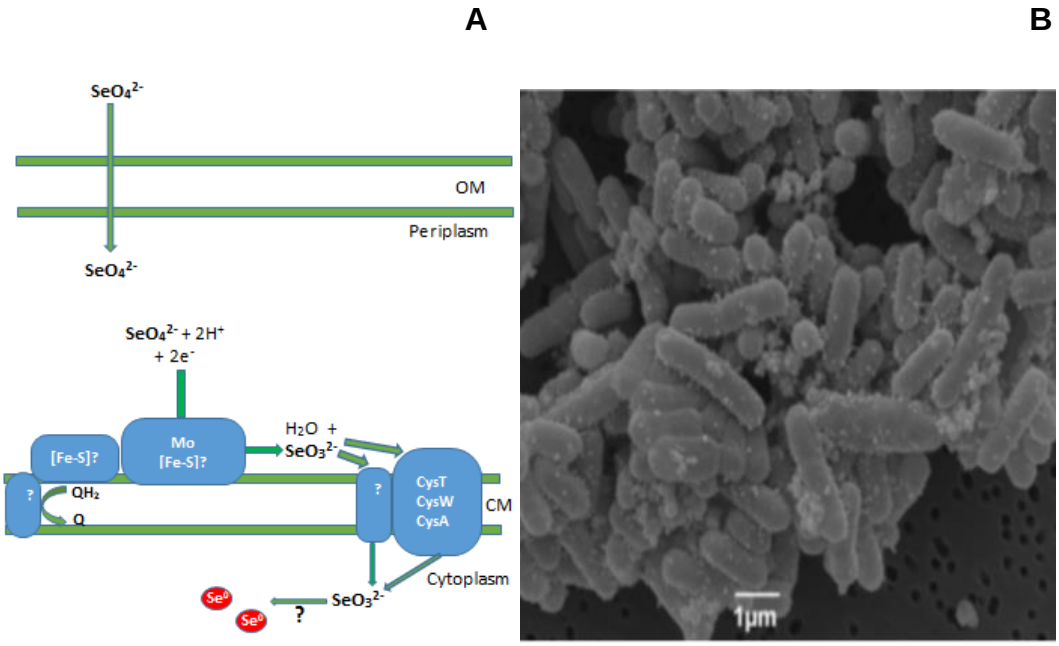

Figure 1.2: A model showing the proposed electron transport pathway involved in selenate reduction in *E. cloacae* SLD1a-1 with an SEM micrograph of selenium deposits on the surface of *E. cloacae* SLD1a-1. (A) Proposed electron transport pathway in selenate reduction in *E. cloacae* SLD1a-1. Adapted from Nancharaiah *et al*., 2015. (B) SEM micrograph of selenium deposits on the surface of *E. cloacae*. (Butler *et al*., 2012).

1.6 *Thauera selenatis*

In 1983, high concentrations of toxic selenate and selenite, and elemental selenium were identified in the agricultural subsurface drainage waters of the Kesterson Reservoir and the San Luis Drain in the San Joaquin Valley, California (Saiki *et al*., 1987). This selenium contamination was identified as the cause of abnormal development and death in aquatic birds inhabiting the San

Joaquin Valley (Ohlendorf *et al*., 1986). A large proportion of the contaminating selenium was present as the soluble oxyanion selenate (SeO_4^{2-}, Se(VI)), with a smaller proportion present as selenite (SeO_3^{2-}, Se(IV)). These two selenium oxyanions can be toxic at low concentrations and can also bioaccumulate, posing a serious threat to aquatic organisms inhabiting the contaminated waters (Presser *et al*., 1987; Weres *et al*., 1989). The potential for removal of these harmful selenium oxyanions by bacterial anaerobic respiration to produce less toxic elemental selenium which is also easier to remove from contaminated waters than the soluble selenate and selenite was investigated. A new species able to use selenate as a respiratory substrate and ultimately form nanospheres of elemental selenium (Se^0) was identified, initially incorrectly on the basis of phenotypic characteristics, as a *Pseudomonas* species in 1989. This species was isolated from the selenium-contaminated waters of the San Joaquin Valley, CA, U.S.A (Macy *et al*. 1989). In 1993, this bacterium was subsequently reclassified as the first member of a new genus and species*, Thauera selenatis,* and was identified as a Gram-negative, rod-shaped β-proteobacteria. *T. selenatis* cells are 1.4 µm long and 0.56 µM wide and are motile, with a single polar flagellum. *T. selenatis* is able to grow aerobically using acetate as the carbon source and electron donor, which is metabolized to CO_2. *T. selenatis* is also able to grow anaerobically using acetate as the carbon source and can simultaneously or exclusively use selenate (reduced to selenite) or nitrate (reduced to N_2O) as the terminal electron acceptor (Macy *et al*. 1993).

Selenate respiration in *T. selenatis* involves a 2 electron reduction of selenate, which is catalysed by the type II molybdoenzyme, selenate reductase (SER), in the periplasm, to form selenite (Dridge *et al.* 2007). The equation for the reduction of selenate can be seen in [1]:

$$SeO_4^{2-} + 2e^- + 2H^+ \rightarrow SeO_3^{2-} + H_2O \qquad [1]$$

A distinct selenate reductase used to catalyze selenate reduction in *T. selenatis* was first investigated in 1992 (Rech *et al.* 1992), and was subsequently purified and characterised (Schoder *et al*. 1997), and the genes encoding the selenate reductase sequenced (Krafft *et al.* 2000). SER is composed of three subunits.

SerA or the α subunit is ~96 kDa and coordinates the molybdopterin cofactor. It is the catalytic subunit that reduces selenate to selenite. The amino acid sequence of SerA demonstrates a conserved N-terminal cysteine-rich motif and it is thought to be coordinated to a [4Fe-4S] cluster. SerB or the β subunit is ~40 kDa, is rich in cysteine residues, and both [3Fe-4S] and [4Fe-4S] clusters have been detected using EPR analysis (Dridge *et al*., 2007). A predicted co-ordination of one [3Fe-4S] cluster and three [4Fe-4S] clusters has been suggested based on the comparison to the structure of the ethylbenzene dehydrogenase (EBH) β-subunit. SerC or the γ subunit is a *b*-type cytochrome, is ~23 kDa, and is the point of electron entry. SerC has a mid-point redox potential of +234 mV (Lowe *et al*. 2010). A cytoplasmic chaperone protein, SerD, has also been identified and it is thought to be involved with cofactor insertion into SerA (Schroder *et al.* 1997; Krafft *et al*. 2000; Dridge *et al.* 2007). Structural models for SerA, SerB, and SerC can be seen in Figure 1.3. The SerABC complex is a soluble periplasmic enzyme and has been shown to accept electrons from the 24 kDa diheme *c*-type cytochrome, cytc_4, *in vitro*, generating sufficient proton-motive force for growth. Whilst multiple *c*-type cytochromes have been shown to be upregulated during selenate respiration in *T. selenatis*, only two have been purified (cyt*c*-TS4 and cyt*c*-TS7), with only cyt*c*TS4 demonstrating electron transfer to SerABC *in vitro*. Cyt c_4 family cytochromes accept electrons from the quinol-cytochrome *c* oxidoreductase (QCR). However, electrons are thought to be transfered from both QCR and quinol dehydrogense (QDH) to cyt*c*-TS4 during selenate-dependent growth of *T. selenatis* due to the inability of the QCR inhibitor myxothiazol to completely inhibit growth. Full inhibition of selenate-dependent growth in *T. selenatis* is only achieved by the presence of 2-heptyl-4-hydroxyquinoline *N*-oxide (HQNO) which inhibits QCR as well as other QDHs (Lowe *et al*. 2010). A model showing the proposed electron transport pathway during selenate respiration in *T. selenatis* can be seen in Figure 1.4 (A).

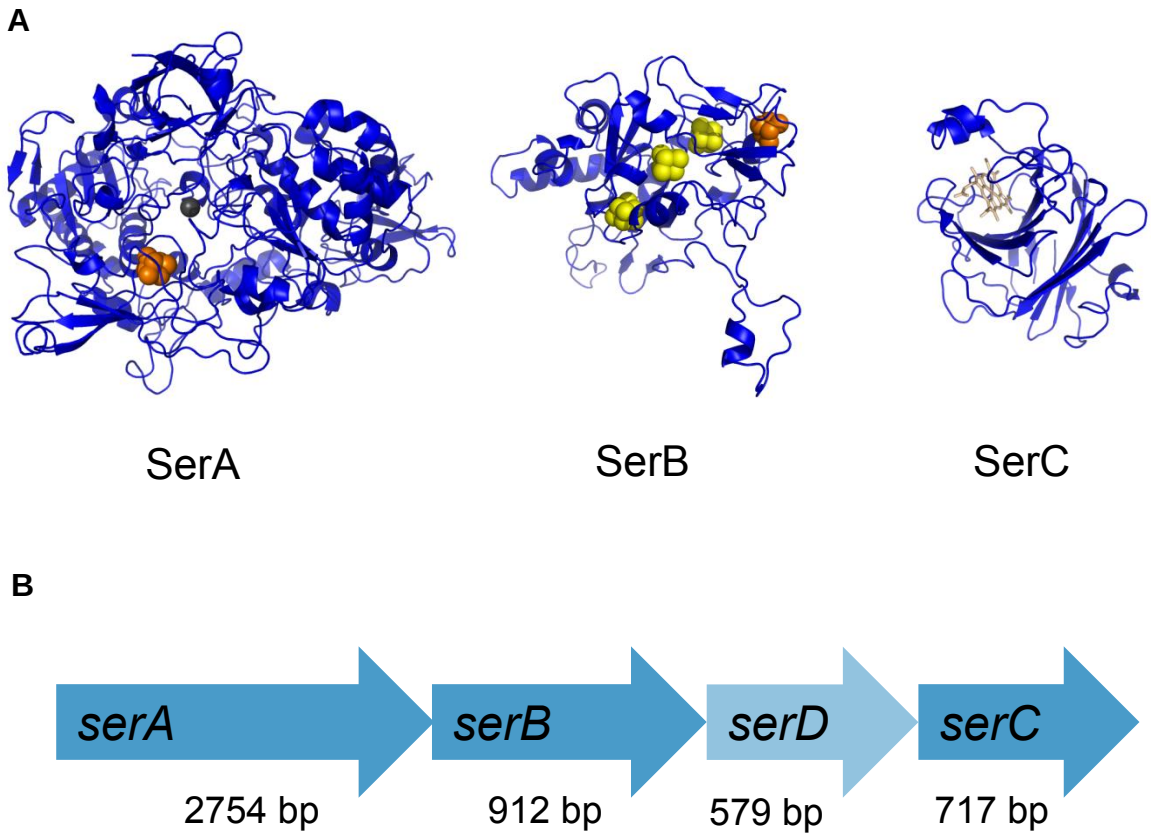

Figure 1.3: Structural models for selenate reductase and the SER subunit genes in the order they are found in the *T. selenatis* genome. (A) SerA showing the location of the [4Fe-4S] cluster and the molybdenum cofactor, SerB showing the location of the [3Fe-4S] cluster in orange and three [4Fe-4S] clusters in yellow, and SerC showing the location of the *b*-type haem. Models sourced from Butler, 2012. (B) SER subunit gene order in the *T. selenatis* genome and the length of the nucleotide sequence for each gene.

The resulting selenite product is not a respiratory substrate and does not support growth in *T. selenatis* under anaerobic conditions. However *T. selenatis* reduces selenite in order to detoxify the cells resulting in the formation of elemental selenium. The equation for selenite reduction to form elemental selenium is shown in [2] (Debieux *et al.*, 2011):

$$SeO_3^{2-} + 4e^- + 6H^+ \rightarrow Se^0 + 3H_2O \qquad [2]$$

The selenite is thought to be transported from the periplasm to the cytoplasm via a sulfate transporter (Debieux *et al.*, 2011; Turner *et al.*, 1998). It was

originally suggested that a periplasmic nitrite reductase might be involved in selenite reduction in *T. selenatis.* This was due to a *T. selenatis* non-specific mutant deficient in nitrite reductase activity, that was also unable to produce Se^0 during growth in selenate-rich medium (DeMoll Decker *et al.* 1993). However, the primary reduced thiol in *Escherichia coli*, glutathione (GSH), which is also abundant in alpha, beta, and gamma groups of the proteobacteria, is now thought to be involved in intracellular bacterial selenite reduction. This followed the agreement that bacterial selenite reduction was more likely to take place in the cytoplasmic compartment due to the commonly observed presence of Se^0 deposits here. GSH reacts with selenite to produce selenodiglutathione (GS-Se-SG) which in turn is reduced by GSH reductase to form a selenopersulfide of GSH ($GS\text{-}Se^-$). The ($GS\text{-}Se^-$) then undergoes dismutation to form elemental selenium (Se^0) and reduced GSH (Butler *et al.*, 2012).

Elemental selenium deposits, produced after selenite reduction, have been observed using transmission electron microscopy in the cytoplasmic compartment of *T. selenatis.* A single particle of selenium can be seen per cell, each possessing a spherical shape, as growth enters the late-exponential phase. When the stationary phase is reached, these selenium particles are excreted from the cell and can be seen both in the surrounding medium, as well as being associated with the cell surface. An SEM image of selenium deposits on the surface of the *T. selenatis* cell can be seen in Figure 1.4 (B). Cultures turn a brick-red colour as the selenium nanospheres are secreted from the cell (Butler *et al*., 2012). The selenium nanoparticles have a diameter of ~150 nm and can be isolated from the culture by fine filtration (0.2 µl) (Debieux *et al.* 2011). Given the potential commercial and medical importance of SeNPs, there has been much interest in the possiblilty of using bacteria like *T. selenatis* as microbial factories for the biogenic sysnthesis of SeNPs. Understanding the mechanisms and protein corona involved in selenium nanosphere assembly and exportation from the cell in *T. selenatis* could therefore allow for the large scale production and use of SeNPs from *T. selenatis* in multiple applications.

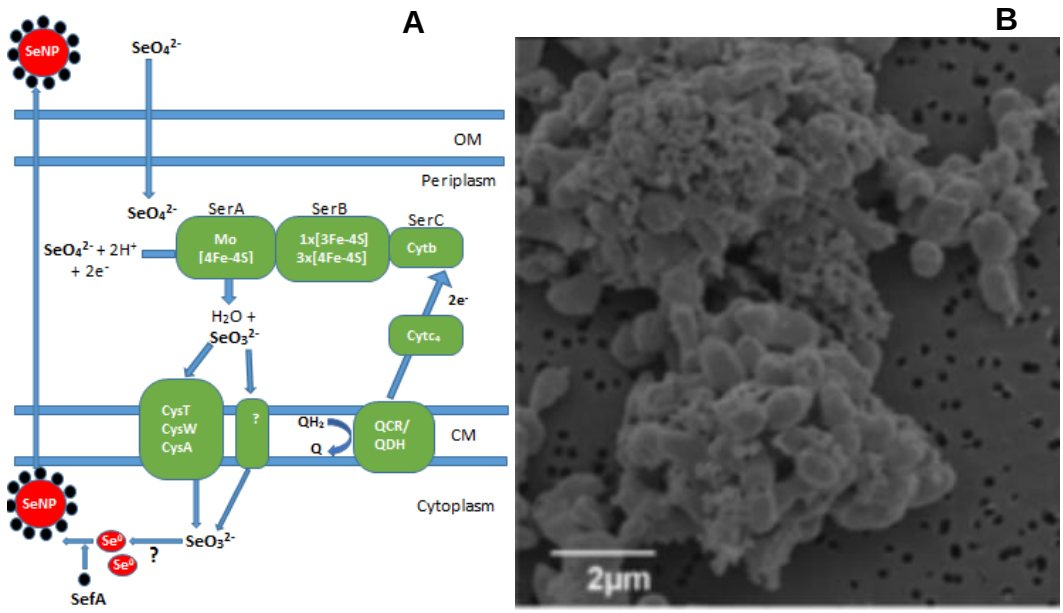

Figure 1.4: A model showing the proposed electron transport pathway involved in selenate reduction and selenium nanoparticle export in *T. selenatis* with an SEM micrograph of selenium deposits on the surface of *T. selenatis* cells grown anaerobically in the presence of selenate. (A) Proposed electron transport pathway in selenate reduction and selenium nanoparticle export in *T. selenatis*. Adapted from Nancharaiah *et al*., 2015. (B) SEM micrograph of selenium deposits on the surface of *T. selenatis* cells grown anaerobically in the presence of selenate (Butler *et al*., 2012).

1.7 The SefA protein corona

A sample from the growth medium of *T. selenatis* undergoing selenate respiration was taken after exportation of selenium nanoparticles from the cell cytoplasm had occurred. Analysis of the secreted protein profile resulted in a protein of ~94.5 kDa being identified. This protein was named Selenium Factor A (SefA), and is composed of 961 amino acids, with 64.3% of the primary sequence consisting of the amino acids; alanine, threonine, glycine, valine and aspartate (Debieux *et al.*, 2011). A BLAST of the SefA protein identifies 10 proteins that align with the SefA sequence (see appendix A1). Two homologues of SefA have previously been identified in the two strains; AL212 and Is79A3 of *Nitrosomonas sp.* Strains of *Nitrosomonas* which are cultured similarly to AL212 and Is79A3 can produce intracellular and extracellular particles (Suwa *et al.*, 1994). Strain AL212 is able to grow in up to 10.7 mM $(NH_4)_2SO_4$ (Suwa *et al.*,

1997). SefA, Is79A3_0436 and NAL212_3002 have a low overall identity but there is 60% identity over the first 25 N-terminal residues. This suggests that the N-terminal region might play a role in essential recognition by the membrane secretion system or by mineral deposits.

SefA is up-regulated by selenite and during selenite reduction the concentration of SefA found in the growth medium increases over time. SefA was found to have no selenite reductase activity, suggesting that it either binds to, or stabilises selenium nanospheres (Debieux *et al.*, 2011). SefA has been cloned, overexpressed, and purified from *E. coli* and following selenite reduction by glutathione, *in vitro*, SefA is able to stabilise selenium nanosphere formation. SefA does not have cysteine residues and therefore could not interact with selenium via thiol groups. SefA may instead interact with selenium via weak interactions using carboxylate ligands (Debieux *et al*., 2011). If this is the case, SefA could therefore form a soft protein corona around selenium nanoparticles. Bovine serum albumin (BSA) has been found to stabilise selenium nanopaticles by a non-specific interaction that allows it to cap the surface of the particle (Bücking *et al*., 2010). It is thought that SefA acts similarly with selenium particles, resulting in reaction sites for the selenium so that nanospheres can be formed, as well as preventing aggregation of the elemental selenium particles (Debieux *et al*, 2011).

How the selenium nanospheres, produced by *T. selenatis* after selenite reduction, are transported out of the cell is still unknown. When transmission electron microscopy (TEM) was used to analyse *T. selenatis* cells carrying out selenate respiration, the spherical selenium nanosphere particles were found to be ~150 nm in diameter. No evidence of cell lysis, Se in the periplasmic compartment, or budding of the outer membrane was found (Debieux *et al.*, 2011). SefA does not contain an N-terminal signal sequence which is necessary for export to the periplasm in the cell. Also, it was concluded unlikely that SefA could be targeted to the periplasm by twin-arginine-translocation (TAT) substrate candidates. It is therefore thought that SefA-Se nanospheres are exported from the cell directly from the cytoplasm (Debieux *et al.*, 2011). Analysis of the *T. selenatis* draft genome assembly found the presence of all

but the Type V secretion system. Two secretion systems have been identified as potential ways that the SefA-Se nanospheres leave the cell. The Type 6 Secretion System (T6SS) is a potential way that SefA is exported from the cell, as other proteins secreted by this system are not translocated to the periplasmic compartment as they also do not contain an N-terminal signal sequence. The Type 1 Secretion System (T1SS) is the other candidate due to other T1SS substrates containing few or no cysteine residues (Baumann *et al*., 1993; Delepelaire, 2004; Debieux *et al*., 2011).

1.8 Aims and objectives

The main aim of this work was to investigate the molecular mechanisms by which *T. selenatis* generates selenium nanospheres during selenate respiration, and how these selenium nanopshere deposits might be expelled from the cell.

The specific objectives were:

- To express and purify His-SefA-His and His-SefA and cleave the N-terminal His-tag from His-SefA-His to form SefA-His.
- To investigate interactions between soluble proteins in cell extracts from *T. selenatis* grown in either sodium selenate or potassium nitrate, and His-SefA-His, His-SefA, and SefA-His.
- To isolate proteins that may interact with the N-terminal of SefA-His and identify them using MALDI-MS.
- To identify the oligomeric state of the His-SefA-His protein.
- To resolve the crystal structure of the SefA protein from *T.* selenatis by crystallising His-SefA-His.
- To investigate differential expression in *T. selenatis* grown with or without sodium selenite using mRNA sequencing.

2. Materials and methods

Bacterial strains, and growth conditions

The strains and constructs used during this study are shown in Table 2.1. The SefA protein from *T. selenatis* was originally isolated and characterised due to its presence in the secreted protein profile from *T. selenatis* after it had been exposed to selenate and selenite, and is thought to be associated with the assembly and exportation of selenium nanospheres. It was subsequently cloned into the pET-33b(+) expression vector with pET-33b/*His-SefA* the construct to produce the His-SefA protein, and pET-33b/*His-SefA-His* the construct to produce the His-SefA-His protein. The two recombinant proteins were expressed in *E. coli* and purified using a nickel affinity column (Debieux *et al.*, 2011). In this work, three versions of differentially His-tagged SefA proteins were expressed. These three versions include SefA with a His-tag on the C-terminal, SefA with a His-tag on the N-terminal, and SefA with a His-tag on both the C- and N-terminals. SefA with a His-tag on the C-terminal will be represented as SefA-His. SefA with a His-tag on the N-terminal will be represented as His-SefA. SefA with His-tags on both the C- and N-terminals will be represented as His-SefA-His.

Table 2.1: Bacterial strains and plasmids with characteristics and growth conditions.

Strains and Plasmids	Characteristics	Growth conditions	Reference
E. coli BL21 CodonPlus (DE3)-RIPL	F–, *dcm, omp*T, *hsd*S (rB– mB–), *gal*, λ(DE3). (For induction in T7 expression systems).	LB media, chloramphenicol kanamycin, 37 ^{o}C, agitation (250 rpm)	Stratagene
pET33b(+) with *His-SefA* and *His-SefA-His*	Kan^{r}, *lac*I gene, IPTG inducible, P_{T7}	(To express SefA protein) LB media, chloramphenicol, kanamycin, 37 ^{o}C, agitation (250 rpm) followed by addition of IPTG (1 mM), 20 ^{o}C, agitation (250 rpm)	Novagen
T. selenatis (ATCC55363)	Proteobacteria of the β subclass able to respire anaerobically using selenate. Selenium nanospheres are produced as waste products of selenate respiration.	Aerobic: LB media, 30 ^{o}C, agitation (250 rpm) Anaerobic: Hungates media, SL8 solution of trace elements, vitamin solution, sodium acetate, sodium selenate/potassium nitrate, magnesium chloride hexahydrate, calcium chloride hydrate, 30 ^{o}C, no agitation	Macy *et al.* 1993

Table 2.1: Continued.			
E. Cloacae (SLD1a-1, ATCC700258)	Gammaproteobacteria able to completely reduce selenate to elemental selenium	Aerobic: LB media, 30 ^{o}C, agitation (250 rpm) Anaerobic: Basal salt medium (BSM), vitamin solution, mineral soution, glycerol, formate, nitrate, 37 ^{o}C. (Leaver *et al.*, 2008)	Losi *et al.*, 1997

2.1 Bacterial Growth

2.1.1 Expression of His-SefA and His-SefA-His in *E. coli* and cell preparation

Two cultures of *E. coli* expressing His-SefA-His and His-SefA were grown aerobically from glycerol stocks by adding the cells to 100 ml Luria-Bertani (LB) medium (casein enzymic hydrolysate, 10 g/L, sodium chloride, 10 g/L, yeast extract, 5 g/l) with added Kanamycin (1 mg/ml) and Chloramphenicol (0.355 mg/ml) at 37^{o}C with agitation (250 rpm) for 16 hours. 10 ml of the *E. coli* cultured for 16 hours was then added to 500 ml of fresh LB media and incubated at 37^{o}C with agitation (250 rpm). Incubation was continued until the optical density of the culture, measured using a colorimeter at 600nm, was 0.4. The culture was then refrigerated for 30 minutes, after which isopropyl β-D-1-

thiogalactopyranoside (IPTG) (1 mM) was added. Further incubation with agitation (250 rpm) at 20^{o}C was then carried out for 16 hours.The culture was then centrifuged (5000 x g, 10 ^{o}C, 15 minutes) to isolate the cells. The supernatant was discarded and the pellet resuspended in 25 ml of Buffer A (50 mM Tris-HCl, pH 7.0, 0.5 M NaCl, 50 mM imidazole), a low concentration imidazole buffer to allow his-tagged proteins to attach to the nickel resin contained within a nickel affinity column and prevent other weak His interactions.

2.1.1.1 Cell Lysis

The resuspended cells were lysed, whilst being kept on ice, using a sonicator with the deflection set at 15 microns. The sonicator was turned on for 25 seconds and then off for 35 seconds, with 6 repeats of these pulses. The sample was then centrifuged (20,000 x g, 4 ^{o}C, 30 minutes) and the supernatant was retained for use in the nickel affinity column.

2.1.2 Anaerobic growth of *T. selenatis* and cell preparation

A solution of Hungates media (see appendix A2., 500 ml) was added to an SL8 solution of trace elements (see appendix A3., 5 ml), a vitamin solution (see appendix A4., 5 ml), sodium selenate (10 mM), sodium acetate (9.9 mM), $MgCl_2.6H_2O$ (1.97 mM), and $CaCl_2H_2O$ (1.35 mM). The solution was degassed by flowing nitrogen gas (N_2) through a needle pierced through the sealed rubber stopper in the top of a flask, and submerged in the growth media for 25 minutes to establish anaerobic conditions. A control was also produced containing the same compositions of each of the solutions except the sodium selenate was replaced by potassium nitrate (10 mM). The nitrate control was also degassed for 25 minutes as above. *T. selenatis* glycerol stock (250 µl) was then added to each of the solutions and incubated at 30 ^{o}C for 96 hours. Another two solutions were made as before with one containing sodium selenate (10mM) and the other containing potassium nitrate (10mM). They were both degassed and

inoculated with the respectively grown *T. selenatis* cultures and incubated at 30 ^{o}C for 96 hours. The subculturing process was repeated. The cultures of *T. selenatis* grown with either selenate or nitrate as the sole electron acceptors were each centrifuged (5000 x g, 10 ^{o}C, 20 minutes). The two pellets were each resuspended in 25 ml of Tris-HCl (30 mM, pH 8.5). The cells were then lysed as in section 2.1.1.1.

2.1.3 Aerobic growth of *T. selenatis*

LB media (100 ml) was inoculated with *T. selenatis* (250 µl) and incubated at 30 ^{o}C for 12 hours with agitation (250 rpm). Fresh LB media (99 ml) was added to sodium selenite (10 mM), or fresh LB media (100 ml) without sodium selenite was prepared and the LB was inoculated with the *T. selenatis* (1 ml) from the first culture that had been growing for 12 hours. *T. selenatis* cultures were then incubated at 30 ^{o}C for 5 hours. Optical density of the *T. selenatis* cultures, when required, was recorded using the Tecan Infinite Pro M200 plate reader at a wavelength of 600 nm.

2.2 Protein purification, concentrating protein samples, and the determination of protein concentration

2.2.1 Nickel affinity chromatography

A 20 ml nickel column was filled with 5 ml of ProBond^{TM} Nickel-Chelating Resin and was equilibrated with 30 ml of Buffer A' (50 mM Tris-HCl, 100 mM imidazole, 0.5 M NaCl, pH 7). Half of the sample was added to the column and agitated for 20 minutes to allow for binding to the nickel resin. The column was allowed to settle before the sample was allowed to run through the column. The second half of the sample was added to the column and agitated for 20 minutes, allowed to settle, and then the sample was run through the column. The nickel affinity column was washed with Buffer A' (20 ml) to remove sample not bound to the nickel resin. The bound sample was eluted with 20 ml of Buffer

B (50 mM Tris-HCl, 0.5M NaCl, 1 M imidazole, pH 7). Samples were collected at each elution and wash step for analysis by SDS-PAGE.

Nickel affinity chromatography was carried out as above in all protein purification experiments. For the nickel affinity columns run to investigate protein-protein interactions between the three variations of the His-tagged SefA protein (His-SefA, His-SefA-His, and SefA-His) and soluble cell extracts from *T. selenatis* grown either with sodium selenate or potassium nitrate the same protocol as above was carried out with the following alterations: the column was equilibrated and washed with Buffer C (30 mM Tris-HCl, pH 8.5) instead of Buffer A'. After the SefA sample had been added to the column and washed with Buffer C the *T. selenatis* sample was added to the column and agitated for 20 minutes to allow for protein binding to SefA, before being allowed to flow through the column, and an extra wash with Buffer C after the *T. selenatis* sample flowed through the column was carried out. Samples of each elution and wash step were collected for analysis by SDS-PAGE.

2.2.2 Concentrating protein samples

Part of the protein sample was added to an Amicon™ Ultra-10 Centrifugal Filter tube and centrifuged (8448 x g, 4 ºC, 15 minutes). The remaining protein mixture was added to the tube and centrifuged again (8448 x g, 4 ºC, 15 minutes). The protein mixture was centrifuged repeatedly (8448 x g, 4 ºC, 15 minutes) until the desired concentration was achieved.

2.2.3 Determing protein concentration

Protein concentration was quantified using a Nanodrop 2000c UV-Vis spectrophotometer (A_{280}). A blank using 2 µl of the protein buffer was first taken and then 2 µl of the protein sample was used to measure protein concentration.

2.3 Analysis of protein samples by SDS-PAGE

2.3.1 Solutions for SDS-PAGE

Solution Name	Ingredients
NuPAGE® Reducing Agent (10X)	500 mM Dithiothreitol
NuPAGE® LDS Sample Buffer (4X)	40-70% Glycerin, 7-13% Sulfuric acid, monododecyl ester, lithium salt
NuPAGE® MOPS SDS Running Buffer (20X)	50 mM MOPS, 50 mM Tris Base, 0.1% SDS, 1 mM EDTA, pH 7.7
NuPAGE® Antioxidant	10-30% Dimethylformamide, 10-30% Sodium bisulfate

2.3.2 Preparation of the protein sample

13 µl from each protein sample was added to NuPAGE® Reducing agent (10X) (2 µl), and NuPAGE® SDS Sample Buffer (4X) (5 µl), and then centrifuged (13,249 x g, 20 ^{o}C, 15 seconds). The samples were heated to 70 ^{o}C for 10 minutes and then centrifuged again (13,249 x g, 20 ^{o}C, 15 seconds).

2.3.3 SDS-PAGE run

NuPAGE® MOPS SDS Running Buffer (20X) (40 ml) was added to distilled water (760 ml) and this was added into the buffer chamber of a NuPAGE®

Novex® 10% Bis-Tris gel along with NuPAGE® Antioxidant (500 µl). The NuPAGE® Novex® 10% Bis-Tris Gel was then loaded with the protein ladder SeeBlue® Plus2 Pre-Stained Standard (5 µl) in lane 1 and each of the samples (20 µl) with an average maximum protein concentration of 0.13 mg were loaded into adjacent wells. The gel was run at 200 V for 50 minutes.

2.3.4 Gel staining

The gel was removed from the gel holder and stained with Expedeon Instant Blue Protein Stain for 1 hour on an agitator. The gel was then agitated in distilled water for 1 hour. A photograph of the gel was then taken.

2.4 Removal of the N-terminal His-tag from His-SefA-His

2.4.1 Sample preparation

The His-SefA-His protein was first purified using nickel affinity chromatography as described in section 2.2.1. The protein sample was then exchanged into Buffer E (50 mM Tris-HCl, 10 mM $CaCl_2$, pH 8) by addition of the sample and Buffer E to an Amicon™ Ultra-10 Centrifugal Filter tube. Centrifugation and protein concentration was carried out as described in section 2.2.2 and the protein concentration was quantified as in section 2.2.3.

2.4.2 Washing the Thrombin CleanCleave™ Kit resin

The Thrombin CleanCleave™ Kit was used. The thrombin-agarose resin (thrombin-agarose 50 % suspension in 50 % glycerol, 20 mM Tris-HCl, pH 8.2) was resuspended. A 100 µl aliquot of resin was centrifuged (500 x g, 15 minutes) to pellet the resin and the supernatant was removed. 500 µl of 1 X Cleavage Buffer (50 mM Tris-HCl, pH 8.0, 10 mM $CaCl_2$) was added to the

pellet to resuspend it. The sample was centrifuged (500 x g, 15 minutes). The supernatant was removed and again, 500 µl of 1X Cleavage Buffer was added to the pellet. The sample was centrifuged (500 x g, 15 minutes), and the supernatant removed.

2.4.3 Cleavage Reaction

The centrifuged beads were resuspended in 100 µl of 10 X Cleavage Buffer (500 mM Tris-HCl, pH 8.0, 100 mM $CaCl_2$) and the His-SefA-His sample containing 1 mg of protein was added. The final reaction volume was made to 1 ml using water. The cleavage reaction tube was incubated at room temperature with agitation for 24 hours. Aliquots (30 µl) were removed from the reaction tube, to be analysed using SDS-PAGE, at 1, 2, 4, 6, and 24 hours and centrifuged (461 x g, 15 minutes) to remove the resin.

2.4.4 Recovery of the fusion protein

After 24 hours the tubes were transferred to the recovery column, rinsed with 5 bed volumes of Cleavage Buffer (1 x), and the eluent containing the cleaved SefA-His was collected.

2.5 Protein preparation and analysis for crystallisation trials

2.5.1 Gel filtration chromatography

A Superdex 200 HiLoad 16/60 120 ml gel filtration column (sourced from GE Healthcare) was equilibrated with Buffer C (25 mM Tris-HCl, pH 7, 0.1 M NaCl) at a flow rate of 1 ml/min. The His-SefA-His protein was loaded (1 ml) at 0.5 ml/min and eluted over one column volume collecting 2 ml fractions. Fractions

containing the highest concentration of His-SefA-His protein (conclusions drawn from analysing the gel filtration trace) were analysed by SDS-PAGE as in section 2.3.

2.5.2 Analytical Gel filtration chromatography

A Superdex 200 10/300 GL 23.56 ml gel filtration column (sourced from GE Healthcare) was equilibrated using Buffer D (10 mM HEPES, pH 7, 0.5 M NaCl) at a flow rate of 0.5 ml/min. The protein was loaded (200 µl) at 0.5 ml/min and eluted over one column volume collecting 2 ml fractions.

2.5.3 Differential Scanning Fluorimetry

A His-SefA-His protein master mix was made containing His-SefA-His protein (0.133 mg/ml), Sypro Orange (5000x, 1.92 µl), and water (added to produce a final volume of 900 µl). 24 separate buffers (5 µl) (see appendix A5.) were added in duplicate to a MicroAmp® Fast Optical 48-Well Reaction Plate. The master mix (15 µl) was added to each of the 48 wells. The plate was sealed with optically transparent sealing tape and centrifuged (2 minutes, 300 x g). The plate was loaded into a StepOne quantitative PCR machine and the samples were heated between 25 ºC and 99 ºC over 50 minutes. The results were analysed using the Protein Thermal Shift Software.

2.6 His-SefA-His Protein Crystallisation Trials

After gel filtration the protein was concentrated as in section 2.2.2. Microbatch crystallisation trials were set up in a 96 well Douglas Vapour Batch Plate (Douglas Instruments Ltd) using a JCSG-*plus* screen, a Morpheus screen, and an SG1 screen (All Molecular Dimensions). An Oryx 8 protein crystallisation robot (Douglas Instruments Ltd) was used. The final droplet volume was 1 µl with a 50:50 ratio of His-SefA-His protein to screen. Each droplet was then

covered with a 50:50 ratio of silicon oil:paraffin and the plates were stored at 18 ºC and checked daily.

2.7 *T. selenatis* cell density determination and RNA extraction for mRNA sequencing

2.7.1. *T. selenatis* cell concentration determination

A culture of *T. selenatis* was grown aerobically as in section 2.1.3 with three cultures being grown in the presence of sodium selenite and three cultures being grown in the absence of sodium selenite, all inoculated from an overnight *T. selenatis* culture. After 5 hours of growth, 100 µl of each culture was transferred into separate first column wells of a 96 well plate and 90 µl of LB was placed in all other wells on the plate. The optical density of the pure culture in the first column wells was then identified as described in section 2.1.3. A serial dilution was then carried out along each row until a dilution of 1×10^{-9} was reached in the final column used. 3 x 10 µl from each culture from each dilution between 1×10^{-4} and 1×10^{-9} was then taken and pipetted onto 12 LB agar plates. The plates were then incubated for 12 hours at 30 ºC and the colonies that had grown after this time were counted.

2.7.2 Enzymatic lysis and proteinase K digestion of *T. selenatis* cells using the QIAGEN RNeasy® Mini Kit

T. selenatis was cultured as described in section 2.1.3 with three cultures containing sodium selenite and three cultures without sodium selenite. RNA bacterial reagent was added to each *T. selenatis* sample so that the total volume was 4 x the volume of the amount of culture added. Each sample was mixed by vortexing for 5 seconds and then incubated for 5 minutes at room temperature. Each sample was centrifuged (5000 x g, 20 ºC, 10 minutes) and the supernatant was removed. For each of the 6 samples QIAGEN proteinase K

(10 µl) was added to Tris-EDTA (TE) buffer (30 mM Tris-Cl, 1 mM EDTA, pH 8.0, 200 µl) containing lysozyme (3 mg) and the mixture was added to each bacterial pellet. Each pellet was resuspended by pipetting up and down several times and then mixed by vortexing for 10 seconds. Each mixture was incubated at room temperature with vortexing every 2 minutes for a total of 10 minutes.

2.7.3 Purification of total RNA from the bacterial lysate using the QIAGEN RNeasy® Mini Kit with on-column DNase digestion using the QIAGEN RNase-Free DNase Set

Buffer RLT (QIAGEN) (700 µl) was added and each sample was vortexed vigorously. Ethanol (500 µl) was added and then each sample was mixed by pipetting. Each lysate (700 µl) was transferred to a separate RNeasy® Mini Spin column which was placed in a 2 ml collection tube. Each lid was closed and then the samples were centrifuged (8000 x g, 20 ^{o}C, 15 seconds), and the flow through was discarded. The remaining volume from each lysate was then transferred into the corresponding RNeasy® Mini Spin column and centrifuged (8000 x g, 20 ^{o}C, 15 seconds) and the flow through was discarded. Buffer RW1 (QIAGEN) (350 µl) was added to each RNeasy® Mini Spin column and centrifuged (8000 x g, 20 ^{o}C, 15 seconds) to wash the spin column membrane and the flow through was discarded.

For each of the 6 samples, DNase I (QIAGEN) (10 µl) was added to Buffer RDD (QIAGEN) (70 µl) and then mixed by inversion and centrifuged (8000 x g, 20 ^{o}C, 15 seconds). The DNase I incubation mix was then added directly to each RNeasy® Spin column membrane and incubated at room temperature for 15 minutes. Buffer RW1 (350 µl) was added to each RNeasy® Mini Spin column, the mixture was incubated for 5 minutes and then centrifuged (8000 x g, 20 ^{o}C, 15 seconds). Each flow through and collection tube was discarded.

Each RNeasy® Mini Spin column was placed in a new 2 ml collection tube and Buffer RPE (QIAGEN) (500 µl) was added to each spin column. Each column was centrifuged (8000 x g, 20 ^{o}C, 15 seconds) and the flow through was

discarded. Buffer RPE (500 µl) was added to each RNeasy® Mini Spin column and centrifuged (8000 x g, 20 ^{o}C, 2 minutes). Each RNeasy® Mini Spin column was removed from the collection tube and the collection tubes were discarded. Each spin column was placed in a new collection tube and RNase-free water (30 µl) was added directly to each spin column membrane and centrifuged (8000 x g, 20 ^{o}C, 1 minute) to elute the RNA. RNase-free water (30 µl) was again added to each spin column and centrifuged (8000 x g, 20 ^{o}C, 1 minute).

2.7.4 RNA concentration and integrity determination and mRNA sequencing

The RNA concentration and RNA integrity number of each of the 6 *T. selenatis* total RNA samples was then identified using electrophoretic analysis in a chip format using an Agilent 2100 Bioanalyzer. For each total RNA sample 1µg of total RNA was used for preparations for mRNA sequencing.

The following was carried out by the Exeter Sequencing Service, Geoffrey Pope Building, Biosciences, Stocker Road, University of Exeter, EX4 4QD; for each of the 6 samples, mRNA was isolated by removing the rRNA using a Ribo-Zero rRNA Removal Kit (Bacteria). ScriptSeq was then used for the library preparation before sequencing of the mRNA for each of the 6 samples was carried out using a HiSeq 2500 standard mode, with a read length of 100, using a paired end read-type, and units of 0.5 lanes.

2.8 PCR trials

2.8.1 Preparation of *T. selenatis*/*E. cloacae* individual colonies

Cultures of *T. selenatis*/*E. cloacae* were grown as described in section 2.1.3. A 100 µl sample of the culture was then used to make 100 µl dilutions of the bacteria using 90µl of fresh LB broth for each dilution, up to a 10^{-9} dilution. The dilution samples were then streaked onto plates containing LB agar and

incubated for 24 hours at 30 ºC. Individual colonies were then picked using a loop and either;

1. Half of the colony was picked and resuspended directly in the PCR mixtures. The other half of the colony was then picked and resuspended in LB media (10 ml) and incubated for 24 hours at 30 ºC with agitation (250 rpm). Half of the colony was incubated so that if a pure *T. selenatis* sample was identified using PCR, the culture could be frozen at -80 ºC for use in further experiments.
2. The whole colony was picked and resuspended in PCR grade water (10 µl) with 5 µl of this mixture being heated to 99 ºC for 10 minutes and then transferred to one or multiple PCR mixtures. The other 5 µl was transferred to LB media (10 ml) and incubated for 24 hours at 30 ºC with agitation (250 rpm) as above.

2.8.2 Colony PCR trials

PCR trials general method:
All PCR solutions were prepared on ice. Where master mixes of PCR reagents were necessary (for temperature gradient reactions), solutions were mixed in 1.5 ml eppendorf tubes. Individual PCR mixtures (final volume of 10 µl) for a single PCR reaction were mixed in a PCR tube. Where a master mix was required, once all components had been added, 10 µl aliquots were pipetted into PCR tubes. All PCR tubes were then centrifuged before being placed into the PCR machine (BioRad T100™ Thermal Cycler) and then the PCR reaction was carried out. Primers (all sourced from Eurofins Genomics) and conditions used are detailed in the appendix A6.

2.8.3 Analysis of PCR trials using horizontal agarose gels

A 1% agarose gel was made by adding agarose (0.6 g) into a conical flask with 1 x Tris-acetate-EDTA (TAE) buffer (60 ml, 40 mM Tris, 20 mM acetic acid, 1 mM EDTA), and heating in a microwave for 1.5 minutes. The mixture was

partially cooled and poured into the gel holder containing either one or two sets of well combs. The gel was allowed to cool completely before the combs were removed, and the gel holder was placed into the electrophoresis gel box. The gel was covered with 1 x TAE buffer, and 10 µl of HyperLadder™ 1kb (Bioline) was loaded into lane 1 of the gel. PCR samples were then loaded into the wells before the gel was run for 35 minutes at 100 V and 200 mA. Once run, the gels were visualised under UV light.

3 Investigating protein-protein interactions between SefA and soluble proteins in cell extracts from *T. selenatis*

3.1 Introduction

Previous investigations (Debieux *et al.*, 2011) have found that selenium deposits produced as a result of selenate reduction in *T. selenatis* are associated with a protein of ~94.5 kDa, SefA. SefA was found to be upregulated with increasing selenite concentrations. Observations of the *T. selenatis* growth medium over time revealed that the selenium nanospheres produced during selenate reduction are exported out of the cell during the exponential growth phase. N-terminal sequence analysis of SefA found no cleavable signal peptide, resulting in the hypothesis that SefA is exported from the cell directly from the cytoplasm. It is believed that SefA facilitates the assembly and exportation of the selenium nanospheres from the *T. selenatis* cell. SefA has previously been cloned and expressed in *E. coli* (Debieux *et al.*, 2011) and two recombinant, differentially His-tagged proteins have been successfully purified; His-SefA-His and His-SefA.

Whilst SefA is thought to faciliate selenium nanosphere assembly and exportation in *T. selenatis*, other proteins yet to be identified could also be involved with this process. The aim of this work was to investigate protein-protein interactions between His-tagged SefA expressed in *E. coli* and proteins located in the soluble cell fractions of *T. selenatis*. The *T. selenatis* cultures were grown in the presence and absence of sodium selenate in order to compare protein-protein interactions when selenate reduction is occurring and when it is not. Identification of proteins that are found to interact with SefA may allow for a more detailed understanding of how the selenium deposits are assembled into nanospheres and exported from the cell and exactly what role SefA and other proteins play in this process.

Whilst His-SefA-His and His-SefA have been expressed in *E. coli*, interactions between the N-terminal of SefA and soluble cell fractions from *T. selenatis* are of particular interest and will be investigated here. Homologues of SefA have

been identified in two strains of *Nitrosomonas* (AL212 and Is79A3). Strains of *Nitrosomonas* which have been cultured under similar conditions to strain AL212 have previously been shown to produce intracellular and extracellular particles (Suwa *et al.*, 1994). Whilst the overall identity between SefA and the two homologues from these strains is low, there is 60% identity over the first 25 N-terminal residues (Figure 3.1). It has been hypothesized (Butler *et al.*, 2012) that these first 25 N-terminal residues may play a role in recognition by a membrane secretion system or are associated with the mineral deposits. The N-terminal His-tag from the His-SefA-His protein expressed in *E. coli* will therefore be cleaved in order to allow for protein-protein interactions to be investigated between the N-terminal of SefA and proteins from the soluble cell extracts of *T. selenatis*. Retaining the C-terminal His-tag will allow the SefA protein to be immobilized onto a nickel column matrix.

```
SefA            MAITATQRTEIVKVVVGLFNAAPGATYLDSFTAYADNIDG------LVNDLVADPAFT-A 53
Is79A3_0436     MAITSTQKTEILKIVAGLFNAAPGGSNLTELANLVSGG---MTTSQLADALAANTLFTNG 57
NAL212_3002     MAITAEQQTSILEVAIGLFNAAPGKIYMTELANMVDANGGNLSIEQLADFLDDTAVFKDN 60
                ****: *:*.*:::. ********   : .::  ..         *.: *   . *.
```

Figure 3.1: N-terminal sequence alignment of SefA, Is79A3_0436, and NAL212_3002 (Butler *et al.,* 2012)

3.1.1 Aims and Objectives

- Express and purify the recombinant His-SefA and His-SefA-His proteins.
- Cleave the N-terminus His-tag from the His-SefA-His protein to produce SefA-His.
- Culture *T. selenatis* anaerobically in the presence of either sodium selenate or potassium nitrate and extract the soluble cell extracts from both samples.
- Investigate protein-protein interactions between His-SefA and His-SefA-His and soluble proteins in cell extracts from *T. selenatis* grown in the two growth conditions using pull-down experiments.
- Investigate protein-protein interactions between SefA-His and soluble proteins in cell extracts from *T. selenatis* grown in the two different conditions using pull-down experiments.
- Isolate proteins from the soluble cell extracts of *T. selenatis* that interacted with SefA-His on a nickel affinity column and identify them using MALDI-MS.

3.2 Preparation of purified His-SefA and His-SefA-His proteins and the soluble cell extracts from *T. selenatis* grown in the presence of sodium selenate or potassium nitrate

Purified samples of both His-SefA-His and His-SefA were required in order to investigate protein-protein interactions between SefA and *T. selenatis* soluble proteins from cell extracts. The two samples of *E. coli* expressing the His-SefA and His-SefA-His proteins were cultured in LB broth, kanamycin, and chloramphenicol overnight at 37 ºC with agitation. Fresh LB broth was then inoculated with the overnight culture and incubated at 37 ºC with agitation until the optical density was 0.4, at which point the cultures were refrigerated for 30 minutes. IPTG was added, and the cultures were incubated overnight at 20 ºC with agitation. The cells were then isolated by centrifugation, resuspended and lysed using a sonicator, before being clarified. The His-SefA-His and His-SefA

proteins were then purified using two consecutive nickel affinity columns. The nickel column was equilibrated with Buffer A' which has a low imidazole concentration. Half of the protein sample was then added into the nickel column before the nickel column was agitated for 20 minutes and the sample was run through. This was repeated with the second half of the protein sample. The nickel column was then washed with Buffer A' to remove contaminating proteins, before the purified protein was eluted in Buffer B, which has a high imidazole concentration, in 20 samples of 1 ml fractions. After the first nickel affinity columns the SefA proteins were not pure and so a second nickel column purification step was employed. The resulting purified proteins after both the first and second nickel affinity columns were then analysed using SDS-PAGE (Figures 3.2 and 3.3).

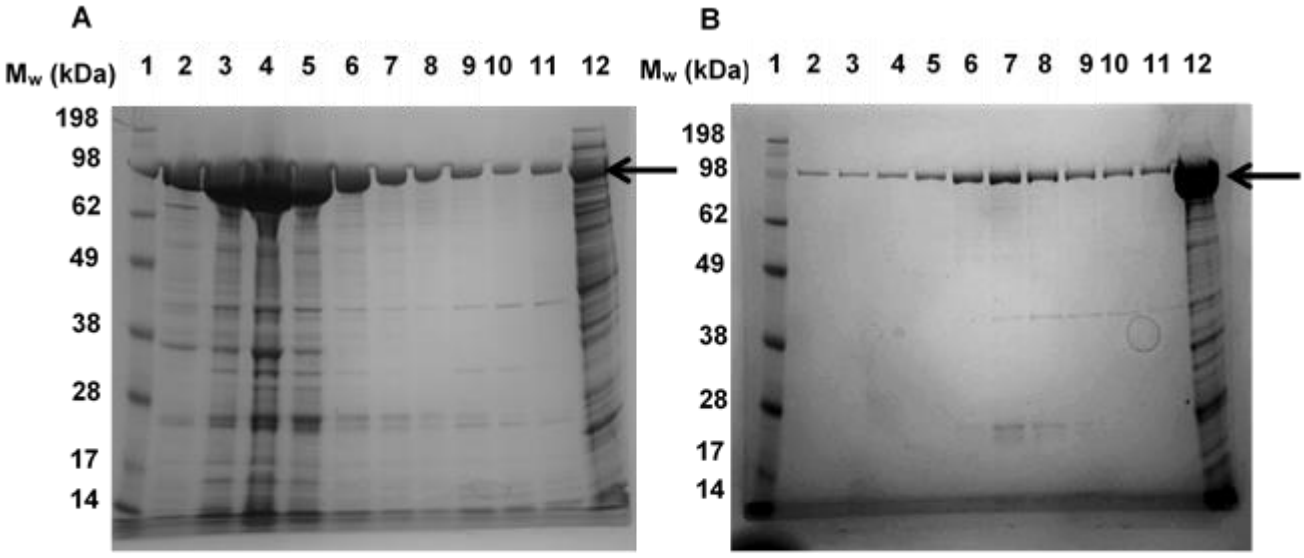

Figure 3.2: SDS-PAGE analysis of fractions eluted from the two nickel affinity columns containing purified His-SefA protein. A: Lane 1: Pre-stained Protein Marker, Lanes 2-11: Fractions 1, 3, 5, 7, 9, 11, 13, 15, 17, 19 all containing His-SefA, Lane 12: sample flow through, B: Lane 1: Pre-stained Protein Marker, Lanes 2-11: Fractions 1, 2, 3, 4, 5, 6, 7, 8, 9, 10 all containing purified His-SefA, Lane 12: sample flow through. Arrows on both images indicate the His-SefA protein.

Figure 3.2(A) shows the His-SefA after the first nickel column purification. Lanes 2-11 show odd numbered fractions between 1-19 eluted from the nickel column and all show clearly the presence of the His-SefA protein at ~94.5 kDa with the most concentrated protein found in lanes 3, 4, and 5. Contaminating proteins can also be seen at ~43 kDa, ~37 kDa, and at ~26 kDa. The SDS-PAGE analysis of the elution from the second nickel column can be seen in Figure 3.2 (B). The His-SefA protein can be seen at ~94.5 kDa in Figure 3.2 (B) with the protein contaminants from the first nickel column almost removed and a substantially pure His-SefA protein remaining. The protein at ~43 kDa can be seen in a lower concentration still in Figure 3.2 (B) in lanes 7-11 and the protein at ~26 kDa can still be seen in lanes 7 and 8 and therefore only fractions 1-5 were used in further experiments to ensure contaminants did not affect results.

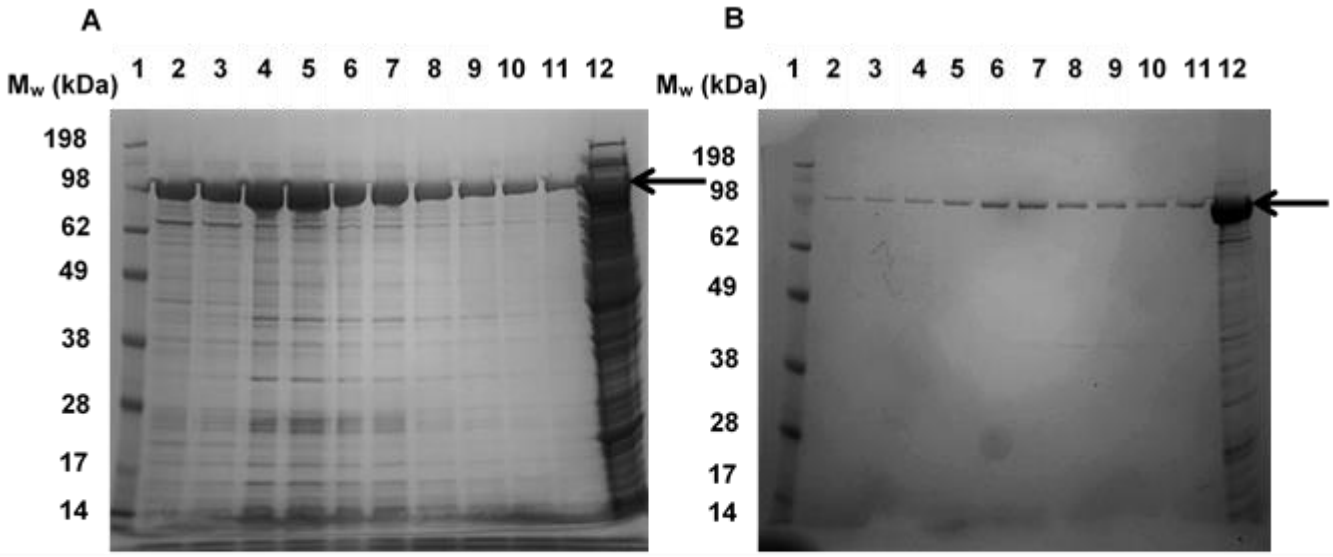

Figure 3.3: SDS-PAGE analysis of fractions eluted from the two nickel affinity columns containing purified His-SefA-His protein. A: Lane 1: Pre-stained Protein Marker, Lanes 2-11: Fractions 1, 3, 5, 7, 9, 11, 13, 15, 17, 19 all containing His-SefA-His, Lane 12: sample flow through, B: Lane 1: Pre-stained Protein Marker, Lanes 2-11: Fractions 1, 2, 3, 4, 5, 6, 7, 8, 9, 10 all containing purified His-SefA-His, Lane 12: sample flow through. Arrows on both images indicate the His-SefA-His protein.

Figure 3.3 (A) shows the SDS-PAGE analysis following the nickel column to purify the twin His-tagged protein, His-SefA-His. The SefA protein can again be seen at ~94.5 kDa in each of the fractions analysed which were odd numbered fractions between 1-19, in lanes 2-11. Contaminating proteins can be seen at ~69 kDa, ~43 kDa, ~37 kDa, ~26 kDa, ~18 kDa, and ~16 kDa and so a second nickel column was carried out to remove these contaminating proteins from the sample. Figure 3.3 (B) shows the SDS-PAGE analysis of the elution from the second nickel column to purify His-SefA-His. The His-SefA-His protein can be seen at ~94.5 kDa with no contaminating proteins present.

After purified His-SefA-His and His-SefA protein were obtained, two *T. selenatis* samples were cultured anaerobically in the presence of either sodium selenate or potassium nitrate. Hungates media was added to hungates vitamins, SL8 trace elements, sodium acetate, $MgCl_2.6H_2O$ (1000x) and $CaCl_2.H_2O$ (1000x) and either sodium selenate or potassium nitrate, and de-oxygenated by flowing nitrogen through the media. *T. selenatis* glycerol stock was then added to each of the two cultures and the *T. selenatis* was cultured for 4 days anaerobically at 30 ºC. *T. selenatis* was again subcultured and grown for another 4 days in the two fresh media mixtures. After 4 rounds of subculturing the *T. selenatis* cells were isolated using centrifugation and lysed using sonification and the soluble cell extracts were retained.

3.3 Investigating protein-protein interactions between His-SefA and His-SefA-His and soluble proteins in cell extracts from *T. selenatis* grown in the presence of sodium selenate

Investigating interactions between the N-terminal of SefA and soluble cell extracts from *T. selenatis* was the main aim of this chapter of work. However, probing interactions between the C-terminal of SefA as well as SefA which has His-tags at both the C and N-terminal was also investigated. Each nickel column was equilibrated with Buffer A'. Purified SefA protein samples were then added, agitated for 20 mins and run through the column. The agitation of the SefA samples was to ensure the nickel column was first 'fully charged' by the binding of either the His-SefA-His or the His-SefA protein. The binding of the His-SefA-His or the His-SefA protein to the nickel column resulted in SefA bound with only the internal regions or C-terminal region exposed respectively. For both samples the N-terminal should not be exposed. The column was washed with Buffer A' and then the soluble cell extracts from *T. selenatis* grown with sodium selenate were added. Each column was then washed again with Buffer A' and the SefA proteins together with any interacting proteins were eluted in Buffer B.

The following samples were analysed by SDS-PAGE; the purified His-SefA-His and His-SefA proteins, *T. selenatis* soluble cell extracts, the His-SefA-His and His-SefA flow through from the column, the first Buffer A' washes, the *T. selenatis* soluble cell extracts flow through from the column, the second nickel column washes, and the final eluted proteins. Figure 3.4 shows the SDS-PAGE analysis for the elutions from the nickel column investigating the interaction between His-SefA and the soluble cell extracts from *T. Selenatis*. Lane 8 shows a very low amount of His-SefA was present in the elution as only a faint band at ~94.5 kDa can be seen. No other proteins can be seen in the elution. Figure 3.5 shows the SDS-PAGE analysis for the elutions from the nickel column investigating the interaction between His-SefA-His and the soluble cell extracts from *T. selenatis*. The His-SefA-His protein at ~94.5 kDa can be seen in the elution from the nickel column (lane 8) but no other proteins have been eluted with it. Whilst there is a distinct SefA band at ~94.5 kDa, it is not as

concentrated as the initial His-SefA-His sample that was added to the column, suggesting some of the sample was lost (as can be seen in the flow through and wash in lanes 5 and 6).

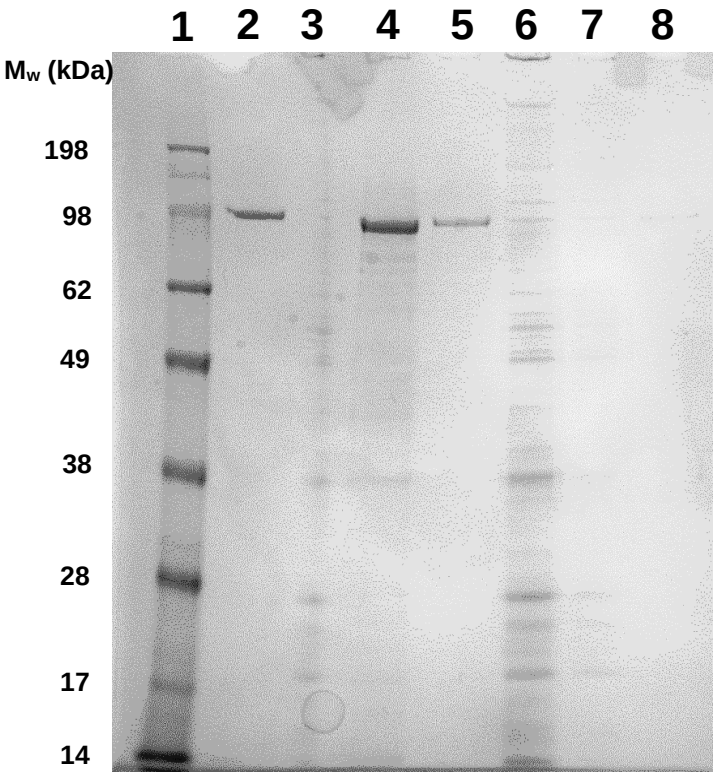

Figure 3.4: SDS-PAGE analysis identifying protein interactions between His-SefA and proteins in soluble cell extracts from *T. selenatis* grown in the presence of sodium selenate. Lane 1: Pre-stained Protien Marker, Lane 2: Purified His-SefA, Lane 3: *T. selenatis* soluble cell extracts (not completely run), Lane 4: Nickel column flow through, Lane 5: Nickel column wash, Lane 6: *T. selenatis* soluble cell extracts flow through, Lane 7: Nickel column wash, Lane 8: Elution of His-SefA and interacting proteins.

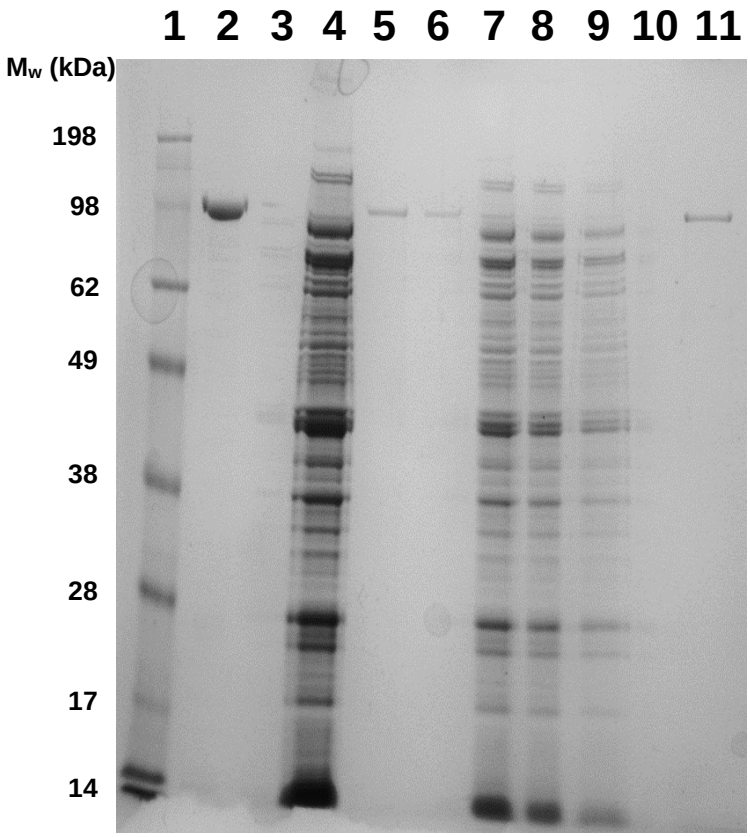

Figure 3.5: SDS-PAGE analysis identifying protein interactions between His-SefA-His and soluble proteins in cell extracts from *T. selenatis* grown in the presence of sodium selenate. Lane 1: Pre-stained Protien Marker, Lane 2: Purified His-SefA-His, Lane 4: *T. selenatis* soluble cell extracts, Lane 5: Nickel column flow through, Lane 6: Nickel column wash, Lane 7: *T. selenatis* soluble cell extracts flow through, Lane 8: Nickel column wash, Lane 9: Nickel column wash, Lane 11: Elution of His-SefA-His and interacting proteins.

3.4 Investigating protein-protein interactions between the N-terminal of SefA-His and soluble cell extracts from *T. selenatis* grown in the presence of sodium selenate or potassium nitrate

The His-SefA-His and His-SefA forms of the SefA protein have been previously cloned, expressed, and purified in *E. coli* (Debieux *et al.*, 2011). However, SefA with a His-tag only at the C-terminal, leaving the N-terminal exposed has not been expressed in *E. coli*. Instead, the N-terminal His-tag on the His-SefA-His form of the protein can be cleaved using the Thrombin CleanCleave™ Kit. The purified His-SefA-His protein (see section 3.2) was exchanged into Buffer E using an Amicon Ultra centrifugation filtration unit with a 10 kDa cutoff point (Millipore) and concentrated until the protein concentration was 1 mg/ml. The N-terminal His-tag was then removed by adding the SefA protein to the thrombin-agarose gel and following the Thrombin CleanCleave™ Kit protocol. The cleavage reaction was run for 24 hours and 30 µl aliquots of the SefA sample were taken at 1, 2, 4, 6, and 24 hours during the cleavage reaction and analysed using SDS-PAGE to ensure the SefA protein remained intact (Figure 3.6). Figure 3.6 shows the SefA protein at 94.5 kDa and shows that it remained undegraded.

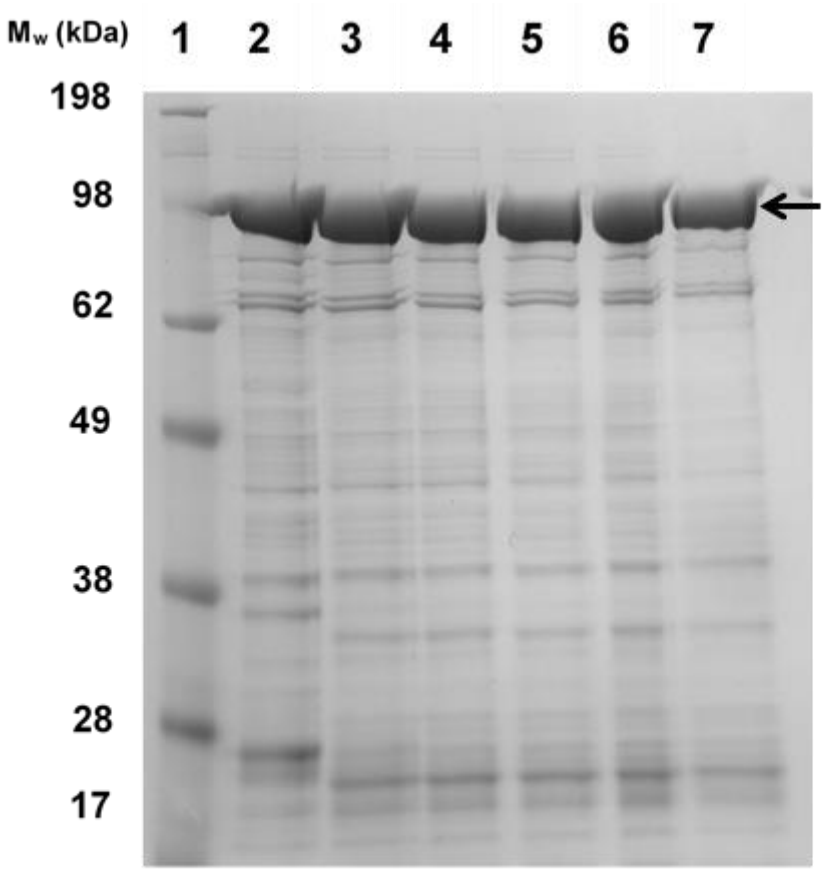

Figure 3.6: SDS-PAGE analysis of the SefA-His protein during cleavage of the N-terminal His-tag. Lane 1: Pre-stained Protein Standard, Lane 2: 0 hr, Lane 3: 1 hr, Lane 4: 2 hr, Lane 5: 4 hr, Lane 6: 22 hr, Lane 7: 24 hr. SefA-His, present in lanes 2-7, is indicated with an arrow.

SDS-PAGE cannot confirm that the N-terminal His-tag has been removed from the His-SefA-His protein. However, previous work (Dridge, 2014) following the cleavage reaction, using western blot analysis, identified the cleavage of the N-terminal His-tag from the His-SefA protein. The removal of the His-tag resulted in the disappearance of the SefA protein when probed with a His antibody, but remained detectable by Coomassie staining.The Thrombin CleanCleave^{TM} Kit cleaves a His-tag from a recombinant protein which contains the thrombin recognition sequence Leu-Val-Pro-Arg-Gly-Ser, cleaving the peptide bond between Arg and Gly. The N-terminal His-tag in His-SefA-His was identified as being able to be cleaved at the Thrombin site in the pET-33b(+) vector, and was successfully completed (Dridge, 2014). Therefore the same method was used here to cleave the N-terminal His-tag from the double His-tagged SefA protein.

Following successful cleavage of the N-terminal His-tag, protein interactions between the N-terminal of SefA-His and soluble proteins in cell extracts from *T. selenatis* were investigated. *T. selenatis* was cultured and prepared as described in section 3.3 with one culture being grown in the presence of potassium nitrate and one culture grown in the presence of sodium selenate. Two nickel columns were run, as described in section 3.3, using the SefA-His protein in both. In one nickel column experiment, protein-protein interactions with the soluble proteins in cell extracts from *T. selenatis* grown in selenate were investigated. This was to identify soluble proteins expressed during selenate respiration that might interact with the N-terminal of SefA. Control experiments using soluble cell extracts from *T. selenatis* grown under nitrate respiration conditions were also investigated. This was to identify whether proteins that interacted with the N-terminal of SefA were also expressed and interacted with SefA when selenate reduction and selenium nanosphere formation was not being carried out. If interacting proteins were expressed only when *T. selenatis* was carrying out selenate reduction, these proteins might also carry out a role specific to selenate reduction and their function and exact interaction with SefA could be further explored. Figure 3.7 shows the SDS-PAGE analysis for the SefA-His-protein interactions with soluble cell extracts taken from *T. selenatis* grown in nitrate. Pre-column samples of SefA-His protein and *T. selenatis* soluble cell proteins can be clearly seen in lanes 2 and 3. Lanes 4 and 5 show the SefA-His flow through and the Buffer A' wash. Some SefA-His protein can be seen in these lanes, suggesting that some of the SefA-His was lost before the final elution, potentially due to an excess of protein that resulted in a saturated column. Lanes 6 and 7 show proteins in the *T. selenatis* soluble cell extracts flow through and the final Buffer A' wash and no SefA-His can be seen in these lanes. The SefA-His protein can be seen in the elution from the nickel column in lane 8 as indicated with an arrow. No other clear protein bands can be seen in this sample.

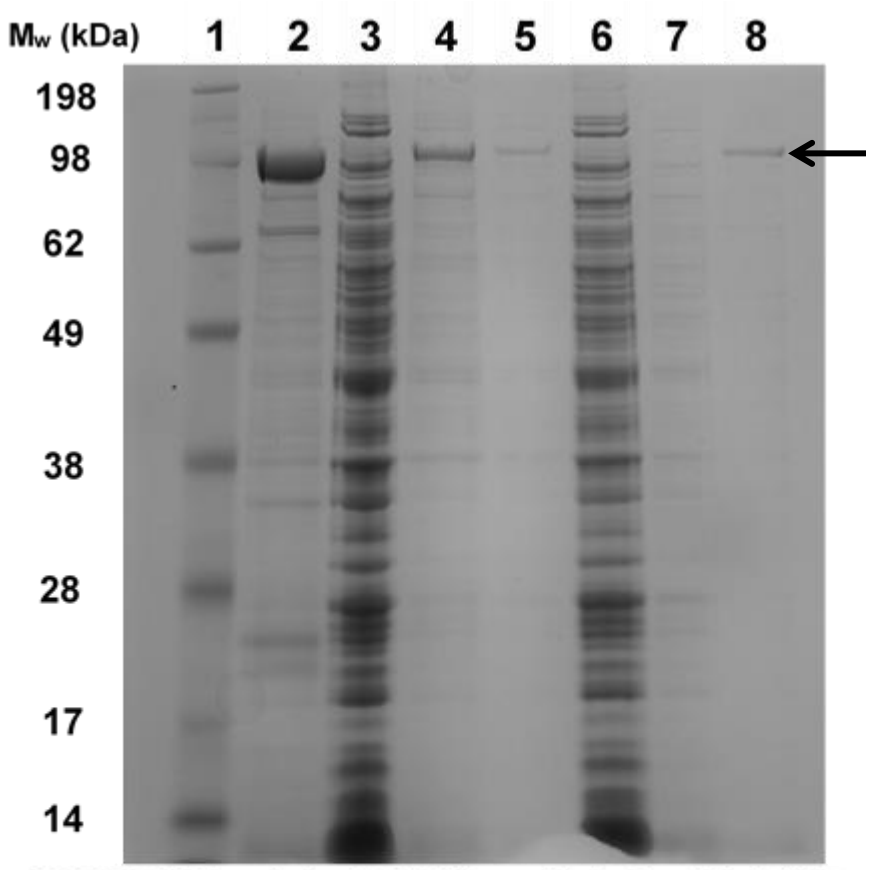

Figure 3.7: SDS-PAGE analysis of SefA-His, purified using nickel affinity chromatography, investigating protein interactions with soluble proteins in cell extracts from *T. selenatis* grown in the presence of potassium nitrate. Lane 1: Pre-stained Protein Standard, Lane 2: Purified SefA-His, Lane 3: *T. selenatis* soluble cell extracts, Lane 4: SefA-His nickel column flow through, Lane 5: Nickel column wash, Lane 6: *T. selenatis* nickel column flow through, Lane 7: *T. selenatis* nickel column wash, Lane 8: SefA-His and interacting proteins elution.

Figure 3.8 shows the SDS-PAGE analysis of SefA-His-protein interactions with soluble proteins in cell extracts taken from *T. selenatis* grown in selenate. Each lane shows the equivalent samples as in Figure 3.7. Lane 8 shows the elution from the nickel column and the SefA-His can be seen clearly, as indicated by an arrow, at ~94.5 kDa. The elution sample contains other protein. Particularly clear are two protein bands at ~66 kDa and ~60 kDa, highlighted in Figure 3.8 with arrows. This elution sample was a dilute sample as 10 ml of Buffer B was used to elute the SefA-His protein and interacting proteins. Therefore the elution sample was concentrated using an Amicon™ Ultra-10 Centrifugal Filter tube to a final volume of 1 ml. This concentrated sample was again analysed using SDS-PAGE (Figure 3.9) along with the pre-column SefA-His (lane 2), the pre-column soluble cell extracts from *T. selenatis* grown in the presence of selenate (lane 3), and the *T. selenatis* soluble cell extracts flow through (lane 4) run in adjacent wells.

The concentrated SefA-His and interacting proteins elution can be seen in lane 8 in Figure 3.9. Successful concentration of the sample can be seen with a clear SefA band at ~94.5 kDa, as well as the potentially interacting proteins. The protein bands at ~66 kDa and ~60 kDa can be seen clearly, as can a protein band at ~16.5 kDa that was not obvious in the diluted sample (Figure 3.8). These protein bands in particular have been chosen because they cannot be seen obviously in protein samples in lanes 2 or 4. If these proteins could also be seen in lane 2 it may indicate that they are contaminating proteins that originate from *E. coli*. Therefore the three proteins at ~66 kDa, ~60 kDa, and ~16.5 kDa have most likely originated from the soluble cell extracts from *T. selenatis* and are therefore soluble proteins expressed by *T. selenatis* during selenate respiration. The protein bands at ~66 kDa and ~60 kDa in the elution column in Figure 3.8 look as though they are also in the sample from the second Buffer A' wash in lane 7. In Figure 3.9 the ~66 kDa and ~60 kDa bands can be seen clearly in the elution sample but cannot be clearly identified in any of the other samples in adjacent lanes. Each protein band was removed from the gel using a scalpel, placed in an Eppendorf tube and sent for MALDI-MS analysis at the University of Bristol.

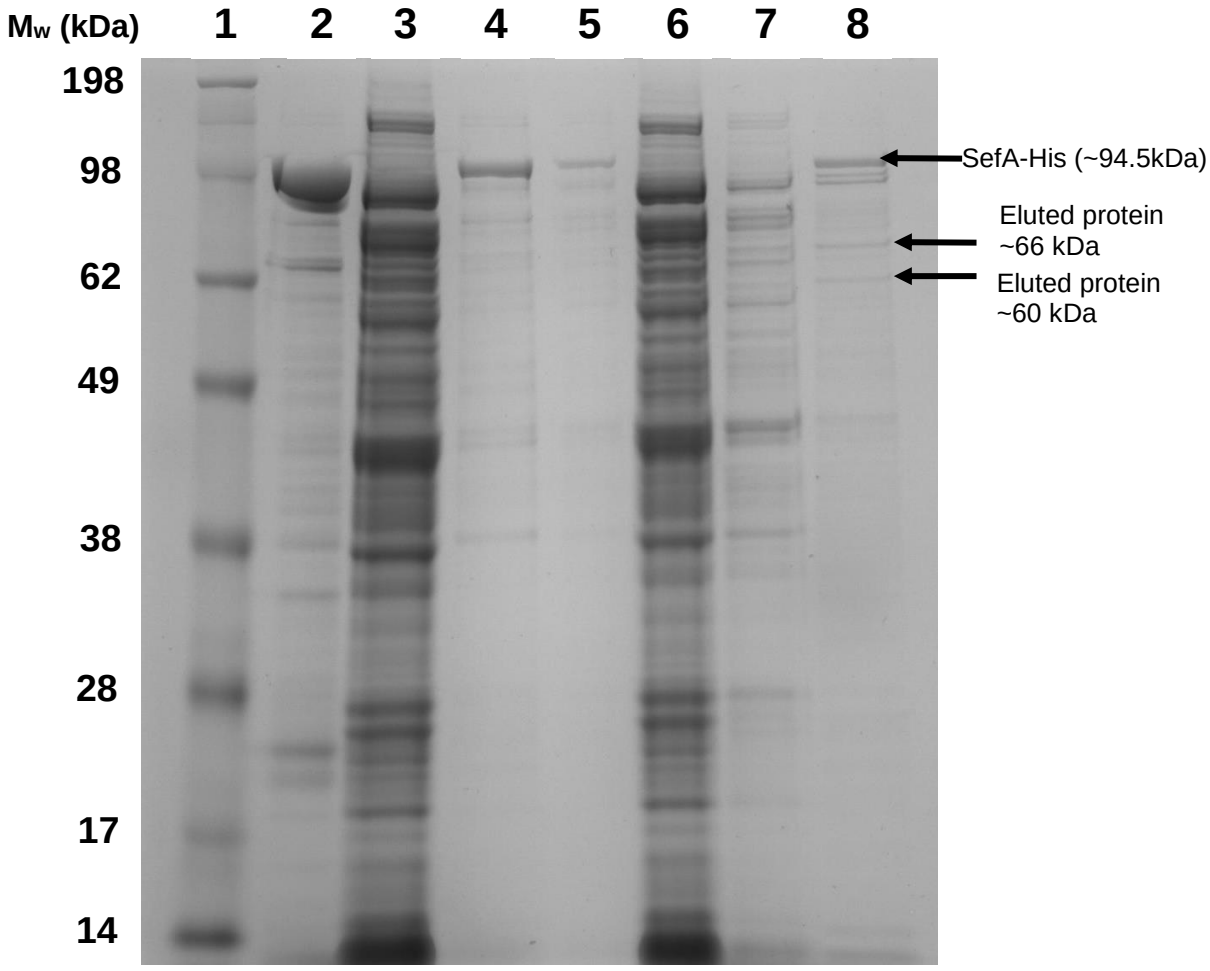

Figure 3.8: SDS-PAGE analysis of SefA-His, purified using nickel affinity chromatography, investigating protein interactions with soluble proteins in cell extracts from *T. selenatis* grown in the presence of sodium selenate. Lane 1: Pre-stained Protein Standard, Lane 2: Purified SefA-His, Lane 3: *T. selenatis* soluble cell extracts, Lane 4: SefA-His nickel column flow through, Lane 5: Nickel column wash, Lane 6: *T. selenatis* nickel column flow through, Lane 7: *T. selenatis* nickel column wash, Lane 8: SefA-His and interacting proteins elution. The SefA protein at ~94.5 kDa is indicated on the SDS-PAGE gel with an arrow.

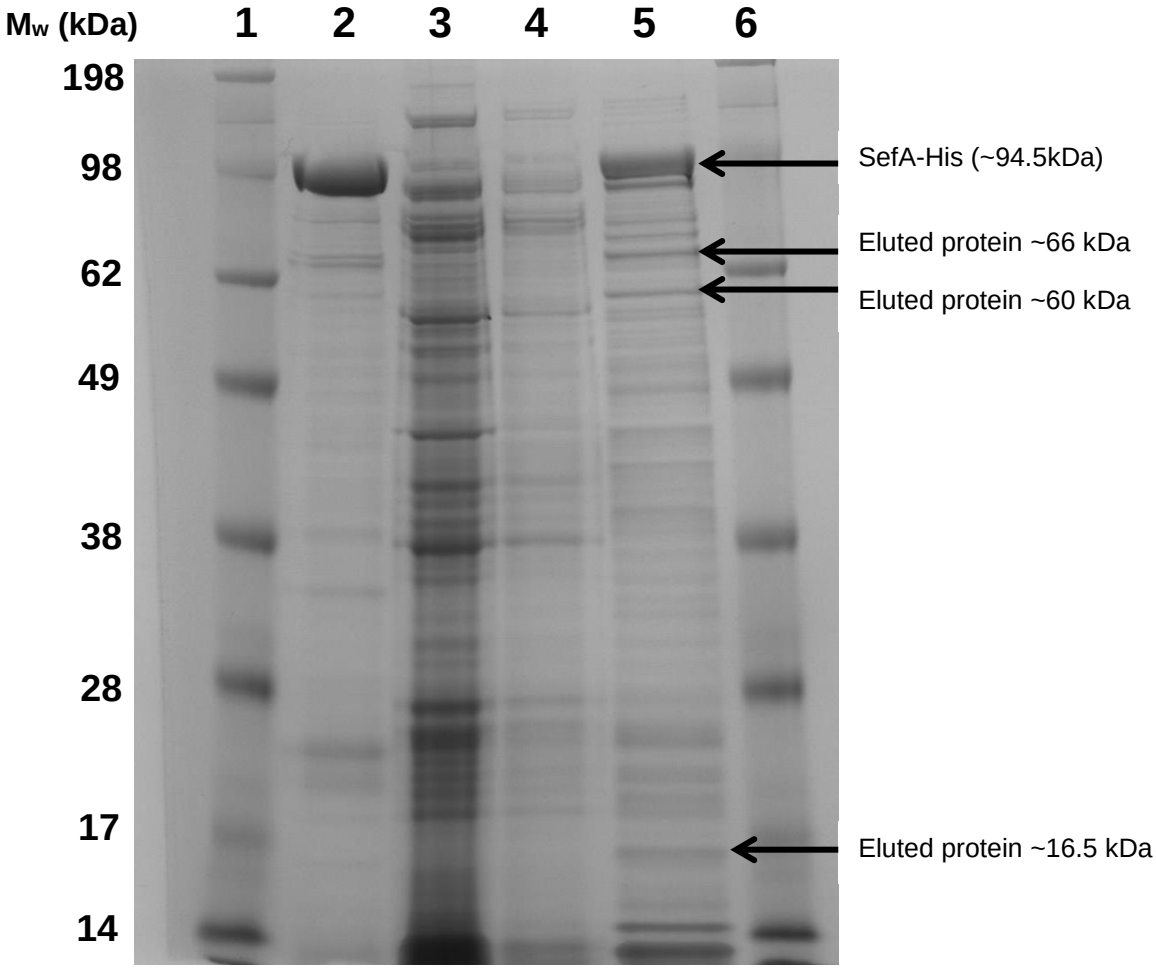

Figure 3.9: SDS-PAGE analysis of a concentrated sample of SefA-His with other eluted proteins from the nickel affinity column investigating protein interactions between SefA-His and proteins from the soluble cell extracts of *T. selenatis* grown in the presence of sodium selenate. Lane 1: Pre-stained protein standard, Lane 2: Purified SefA-His, Lane 3: *T. selenatis* soluble cell extracts, Lane 4: *T. selenatis* nickel column wash, Lane 5: Concentrated elution of SefA-His and soluble cell extracts from *T. selenatis* grown in the presence of sodium selenate, Lane 6: Pre-stained protein standard. The three bands labelled 'Eluted protein' highlighted with arrows above underwent identification using MALDI-MS.

3.5 Identification of the three proteins that potentially interact with SefA-His on a nickel affinity column, using MALDI-MS

The three protein bands extracted from the SDS-PAGE gel shown in Figure 3.9 were sent to Kate Heesom at the University of Bristol for identification using MALDI-MS. Fragments identified during MALDI-MS can be seen for the ~66 kDa protein, ~60 kDa protein, and the ~16.5 kDa protein in tables 3.1, 3.2, and 3.3 respectively. The fragments identified from the proteins isolated were analysed using NCBI's BLASTp (protein Basic Local Alignment Search Tool) using the non-redundant protein sequences (nr) database. The proteins which were identified as having the closest sequence matches to the fragments identified from the 3 proteins isolated in section 3.4 are listed for each protein in tables 3.1, 3.2, and 3.3.

Table 3.1: Protein properties and observed results for the ~66 kDa protein identified using MALDI-MS.

Protein properties	Observed results	
Estimated size of protein (kDa)	66	
Proteomic peptides identified	PVITLPDGSQRGFTQDDAH IFCTEDQVRMVYDMYSTFG FEKIEFTLYDCLDRLSASYV GEDNERHGNILEIAQRYFDE DHSNLIVGPVNKPR	
Blastp (non-redundant protein sequences) results	Threonine-tRNA ligase	
Size (kDa)	73.792	
Number of amino acids	642	
Theoretical pI	5.77	
Sequence coverage (%)	13.20	
Identity (%)	41	
Query cover (%)	64	
Matching peptides with score	M.PVITLPDGSQR.H R.GFTQDDAHIFCTEDQVR.E R.MVYDMYSTFGFEK.I K.IEFTLYDCLDR.A R.LSASYVGEDNER.Q	30.6 35.5 50.1 64.1 28.1

Table 3.2: Protein properties and observed results for the ~60 kDa protein identified using MALDI-MS.

Protein properties	Observed results	
Estimated size of protein (kDa)	60	
Proteomic peptides identified	GYDSAGLAVVDAEGHMTRRP EIESNLQYDAGDKGLDASVEH DIVHGLQALPSRIEALAEDFSD KHHALFLGR	
Blastp (non-redundant protein sequences) results	Glucosamine-fructose-6-phosphate aminotransferase	
Size (kDa)	66.60	
Number of amino acids	609	
Theoretical pI	5.61	
Sequence coverage (%)	13.60	
Identity (%)	80	
Query cover (%)	100	
Matching peptides with score	R.GYDSAGLAVVDAEGHMTR.L K.RPEIESNLQYDAGDK.G K.GLDASVEHDIVHGLQALPSR.I R.IEALAEDFSDKHHALFLGR.G	58.1 98.6 77.2 78.1

Table 3.3: Protein properties and observed results for the ~16.5 kDa protein identified using MALDI-MS.

Protein properties	Observed results	
Estimated size of protein (kDa)	16.5	
Proteomic peptides identified	GANFIAVHEMLDGFRTALVTH LDTMAERSYPLDIHTVQDHLK YAIVANDVRDEDTADMLTAASR	
Blastp (non-redundant protein sequences) results	DNA starvation/stationary phase protection protein Dps/ferritin	
Size (kDa)	18.70	
Number of amino acids	167	
Theoretical pI	5.93	
Sequence coverage (%)	38.3	
Identity (%)	63	
Query cover (%)	100	
Matching peptides with score	R.GANFIAVHEMLDGFR.T R.TALVTHLDTMAER.A K.SYPLDIHTVQDHLK.E R.YAIVANDVR.K	46.0 27.4 48.3 48.1

3.6 Discussion

His-SefA-His and His-SefA were successfully expressed and purified. *T. selenatis* cultures were grown and the soluble cell extracts were isolated. Previous work had identified that the N-terminal sequence of SefA, particularly the first 25 N-terminal residues, may be linked to the formation and exportation of selenium nanospheres as previously described in section 3.1 (Debieux *et al*., 2011). Protein-protein interactions between proteins from the soluble cell extracts from *T. selenatis* and the SefA protein which had either double His-tags or a His-tag attached to the N-terminal only were first investigated. SDS-PAGE analysis of samples taken from the nickel column investigating protein-protein interactions with His-SefA show no interacting proteins in the elution column. This suggests that no proteins from the soluble cell extracts from *T. selenatis* grown with selenate interact with SefA when the N-terminal residues are not exposed. However, the concentration of His-SefA protein present in the elution was very low as the band at ~94.5 kDa is faint. This therefore does not provide conclusive proof that proteins within the soluble cell extracts of *T. selenatis* do not interact with the C-terminal of the SefA protein and further experments with this protein would be needed. SDS-PAGE analysis of samples taken from the nickel column investigating protein-protein interactions with His-SefA-His shows a clear band in the elution sample at ~94.5 kDa, suggesting a high concentration of the SefA protein bound to the nickel column. No other protein bands can be seen in the elution lane. This suggests that the proteins from the soluble cell extracts from *T. selenatis* did not interact with the His-SefA-His protein. From this it can be hypothesised that when both the N-terminal and C-terminal of the SefA protein have a His-tag attached to them, and therefore only internal regions of SefA are exposed for interaction, no interaction occurs with soluble proteins from *T. selenatis* cells grown in the presence of sodium selenate.

Protein-protein interactions with SefA-His and soluble proteins from cell extracts from *T. selenatis* grown in the presence of selenate were investigated. The SDS-PAGE analysis of the resulting nickel column samples identified three potentially interacting proteins at ~66 kDa, ~60 kDa, and ~16.5 kDa. The

presence of these three proteins in the same elution sample as SefA-His suggests that they interacted with the SefA-His bound to the nickel column. The SefA-His protein has an exposed N-terminal and therefore these three proteins could be interacting with the N-terminal of SefA. Interactions between SefA-His and soluble proteins from *T. selenatis* grown in the presence of nitrate were also investigated and the SefA-His elution was analysed by SDS-PAGE. This experiment was run as a control to see whether soluble proteins produced when *T. selenatis* is respiring using selenate, that may interact with SefA-His, are also present and interact with SefA-His when *T. selenatis* is not respiring using selenate. No other proteins can be seen in the elution on the nitrate SDS-PAGE analysis. This indicates that the three proteins identified that are potentially interacting with the N-terminal of SefA-His under selenate conditions are either not expressed at such a high concentration when *T. selenatis* is not carrying out selenate respiration, or are altered so that they do not interact with the N-terminal of SefA-His.

The sequences for the three identified proteins received from Bristol after MALDI-MS were first mapped against the draft *T. selenatis* genome and matches to all three proteins where found with peptide hits located on nodes (15; 18; 127; 627; 726; 2106). To confirm the identity of each protein, the fragments were entered into NCBI's BLASTp. The closest hit for the ~66 kDa protein with a 41 % identity and a 64 % query cover was the threonyl-tRNA synthetase protein from the gammaproteobacterium *Enterobacter cloacae,* which is 74 kDa. Whilst there was only a 13.2 % sequence coverage between the peptide fragment analysed by MALDI-MS and the threonyl-tRNA synthetase protein, the fragments returned from the MALDI-MS investigation were not complete, so the whole protein sequence is not known. The threonyl-tRNA synthetase is an aminoacyl-tRNA synthetase that catalyses the reaction between threonine and tRNA to form threonyl-tRNA. Aminoacyl-tRNA synthetases allow peptide bonds to form between amino acids as they activate free amino acids for which peptide bond formation would otherwise be thermodynamically unfavourable. This ultimately allows translation of the nucleotide sequence into an amino acid sequence and therefore allows for protein synthesis. Threonyl-tRNA synthetase first binds ATP to threonine to

form threonyl-AMP. Next, threonyl-tRNA synthetase catalyses the reaction between threonyl-AMP and a tRNA molecule to allow for the transfer of the threonyl group to a tRNA to form threonyl-tRNA (Ibba *et al.*, 2000). The threonyl-tRNA synthetase amino-acid binding site contains a zinc ion that is used to help recognise threonine, as threonine is coordinated to the zinc ion through the side-chain hydroxyl group it contains, as well as its amino group (Berg *et al.*, 2012). Aminoacyl-tRNA synthetases bind complex tRNA molecules with a relatively low error rate helped by a kinetic proof-reading mechanism (Guth *et al.*, 2007). However, binding to the correct amino acid is more difficult and the active sites of aminoacyl-tRNA synthetases do bind to amino acids that have a similar structure to the cognate amino acid (Ling *et al.*, 2009). Threonyl-tRNA synthetase can mis-activate serine (Dock-Bregeon *et al.*, 2000). However threonyl-tRNA synthetase contains an editing site that hydrolyzes Ser-tRNA^{Thr}, which allows it to correct these binding mistakes. The editing sites and activation sites in aminoacy-tRNA synthetases act as a 'double sieve' which allows them to have high fidelity (Fersht, 1977; Schmidt *et al.*, 1994; Nureki *et al.*, 1998). Although the nature of the interaction between SefA and threonyl-tRNA synthetase is not known, interestingly, 64.3% of the primary sequence of SefA is derived from only five amino acids (16.4% Ala; 15.4% Thr; 12% Gly; 10.4% Val; 10.1% Asp) (Debieux *et al*, 2011). Given that 15.4% of the primary sequence of SefA is made up of threonine residues, there is a high requirement for Thr during protein synthesis. This could explain why the threonyl-tRNA synthestase might be upregulated during selenate respiration and therefore an excess could be binding to the SefA protein during a nickel column experiment.

The peptide fragments sequence from the ~60 kDa protein was also entered in to NCBI's BLASTp after being mapped to the *T. selenatis* draft genome, and a search within the non-redundant protein sequences database was carried out. The closest hit with an 80 % identity and a 100 % query cover was the glucosamine-fructose-6-phosphate protein again from *E.* cloacae which is 66.60 kDa. The sequence coverage for this protein compared to the fragments was 13.6 %. This protein is the catalyst for the formation of glucosamine 6-phosphate from glutamine and fructose-6-phosphate. This process is the rate limiting step and the initial reaction in the hexosamine biosynthetic pathway.

The hexosamine biosynthetic pathway is responsible for the formation of the precursors for macromolecules that contain amino sugars. The final product of the hexosamine biosynthetic pathway is UDP-N-acetlyglucosamine (UDP-GlcNAc). The formation of UDP-GlcNAc from fructose-6-phosphate is a conserved pathway in bacteria, as well as lower and higher eukaryotes (Kato *et al.*, 2002). UDP-GlcNAc is then used to form glycoproteins, proteoglycans and glycolipids. These processes involve the metabolisation of UDP-GlcNAc by glycosyltransferases. UDP-GlcNAc is also a donor substrate for O-GlcNAc transferase. Addition to intracellular proteins of O-GlcNAc to serine or threonine residues is catalysed by this transferase. O-GlcNAcylation is a key process able to control protein stability, localisation, and many other functions within the cell (Bond *et al.*, 2015; Hart *et al*., 2007). The exact interaction that might be occurring between SefA and glucosamine-fructose-6-phosphate aminotransferase is unknown. SefA is very rich in threonine residues however, and as the glucosamine-fructose-6 phosphate aminotransferase is involved in a pathway whose product is a donor substrate for a catalyst implicated in addition of threonine residues to proteins, threonine could be involved in the interaction here. Also SefA and glucosamine-fructose-6-phosphate aminotransferase could be targets for the transfer of threonine residues by O-GlcNAc transferase, and the transfer of threonine residues could provide stability for SefA and potentially help with transport of the SefA protein across the cell membrane and out of the cell.

After being mapped to the *T. selenatis* draft genome, the peptide fragments sequence from the ~16.5 kDa protein was entered in to NCBI's BLASTp and the closest hit with a 63 % identity and a 100 % query cover was found to be the 18.7 kDa DNA starvation/stationary phase protection protein Dps again from *E. cloacae*. The sequence coverage for this protein was 38.3 %. Dps proteins in *E. coli* have been studied extensively. The *E. coli* Dps protein is formed from 12 identical subunits and overall has a shell-like structure. A spherical hollow cavity is produced from the subunit assembly and this is the iron storage compartment and has a diameter of ~40-50 A^{o}(Zhao *et al.,* 2002; Haikarainen *et al.*, 2010). *E. coli* Dps is very stable once it has been assembled and has the N-terminus of each of its momomers extending out from the dodecamer. These N-termini are

very lysine-rich and are flexible (Haikarainen *et al.*, 2010). The Dps protein when bound to DNA is very stable but shows no apparent sequence specificity when binding to DNA (Almiron *et al*., 1992). When DNA is added to Dps protein, aggregation occurs and then crystals form (Wolf *et al.,* 1999). This co-crystallisation allows DNA to be protected against environmental assaults. Dps protein surfaces in *E. coli* are dominated by negative charges and therefore negatively charged DNA molecules are not thought to directly bind Dps. Instead the self-aggregation of Dps forms a crystal lattice containing three dodecamers and holes that are lined with the protruding lysine-rich N-termini with which DNA interacts (Grant *et al*., 1998). Dps has the ability to oxidise ferrous ions, which are bound to the protein, to the ferric state (Nair *et al.,* 2004). Dps has twelve catalytic ferroxidase sites which are thought to be bimetallic, containing a high-affinity and a low-affinity binding site (Ilari *et al.,* 2002; Zhao *et al.,* 2002). These ferroxidase sites catalyse H_2O_2-mediated oxidation of ferrous ions to form a ferrihydrite mineral core, saturated with Fe^{3+}. As H_2O_2 is reduced during this process, this also prevents hydroxyl radical formation that would damage macromolecules, as the Dps protein traps hydroxyl radicals within the protein shell (Velayudhan *et al.,* 2007; Zhao *et al*., 2002; Bellapadrona *et al*., 2010). This is unusual, as in other ferritins O_2 is used most efficiently to oxidise ferrous ions, and is thought to be why Dps is described as a ‘ferritin-like’ protein. It has been suggested that the main role of Dps proteins in *E. coli* is actually not to act as an iron storage molecule but to act as a form of protection for macromolecules from the harmful combination of ferrous ions and H_2O_2. Dps has a number of regulatory elements (Calhoun *et al.*, 2010). However, expression of the Dps protein is induced by the redox-sensitive OxyR during the exponential growth phase. OxyR regulates genes involved in hydrogen peroxide stress and therefore Dps transcription is induced by OxyR in response to hydrogen peroxide exposure during exponential growth (Altuvia *et al.,* 1994; Tartaglia *et al*., 1989; Storz *et al*., 1990). Dps has been found to be one of the most overexpressed proteins during stress and has been found to protect *E. coli* from multiple stresses including copper and iron toxicity, thermal stress, oxidative stress, and extreme acidic and alkaline conditions (Choi *et al*., 2000; Nair *et al.*, 2004; Yu *et al.,* 2009).

Why would the Dps protein interact with SefA? SefA is thought to coat the selenium particles produced during selenate respiration and potentially act to stabilise the selenium deposits and help in the assembly of selenium nanospheres (Debieux *et al*., 2011). Ferritins contain iron storage compartments and Dps proteins from *E. coli* store a ferrihydrite mineral core, the formation of which is catalysed by its ferroxidase sites, formed from ferrous ions (Nair *et al.*, 2004). Recombinant purified SefA expressed in *E. coli* has previously been shown to stabilise selenium nanospheres when selenite is reduced by glutathione (Debieux *et al*., 2011). It is interesting that SefA may interact with Dps due to SefA also being thought to be involved with metal binding and stabilisation. SefA may have a similar stabilising function with selenium as Dps has with iron, and SefA, like Dps, may have a spherical hollow cavity which is self-assembled, forming a cage-like protein, where elemental selenium readily binds. The Dps protein is upregulated by OxyR during the exponential phase in response to oxidative stress (Altuvia *et al.,* 1994; Tartaglia *et al*., 1989; Storz *et al*., 1990). Selenate respiration results in the formation of superoxide anions and causes oxidative stress. Superoxide anions are produced during selenite reduction when GSH reacts with selenite to form GS-Se-SG (Butler *et al*., 2012). Superoxide anions result in the damage of DNA indirectly due to their damaging effect on dehydratase clusters causing iron to be released (Liochev *et al*., 1994). This stress to the cell would result in increased transcription of the Dps protein and as Dps is one of the most overexpressed proteins during stress, a high concentration of the Dps protein may have been present in the *T. selenatis* soluble cell extracts used in nickel column experiments (Choi *et al*., 2000). It seems that the Dps protein, as well as the other two isolated proteins, were likely interacting with the N-terminal of SefA because the proteins were not seen in elution samples where His-SefA-His and His-SefA proteins were used. However, the elution samples from the other two nickel columns using His-SefA-His and His-SefA were not concentrated and therefore the three isolated proteins could still have been present and therefore could still interact with internal regions of SefA. The interaction between SefA and Dps could also be due to charge. The theoretical pI of the Dps protein is 5.93 and the theoretical pI of SefA is 3.65. The pH of the nickel column will be higher than both protein's pI values with buffers ranging

from pH7 – pH8.5. Therefore, the protein surfaces will be predominantly negatively charged in this environment. However, as the pI values for these two proteins differ by 2.28, SefA would be more negatively charged than the Dps protein. The three proteins isolated all have similar pI values of 5.77, 5.61, and 5.93, suggesting that these three proteins could have a charged surface containing a charged component that is favourable for interaction with the N-terminal of SefA.

4 Optimisation of the stability of the His-SefA-His protein and crystallisation trails

4.1 Introduction

Having investigated protein-protein interactions between SefA and proteins in the soluble cell fractions of *T.selenatis*, the stability and oligomeric state of the His-SefA-His protein was investigated and crystallisation trials were performed with the aim of resolving the crystal structure of the His-SefA-His protein. Understanding more about the structure of the His-SefA-His protein would help to identify possible areas of interaction between the SefA protein and selenium nanospheres, and how the SefA protein may facilitate the assembly of these selenium nanospheres. This would also allow a more detailed hypothesis to be formed regarding the mechanism by which the SefA protein and the selenium nanospheres are exported out of the *T. selenatis* cell. Previous work (Dridge, 2014) attempted to crystallise His-SefA-His with a JCSG screen being used in initial crystallisation trials. Three rhombus-shaped crystals of 1.6 mm in size were successfully grown in 0.1 M CAPS buffer (pH 10.5), 1 M NaBr, 40% MPD. However, the crystals did not diffract and therefore the crystal structure could not be obtained. In these experiments, a wider range of conditions were used as well as varying concentrations of protein to try to optimise the conditions, to grow crystals that successfully diffract. Whilst the His-tags attached to the SefA protein may have an effect on the structure of SefA as well as its ability to crystallise, a crystal structure of the His-SefA-His protein will still provide key information about how the protein may interact with the selenium nanospheres.

4.1.1 Aims and Objectives

- Express and purify the recombinant His-SefA-His protein.
- Identify the oligomeric state of the His-SefA-His protein using analytical gel filtration.
- Attempt to crystallise the His-SefA-His protein.
- Investigate stabilisation of the His-SefA-His protein using differential scanning fluorimetry.

4.2 The expression and purification of His-SefA-His to homogeneity

The His-SefA-His protein was overexpressed in *E. coli* BL21 CodonPlus (DE3) – RIPL cells. The *E. coli* was cultured in LB broth with antibiotics and incubated overnight at 37 ºC with agitation. Four separate flasks of fresh LB broth (four cultures worth of cells were used in order to obtain a high concentration of the His-SefA-His protein to be used in crystallisation trials) were then inoculated with the overnight culture and incubated at 37 ºC with agitation until the optical density was 0.4, at which point the cultures were refrigerated for 30 minutes. IPTG was added, and the cultures were incubated overnight at 20 ºC with agitation. The cells were then isolated by centrifugation, resuspended and lysed using a sonicator, before being clarified. The His-SefA-His protein was then purified from each of the four cultures using a nickel affinity column. The His-SefA-His protein was then purified to homogeneity using a gel filtration column and the protein was eluted in 25 mM Tris-HCl pH 7.0, 100 mM NaCl (Figure 4.1). The eluent from the gel filtration column was collected into 55 separate 2 ml fractions, starting at 25.13 ml, and these fractions were labelled; A1 - A12, B1 - B12, C1 - C12, D1 - D12, E1 - E7. The labels correspond to the following elution volumes; A1 - A12 (25.13 ml – 49.13 ml), B1 - B12 (49.13 ml – 73.13 ml), C1 - C12 (73.13 ml – 97.13 ml), D1 – D12 (97.13 ml – 121.13 ml), and E1 – E7 (121.13 ml – 135.13 ml). The fractions found to contain His-SefA-His protein have been indicated on Figure 4.1 with the location of the highest His-SefA-His concentration indicated with arrows. The fractions predicted to contain the

purified protein were visualised on an SDS-PAGE gel (Figure 4.2). Figure 4.2 shows that the His-SefA-His protein was present in samples run in lanes 2-9 of the gel with the highest concentration seen in samples in lanes 3 - 7. Fractions A9 - A11 and B1 - B4 were then pooled and used in further experiments.

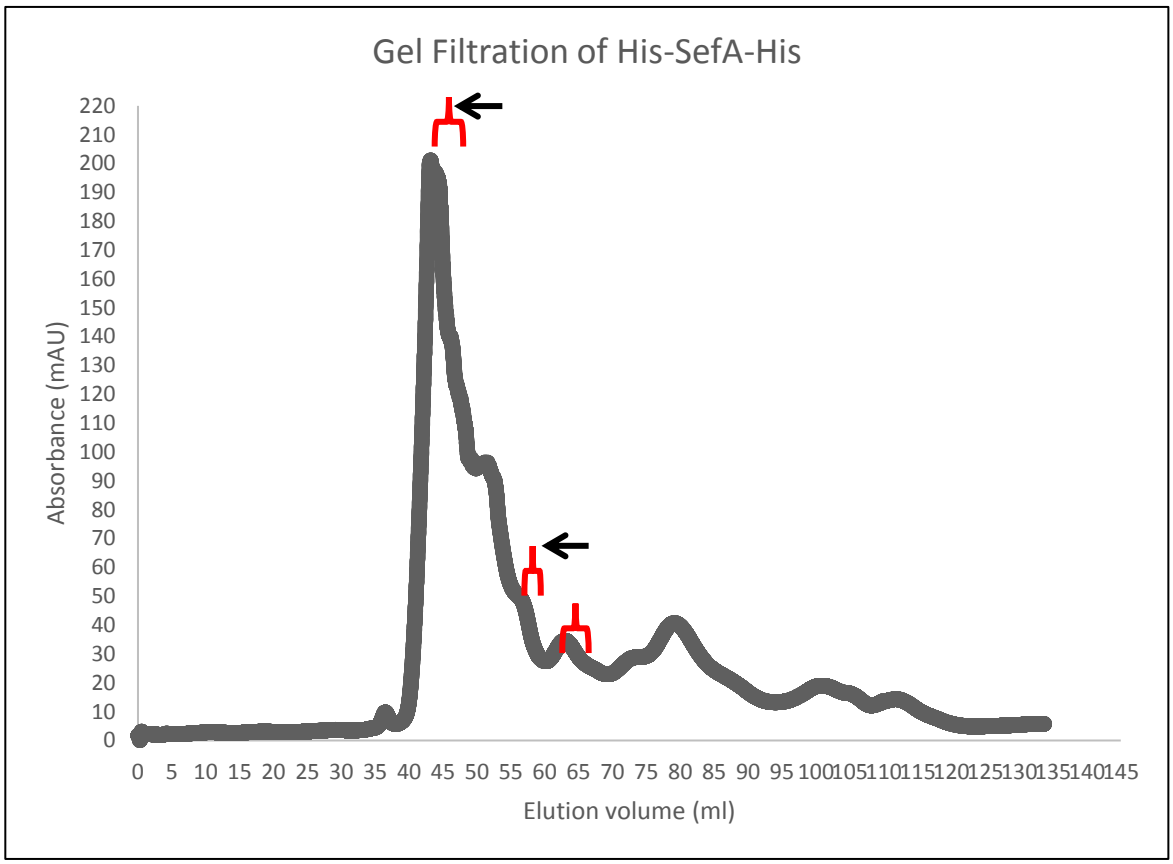

Figure 4.1: Gel filtration elution profile of the His-SefA-His protein. Fractions taken for SDS-PAGE analysis were eluted at: 41.13 – 53.13 ml, 55.13 – 57.13 ml, 61.13 – 63.13 ml, 79.13 – 81.13 ml, 99.13 – 101.13 ml, and 111.13 – 113.13 ml. Fractions in which His-SefA-His is present have been indicated on the graph with red indicators. Arrows indicate where the highest concentration of His-SefA-His was found.

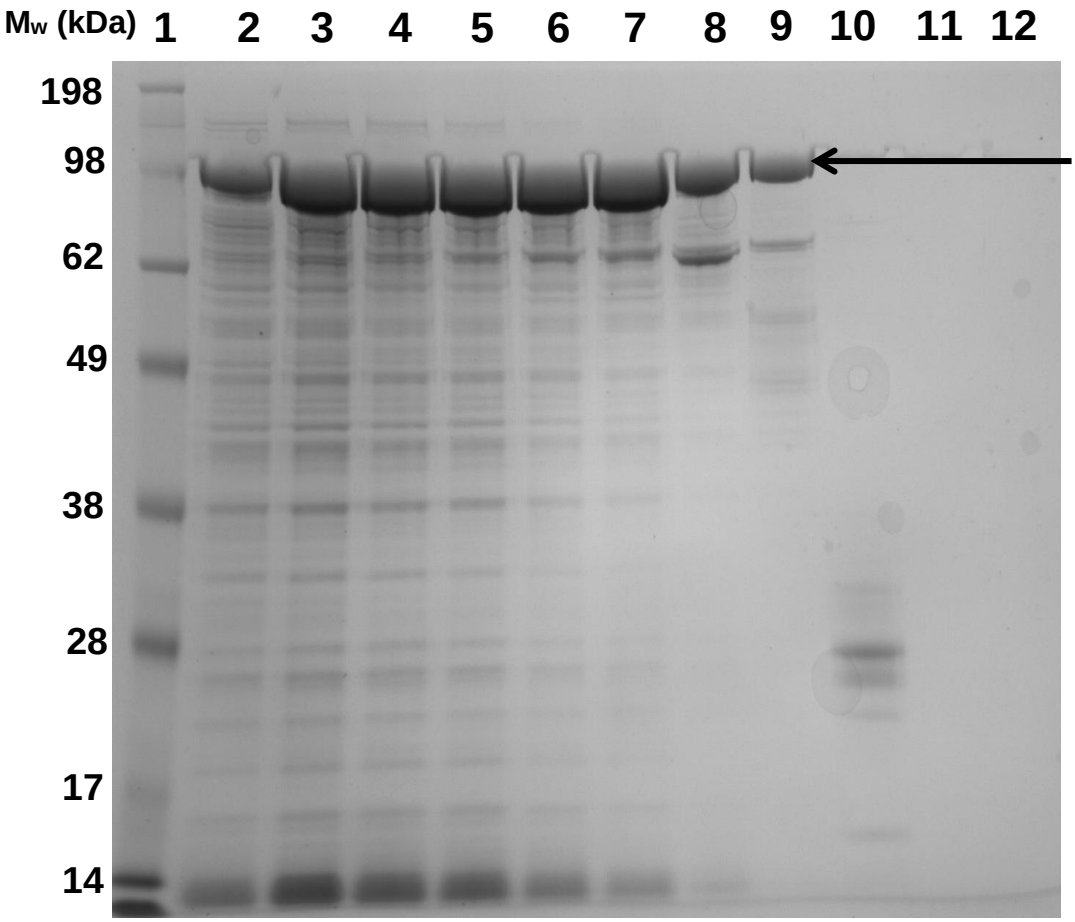

Figure 4.2: SDS-PAGE analysis of fractions taken from the gel filtration purification of the His-SefA-His protein. Lane 1: Pre-stained Protein Marker, Lane 2: Fraction A9, Lane 3: Fraction A10, Lane 4: Fraction A11, Lane 5: Fraction A12, Lane 6: Fraction B1, Lane 7: Fraction B2, Lane 8: Fraction B4, Lane 9: Fraction B7, Lane 10: Fraction C4, Lane 11: Fraction D2, Lane 12: Fraction D8. The His-SefA-His protein is indicated with an arrow.

4.3 Identification of the oligomeric state of the His-SefA-His protein

The oligomeric state of the His-SefA-His protein was investigated using analytical gel filtration. The purified His-SefA-His protein was eluted in 10 mM Hepes, pH 7.0, 0.5 M NaCl (Figure 4.3). The point of elution of the His-SefA-His protein was determined to be at 11.07 ml (shown with an arrow on Figure 4.3) and the presence of the His-SefA-His protein was confirmed using an SDS-PAGE gel (Figure 4.4). The elution volumes of a series of proteins with known molecular weights and oligomeric states (carbonic anhydrase, albumin, alcohol dehydrogenase, apoferritin, thyroglobulin, and dextran) were determined using the same conditions as the His-SefA-His analytical gel filtration. The log of the molecular weight of the known proteins was plotted against their elution volumes in these conditions. The His-SefA-His elution volume of 11.07 was interpolated onto the graph of these known proteins (Figure 4.5) in order to find the log of the molecular weight of the His-SefA-His protein in it's oligomeric state. The log of the molecular weight of the His-SefA-His protein is 5.574 and therefore the antilog of this is 374973. This is equivalent to 375 kDa. SefA has a molecular weight of 94.5 kDa and therefore 375 kDa divided by 94.5 gives 3.97 which can be rounded to 4. Therefore from this experiment it can be concluded that the SefA protein's oligomeric state is a tetramer.

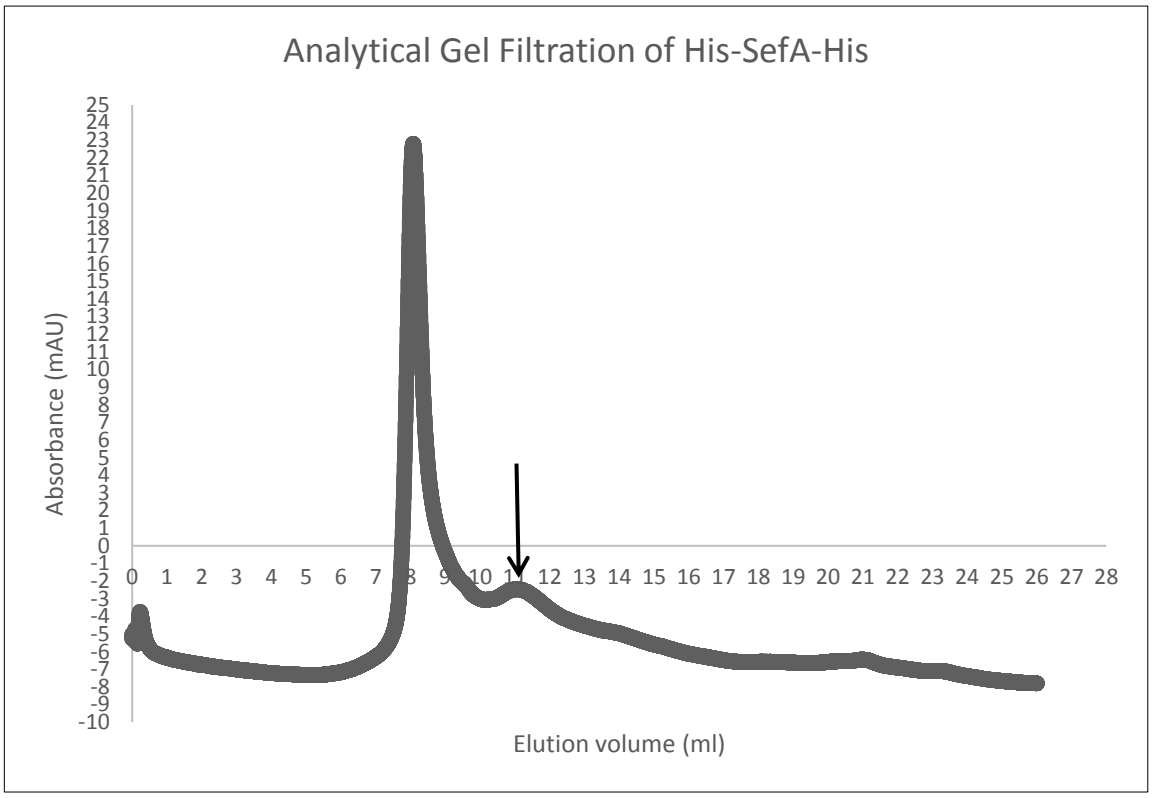

Figure 4.3: Analytical gel filtration elution profile of His-SefA-His. An arrow indicates the point of elution of the His-SefA-His protein, at 11.07 ml.

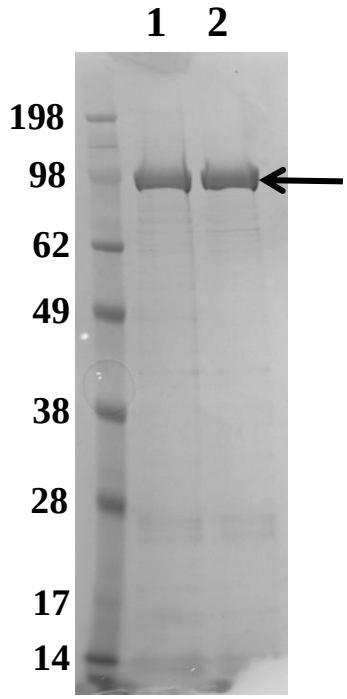

Figure 4.4: SDS-PAGE gel showing the presence of the His-SefA-His protein in the analytical gel filtration fraction eluted at 11.07 ml. Lane 1: Pre-stained protein marker, Lane 2: Elution at 11.07 ml sample 1, Lane 3: Elution at 11.07 ml sample 2. The His-SefA-His protein is indicated with an arrow.

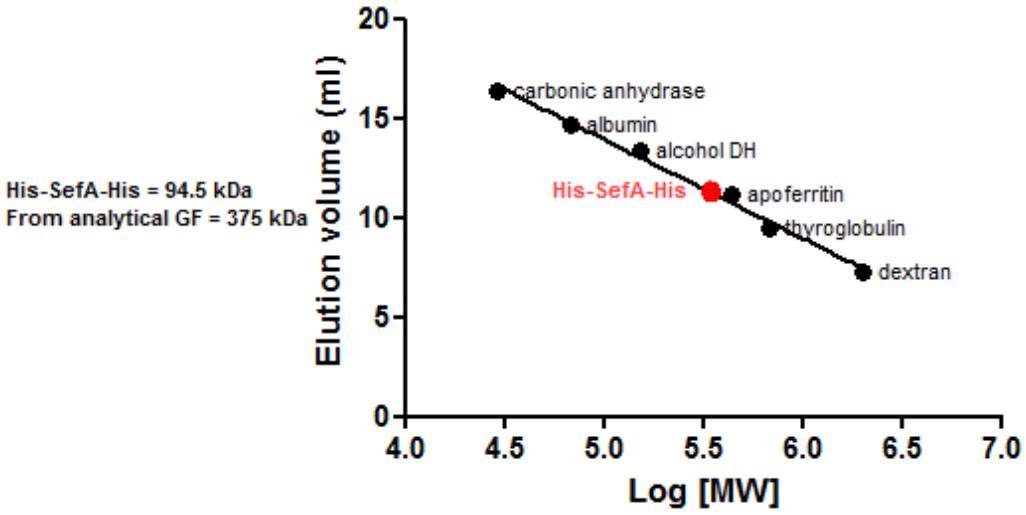

Figure 4.5: Graph to show the linear regression of the elution volume of the standard proteins used, against the log of their molecular weight. The position of the His-SefA-His protein on the line of best fit according to the volume at which it was eluted is shown on the graph in red. The protein has a log[MW] value of 5.574.

4.4 Crystallisation trials for the His-SefA-His protein

Crystallisation trials were undertaken for the His-SefA-His protein using a JCSG-plus screen, a Morpheus screen, and an SG1 screen. Three rounds of crystallisation trials were attempted with increasing protein concentration (determined using the Nanodrop 2000c UV-Vis spectrophotometer (A_{280})) used in the final drop for the microbatch screening. The first set of trials were carried out using 14.652 mg/ml of His-SefA-His protein, the second set using 17.323 mg/ml, and a protein concentration of 19.399 mg/ml was used for the third set of crystallisation trials. To reach a concentration of 19.399 mg/ml, 8 l of *E. coli* expressing the His-SefA-His protein was grown and the protein prepared as described in section 4.2. The duration of each trial was 31 days with observations of the plates taken each day. In all experiments no crystals were seen and a representative image of a well in the final set of trials was captured (Figure 4.6).

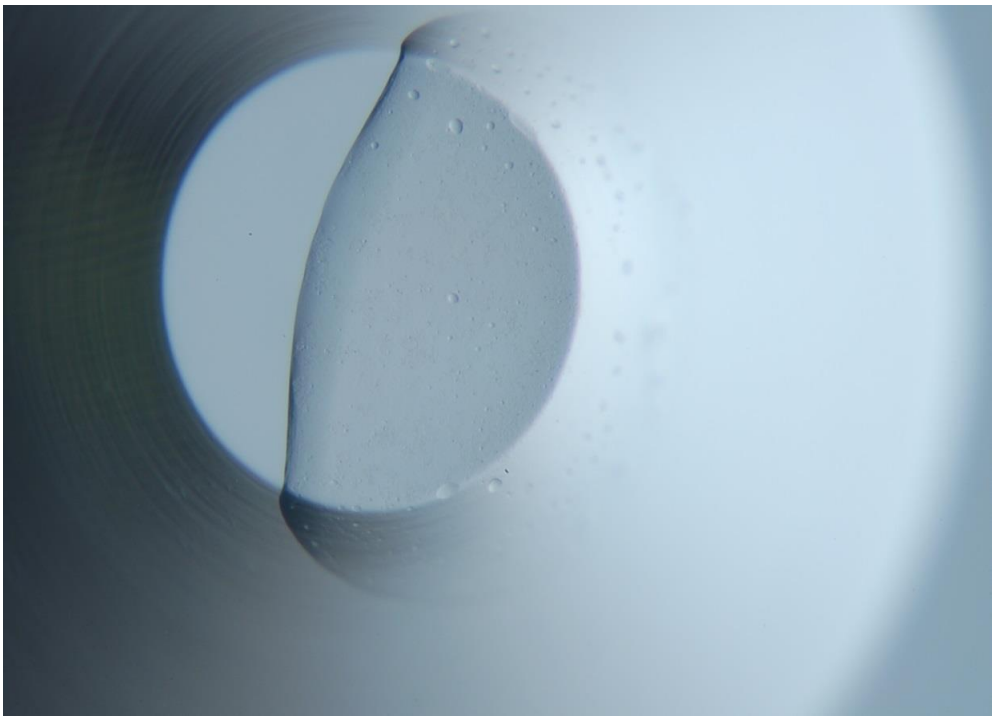

Figure 4.6: An image of a well in a Morpheus crystallisation trial plate in the final attempt to crystallise His-SefA-His, representative of the result of all crystallisation trials of the His-SefA-His protein. No crystals grown.

4.5 Investigating the stability of the His-SefA-His protein using differential scanning fluorimetry

The stability of the purified His-SefA-His protein in the presence of 24 buffers was analysed using differential scanning fluorimetry. Differential scanning fluorimetry quantifies the change in thermal denaturation temperature of a protein under varying conditions, in this case, varying buffer types. This is due to hydrophobic parts of the protein being exposed and binding dye with which it is mixed, upon melting or unfolding of the protein due to heat being applied. This increase in fluoresence can then be detected by a PCR machine. Thermostable proteins are useful, as protein crystallisation is generally more successful for proteins with a higher melting point (Dupeux *et al.*, 2011). A set of 24 buffer conditions were used (see appendix A5.) in duplicate and a concentration of 7.63 mg/ml of the purified His-SefA-His protein was used. Figure 4.7 shows graphs of the buffer types, that showed stabilisation, against mean Tm D (Figure 4.7 A.) and Tm B (Figure 4.7 B.). The Protein Thermal Shift^{TM} software (Life Technologies) calculates the Tm D and the Tm B. Tm D is the melting point calculated from the dFluorescence (derivative method) and the derivative Tm values are taken from the top of the peak in the derivative plot (also produced by the Protein Thermal Shift^{TM} software). Tm B is the melting point calculated from each fluorescence profile (Boltzmann method) and boltzmann Tm values are taken from the inflection point of the fluorescence plot (Protein Thermal Shift^{TM} software). Both graphs (Figure 4.7 A and B) demonstrate that buffer 3 which contained 400 mM CHES-NaOH, pH 9.5, and 600 mM NaCl was the most thermostabilising buffer for the His-SefA-His protein. The maximum Tm D value, which was reached when His-SefA-His was in buffer 3, was 62.8 ºC, and the maximum Tm B value, also when His-SefA-His was in buffer 3, was 62.7 ºC.

A.

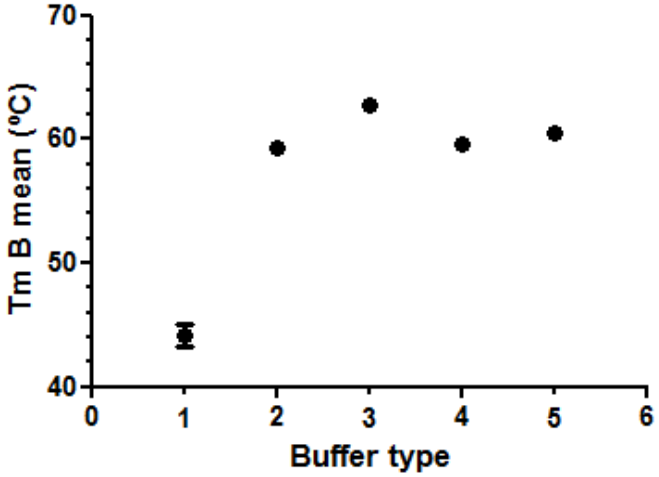

B.

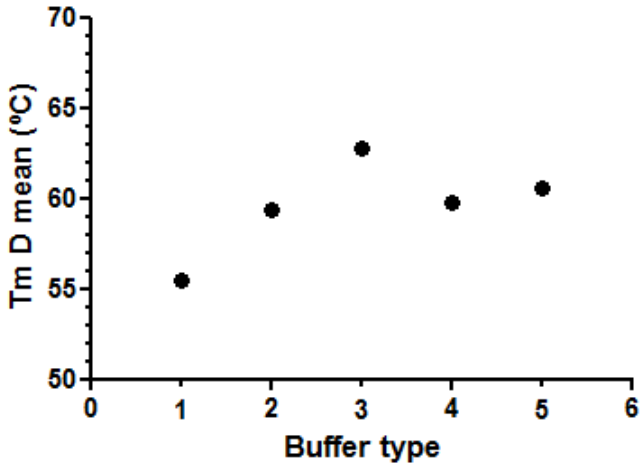

Figure 4.7: Thermostabilising buffers identified during differential scanning fluorimetry. A. Tm B mean values with standard deviation plotted for the 5 stabilising buffers. B. Tm D mean values with standard deviation plotted for the 5 stabilising buffers. Buffer compositions relating to the buffer numbers on both A. and B. graphs: 1. 400mM pyridine/ HCl & 600mM NaCl, 2. 400mM MES/ NaOH pH6 & 600mM NaCl, 3. 400mM CHES-NaOH pH9.5 & 600mM NaCl, 4. 400mM BIS-TRIS/ HCl pH6 HCl & 600mM NaCl, 5. 400mM imidazole/ HCl pH7 & 600mM NaCl.

4.6 Discussion

Purification of the His-SefA-His protein to homogeneity was achieved using gel filtration followed by analytical gel filtration. The analytical gel filtration experiment allowed the oligomeric state of the His-SefA-His protein to be established using a set of standard proteins by plotting the linear regression of the elution volume of the standard proteins used against the log of their molecular weight. From these data, a molecular weight of 375 kDa for the His-SefA-His oligomeric form was established, therefore suggesting that His-SefA-His forms a tetramer. It has been suggested that SefA may cap selenium in a similar way to the ligand stabilising interaction thought to occur between BSA and quantum dots. This stabilisation is thought to allow the selenium functional groups to interact with water and therefore sterically avoid aggregation of selenium. Therefore if SefA caps selenium deposits in a similar way to BSA, it could provide essential stabilisation for the formation of the ~150 nm nanospheres that are exported form the *T. selenatis* cell (Bücking *et al*., 2010; Butler *et al.*, 2012). The SefA protein used here has His-tags attached to the C- and N-terminals which could affect the surface charge of the SefA-Selenium nanocage. However, the addition of a His-tag is unlikely to affect the SefA protein itself and SefA may still be a tetramer within the *T. selenatis* cell. If this is the case then SefA may aid in the assembly of the selenium nanospheres by interacting with the Selenium deposits as a tetramer.

Crystallisation trials for the His-SefA-His protein proved unsuccessful. Despite varying the concentration of the His-SefA-His protein and using three different screens, no crystals were grown. SefA has some sequence similarity to S-layer proteins (Debieux *et al*., 2011). S-layer proteins are usually T1SS substrates and have a distinctive glycine-rich GGXGXDXXX motif that is located generally in the C-terminal part of the protein. This glycine-rich motif ususally binds calcium ions and is implicated in the rapid and stable folding of the proteins after secretion (Baumann *et al*., 1993; Delepelaire, 2004). The His-SefA-His protein was overexpressed in *E. coli* and no additional source of calcium ions was added and so this lack of calcium ions could have resulted in the His-SefA-His protein not being able to fold properly and therefore not forming crystals. As

SefA has been shown to stabilise selenium nanospheres *in vitro* and no selenium was present at any stage in the preparation of the His-SefA-His for crystallisation, this could also have had an effect on the stabilisation and folding of the SefA protein. It may be that SefA requires selenium to form a stable protein structure. Difficulty in growing 3D crystals that can be used for X-ray crystallography is common among S-layer proteins due to their tendency to spontaneously form 2D crystals *in vitro*. Previous groups have used a 'divide and conquer' approach that involved crystallizing recombinant or proteolytically derived fragments of S-layer proteins (Fagan *et al*., 2014). Perhaps this would be a method to use in future work relating to the identification of the crystal structure of SefA.

Differential scanning fluorimetry was used to analyse the stability of the His-SefA-His protein in the presence of a set of 24 different buffers (see appendix A5.). 5 out of the 24 buffers tested produced fluorescence signals that were analysed by the Protein Thermal Shift^{TM} software to give mean melting temperatures. However, one particular buffer (buffer 3) which consisted of: 400 mM CHES-NaOH, pH 9.5, and 600 mM NaCl, was found to be the most stabilising when the melting temperature was calculated using both the derivative method and the Boltzmann method. The maximum melting temperature was the melting temperature calculated using the derivative method and was 62.8 ºC. This is similar to the SerABC enzyme from *T. selenatis* which was found to be stable and active with incubation temperatures of up to 60 ºC to the nearest 10 ºC, and an optimum activity of the enzyme was recorded at 65 ºC (Dridge *et al*., 2010). The buffer found to stabilise His-SefA-His (buffer 3) could be used in future crystallisation trials with varying concentrations of the SefA protein in order to optimise conditions for crystal growth. The other 4 buffers that gave a Tm result could also undergo crystallisation trials with varying concentrations of SefA protein even though they showed less stabilising effects. The thermal stabilisation of SefA could also be analysed when the protein is in the presence of differing pH solutions. Both differential scanning fluorimetry thermostabilising buffer graphs show an increase in melting temperature with an increase in pH. This may not be due to pH but analysing the stability of SefA in different pH solutions may provide

further information about optimal conditions for SefA crystallisation. Optimising buffer conditions may allow for increased stability of the SefA structure, as well as prevent aggregation of the protein and therefore result in the growth of His-SefA-His crystals that could successfully diffract, allowing for the SefA crystal structure to be identified.

Further optimisation of the methods used to grow the *E. coli* and express the His-SefA-His protein could also be explored in future work. The concentration of IPTG added to the *E. coli* could be lowered and the bacteria could be subsequently incubated at a lower temperature. This would allow for slower expression of the His-SefA-His protein and help prevent the formation of inclusion bodies and aggregation of the SefA protein. This may result in an increased concentration and quality of SefA protein isolated for use in crystallisation trials. Also the *E. coli* culture could be refrigerated overnight after expression of the SefA protein has occurred and before the protein is isolated and purified. This may help with protein folding and therefore provide a more stable SefA structure for crystallisation. Autoinduction media could also be used to grow *E. coli* and express SefA (potentially the Overnight Express™ Autoinduction System 1 from Novagen). Addition of the autoinduction system to glucose-free LB media can result in higher cell densities and higher yields of soluble overexpressed protein. (Grabski, 2003)

5 A transcriptome analysis of *T. selenatis* grown in the presence and absence of sodium selenite

5.1 Introduction

Mechanisms and reductases involved in selenate reduction in multiple bacteria have been studied, with *T. selenatis* being the most extensively studied. However, mechanisms and reductases involved in selenite reduction have not been as extensively studied. Bacterial selenite reduction is broadly separated into detoxification and anerobic respiration (Nancharaiah *et al.,* 2015). Only a small number of selenite-respiring bacteria have been isolated (Stolz *et al.,* 2006) an example being *Shewanella oneidensis* MR-1 (Li *et al*., 2014). Selenite detoxification is carried out by a number of bacteria including *T. selenatis*, *E. cloacae* SLD1a-1, and *Rhodospirillium rubrum* (Butler *et al.,* 2012*;* Kessi *et al*., 2004; Losi *et al*., 1997). Selenite reduction in *T. selenatis* is thought to be mediated by the reduced thiol, glutathione. The reduction of selenite to elemental selenium, mediated by GSH, occurs as follows:

$6GSH + 3SeO_3^{2-} \rightarrow 3GS\text{-}Se\text{-}SG + 3O_2^{-} + 3H_2O$
$GS\text{-}Se\text{-}Sg + NADPH \rightarrow GSH + GS\text{-}Se^{-} + NADP^{+}$
$GS\text{-}Se^{-} + H^{+} \rightarrow GSH + Se^{0}$ (Nancharaiah *et al*., 2015)

In this chapter, a transcriptome analysis of *T. selenatis* was carried out and gene expression was compared when the bacteria were grown aerobically with and without selenite. A comparison of the upregulated and downregulated genes when selenite is present in the growth medium was made and protein products of these genes investigated. Identifying genes upregulated during selenite reduction could allow for further insight into the proteins that *T. selenatis* uses to deal with selenite detoxification. Analysing upregulated proteins may also highlight proteins that interact with elemental selenium particles in a similar way to SefA, aiding in the assembly of nanospheres. The regulation of the three proteins identified in chapter 1 as interacting with SefA was also investigated.

5.1.1 Aims and Objectives

- Quantify *T. selenatis* cell density over a 12 hour period and identify the late-exponential growth phase when *T. selenatis* is grown aerobically in the presence or absence of sodium selenite (10 mM).
- Extract total RNA from *T.* selenatis cells, and analyse the quality and concentration of the RNA extracted.
- Sequence mRNA to identify differences in mRNA expression between *T. selenatis* grown in the presence and absence of selenite.
- Isolate a pure sample of *T. selenatis* in order to extract genomic DNA from *T. selenatis* for sequencing.

5.2 *T. selenatis* growth and cell density determination

In order to ensure a high concentration of high quality mRNA can be purified and used in the sequencing of the transcriptome, bacteria should be harvested in the late-exponential growth phase. The RNeasy® Mini Kit (used to extract total RNA from *T. selenatis*) also required a maximum number of 1 x 10^9 bacteria be used in the RNeasy® Mini spin column and therefore the *T. selenatis* bacterial cell density needed to be established relative to the optical density of the culture. *T. selenatis* was grown aerobically on LB media in two different conditions; one culture was grown with sodium selenite (10 mM) added and one culture was grown without sodium selenite. An initial overnight *T. selenatis* culture was grown in LB media and then 3 fresh pure LB media solutions or 3 LB media solutions with sodium selenite (10 mM) added were inoculated with the overnight culture. The cultures were incubated and monitored over a 12 hour period, with optical density being quantified every hour from 0 hours using a Tecan Infinite Pro M200 plate reader at a wavelength of 600 nm. The average value for the optical density for each of the two growth conditions was then plotted against time (Figures 5.1 and 5.2). Both Figure 5.1 and 5.2 show that the the late-exponential growth phase, for *T. selenatis* grown with and without selenite, is reached at approximately 5 hours. Therefore total

RNA extraction, using the RNeasy® Mini spin kit, from *T. selenatis* samples was carried out after 5 hours of growth.

The number of *T. selenatis* cells in a sample relative to optical density measured was required in order to not exceed 1 x 10^9 cells in a sample added to the RNeasy® Mini spin column. Therefore *T. selenatis* was grown as described in section 2.1.3 and samples were taken at 5 hours, the optical density was measured, and a serial dilution was carried out followed by plating of the dilution samples, as described in 2.7.1. It was identified that for *T. selenatis* grown with sodium selenite present and diluted to 10^{-7}, an optical density of 0.7 resulted in the growth of 9.3 bacterial colonies on average. Therefore, in an original 10 µl sample there would be 9.3 x 10^7 cells. It was found that for *T. selenatis* grown without sodium selenite present and diluted to 10^{-7}, an optical density of 1.0 resulted in the growth of 14.6 bacterial colonies on average. Therefore in a original 10 µl sample, there would be 14.6 x 10^7 cells . This information was used to ensure the maximum number of *T. selenatis* cells were added to the RNeasy® Mini spin column without over-loading the column and preventing RNA extraction from successfully being carried out.

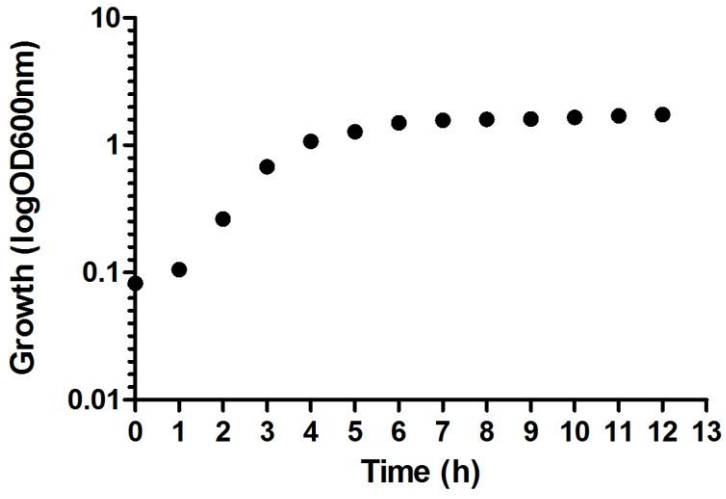

Figure 5.1: Growth curve of *T. selenatis* grown with sodium selenite (10 mM) (error bars are SEM; n = 3 cultures) over a 12 hour period.

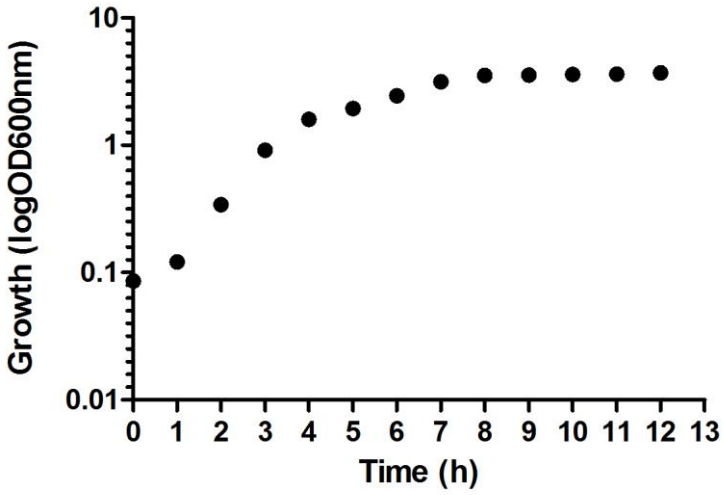

Figure 5.2: Growth curve of *T. selenatis* grown without sodium selenite (error bars are SEM; n = 3 cultures) over a 12 hour period.

5.3 RNA integrity and concentration determination and mRNA sequencing

In order to carry out a transcriptome analysis, mRNA was extracted from 6 samples of *T.* selenatis. All 6 samples were grown aerobically on LB media with 3 samples being grown in added sodium selenite (10 mM) and 3 samples being grown without sodium selenite added. Enzymatic lysis and proteinase K digestion of *T. selenatis* cells was then carried out, followed by purification of the total RNA from the bacterial lysate using the QIAGEN RNeasy® Mini Kit, with on-column DNase digestion using the QIAGEN RNase-free DNase set. The total RNA samples from each of the 6 *T. selenatis* cultures then underwent electrophoretic analysis in a chip format using an Agilent 2100 Bioanalyser to identify the RNA concentration and RNA integrity number. The RNA integrity number is the integrity of the RNA sample including whether there were any degradation products present. A score of 10 represents a perfect RNA sample without any degradation products and a score of 1 represents a completely degraded sample. Results from the electrophoretic analysis can be seen in

Table 5.1. All samples had an exceptionally high RNA integrity number as well as containing a sufficient concentration of RNA to be used for mRNA sequencing. For each total RNA sample 1µg of total RNA was used for mRNA sequencing. The following was carried out by the Exeter Sequencing Service; for each of the 6 samples, mRNA was isolated by removing the rRNA using a Ribo-Zero rRNA Removal Kit (Bacteria). ScriptSeq was then used for the library preparation before sequencing of the mRNA for each of the 6 samples was carried out.

The differential gene expression results were then organised into the top 100 upregulated and top 100 downregulated genes when the *T. selenatis* cells were grown in sodium selenite compared to being grown in the absence of sodium selenite. The top 20 upregulated and downregulated genes can be seen in Tables 5.2 and 5.3 with the log2(foldchange) for each gene, as well as the gene product. Figure 5.3 shows the principal component analysis (PCA) plot for no selenite vs selenite which demonstrates that there is a significant difference in differentially expressed genes between the treated and untreated samples. A search for each of the three proteins identified in chapter 1 was carried out to see whether they were differentially expressed accross the two growth conditions. The threonyl-tRNA synthetase and the glucosamine-fructose-6-phosphate aminotransferase proteins were not identified as being differentially expressed gene products. However, the DNA protection during starvation (Dps) protein was found to be downregulated when *T. selenatis* was grown in selenite compared to when it was not (Table 5.4). 10 differentially expressed genes producing proteins related to selenate and selenite reduction in *T. selenatis* were identified in the complete list of differentially expressed genes, and their regulation is shown in Table 5.5.

During the mapping of the reads to the *T. selenatis* genome, it was discovered that >97 % of the reads mapped to the *T. selenatis* genome but >80 % of the reads also mapped to the genome of the gammaproteobacterium *E. cloacae*. It was also discovered at this stage that the original draft *T. selenatis* AX genome was twice the size of other *Thauera* assemblies and that when running a BLAST comparison between *T. selenatis* and *E. cloacae*, 33 kilobase contigs

were 99 % identical to each other. It was therefore concluded that both the mRNA samples sequenced in this work, and the original genomic sequencing samples contained a mixture of *T. selenatis* and *E. cloacae*.

Table 5.1: Agilent 2100 Bioanalyser RNA concentration and RNA integrity number results for the 6 *T. selenatis* total RNA samples.

Sample identification	Selenite/no selenite	RNA concentration (ng/µl)	RNA integrity number
1C	Selenite	242	9.7
2C	Selenite	195	9.6
3C	No selenite	151	10
4C	No selenite	63	10
5C	Selenite	251	9.3
6C	No selenite	201	10

Table 5.2: The top 20 downregulated genes when *T. selenatis* was grown in the presence of sodium selenite compared to being grown in the absence of sodium selenite.

Top 20 downregulated genes	Log2(foldchange)	Gene	Product
1	-6.80189	arcA_4	Arginine deiminase
2	-6.00509	arcC1_1	Carbamate kinase 1
3	-5.62996	sodB_1	Superoxide dismutase [Fe]
4	-5.58864	ompW	Outer membrane protein W precursor
5	-5.15633	lsrB	Autoinducer 2-binding protein LsrB precursor
6	-4.97573	lsrA	Autoinducer 2 import ATP-binding protein LsrA
7	-4.64734	NA	hypothetical protein
8	-4.61418	tynA	Primary amine oxidase precursor
9	-4.59789	lsrG	Autoinducer 2-degrading protein LsrG
10	-4.55373	NA	C4-dicarboxylate anaerobic carrier
11	-4.38183	lsrD	Autoinducer 2 import system permease protein LsrD
12	-4.16742	NA	hypothetical protein
13	-4.14465	lsrC	Autoinducer 2 import system permease protein LsrC

Table 5.2 continued			
14	-4.13855	rpmE2	50S ribosomal protein L31 type B
15	-4.13505	NA	spherodin-like protein
16	-4.01149	murQ_2	N-acetylmuramic acid 6-phosphate etherase
17	-3.96114	aceB	Malate synthase A
18	-3.88257	NA	Helix-turn-helix domain protein
19	-3.66404	rbsB_3	D-ribose-binding periplasmic protein precursor
20	-3.66135	pyrI	Aspartate carbamoyltransferase regulatory chain

Table 5.3: The top 20 upregulated genes when *T. selenatis* was grown in the presence of sodium selenite compared to being grown in the absence of sodium selenite.

Top 20 upregulated genes	Log2(foldchange)	Gene	Product
1	6.205766	NA	Phage minor tail protein U
2	6.187741	NA	Phage-related protein
3	6.128472	NA	hypothetical protein
4	6.110264	NA	phage minor tail protein G
5	6.101268	NA	hypothetical protein
6	5.905588	NA	Lysis protein S
7	5.834782	NA	phage tail tape measure protein, lambda family
8	5.832372	clpP1	ATP-dependent Clp protease proteolytic subunit 1
9	5.780401	NA	phage portal protein, lambda family
10	5.739443	NA	Prophage minor tail protein Z (GPZ)
11	5.71813	NA	Acetyltransferase (GNAT) family protein

Table 5.3 continued			
12	5.700234	NA	Bacterial Ig-like domain (group 2)
13	5.6444	dpnA	Modification methylase DpnIIB
14	5.610584	NA	hypothetical protein
15	5.537155	NA	hypothetical protein
16	5.485729	NA	DNA-binding transcriptional regulator DicC
17	5.365116	NA	hypothetical protein
18	5.34644	rrrD_2	Lysozyme RrrD
19	5.330991	NA	Phenylacetic acid-responsive transcriptional repressor
20	5.326164	NA	Bacteriophage tail assembly protein

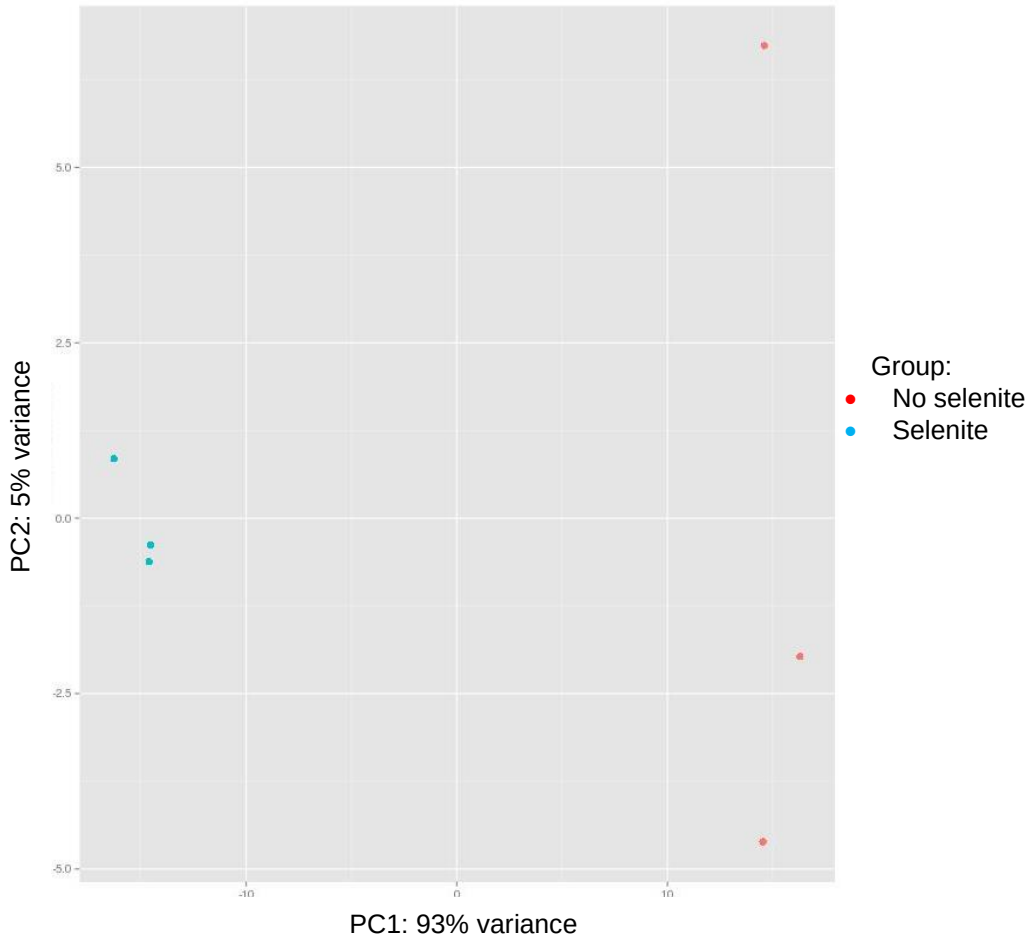

Figure 5.3: Principle component analysis (PCA) plot showing variance in differentially expressed genes in *T. selenatis* grown in no selenite compared to selenite.

Table 5.4: Regulation of the genes of the proteins identified in chapter 1 when *T. selenatis* was grown in the presence of sodium selenite compared to being grown in the absence of sodium selenite.

Protein	Regulation	Log2(foldchange)
DNA protection during starvation protein	Downregulated	-1.64157
Glucosamine-fructose-6-phosphate aminotransferase	Not differentially expressed	Not differentially expressed
Threonyl-tRNA synthetase	Not differentially expressed	Not differentially expressed

Table 5.5: Regulation of genes producing proteins related to selenate or selenite reduction in *T. selenatis*

Protein	Regulation	Log2(foldchange)
Selenate reductase SerB	Downregulated	-0.36923
Respiratory nitrate reductase 1 alpha chain narG_1	Upregulated	4.312444
Respiratory nitrate reductase 1 beta chain narH_1	Upregulated	2.957347
Redox enzyme maturation protein NarJ narj_1	Upregulated	3.318653
Respiratory nitrate reductase 1 gamma chain narI_1	Upregulated	1.738608
DMSO reductase anchor subunit dmsC_1	Upregulated	1.060354
DMSO reductase iron-sulfur subunit dmsB_1	Upregulated	0.251167
Dimethyl sulfoxide reductase DmsA precursor dmsA_2	Upregulated	0.706652
Sulfite reductase [NADPH] hemoprotein beta-component cysI	Upregulated	1.081889
Sulfite reductase [NADPH] flavoprotein alpha-component cysJ_3	Upregulated	1.47425

5.4 PCR trials to isolate a pure *T. selenatis* sample for genomic DNA extraction

After identifying that the *T. selenatis* samples contained *E. cloacae* and that the genome thought to be from *T. selenatis* was actually a mixture of both the *T. selenatis* and *E. cloacae* (or an organism very similar) genomes, attempts to isolate a pure sample of *T. selenatis* were made. If a pure sample of *T. selenatis* could be obtained, genomic DNA extraction would be carried out followed by re-sequencing of the *T. selenatis* genome. Bacteria were cultured aerobically and then bacterial dilution samples (100 µl) between 10^{-4} and 10^{-9} were streaked onto LB agar plates and incubated for 24 hours at 30 ^{o}C. Individual colonies were then picked and either resuspended in a PCR mixture directly or resuspended in PCR grade water and heated before being added to the PCR mixture. Individual colonies were treated in two different ways to see whether heating the bacterial cells and breaking them open to allow DNA to be released would result in the successful identification of a *T. selenatis* colony. PCR mixtures were prepared with different combinations of: DNA polymerases with buffers, DMSO concentrations, temperatures and run times for each stage in the PCR reaction, treatments of individual colonies before addition to the PCR mixtures, and primers. One set of primers was produced to identify *E. cloacae* colonies, as a negative control if *T. selenatis* was isolated. *T. selenatis* primers were produced using the sequences for the SefA, SerA, SerB, SerC, and SerD proteins. Two previously produced sets of primers were used (Debeiux, 2011) (Lowe, 2008) in an attempt to identify the SefA protein and SerC protein. New primers were formed with the aim of identifying the presence of the SefA, SerA, SerB, and SerD proteins. PCR products were analysed using horizontal agarose gel electrophoresis with 1 % agarose gels and visualised using UV light. *E. cloacae* colonies were identified in the PCR reactions with one gel example shown in Figure 5.4. The amplified PCR product produced using the ECLO_1 and ECLO_2 primers should be 657 bp. All 6 samples show DNA bands at ~660 bp, therefore providing a positive result for the presence of *E. cloacae* in each of the 6 colonies used in this particular PCR experiment. Despite multiple alterations to the PCR conditions, no colonies containing *T. selenatis* were identified. Multiple colonies used from the contaminated *T.*

selenatis samples did not contain *E. cloacae,* as highlighted by no DNA band being seen on agarose gels from PCR products containing the ECLO_1 and ECLO_2 primers. However, no bands were seen on any of the gels containing PCR products from PCR trials using the primers identifying the presence of SefA, SerA, SerB, SerC, or SerD. A typical example of a gel analysing PCR products from PCR reactions using *T. selenatis* primers can be seen in Figure 5.5. In this PCR experiment, primers identifying the presence of the SerC protein were used with 3 different colonies and temperature gradients for each. No DNA band was seen at 700 bp for any of the samples on the horizontal agarose gel which would have provided a positive result for the presence of SerC.

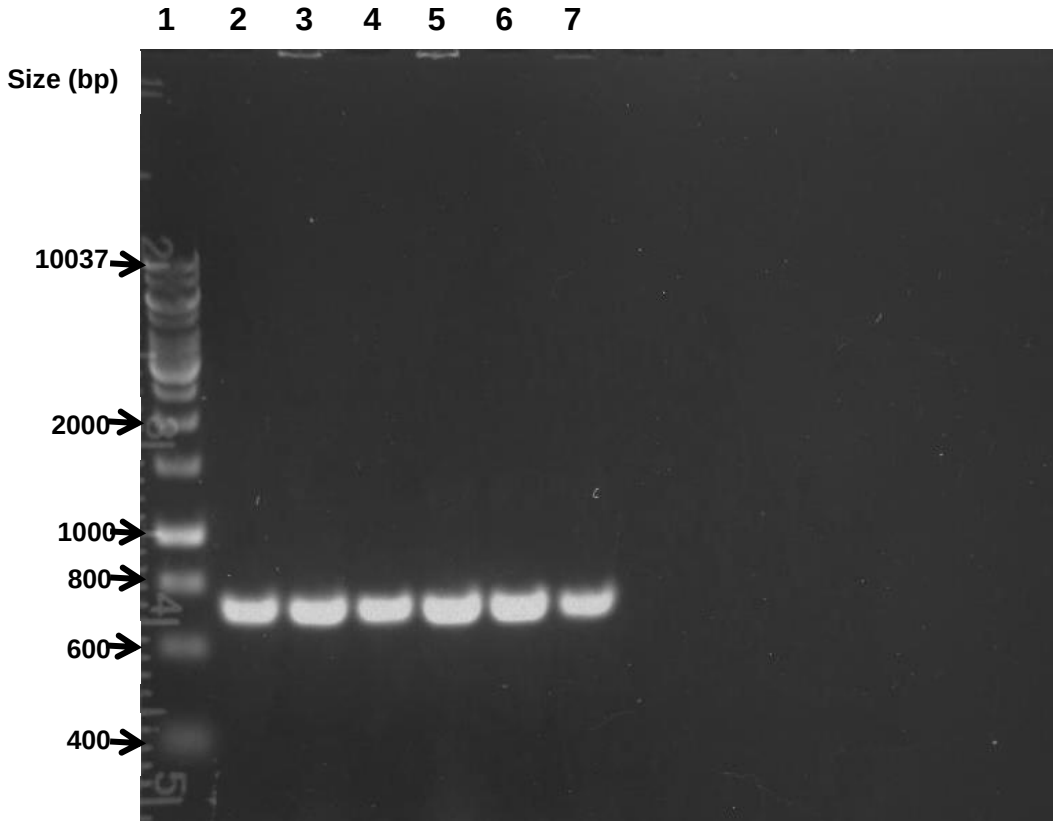

Figure 5.4: Agarose gel analysis of PCR products from 6 different colonies taken from a contaminated *T. selenatis*/*E. cloacae* culture using ECLO_1 and ECLO_2 primers. Lane 1: HyperLadder™ 1kb, Lane 2: Colony 1 with ECLO_1 and ECLO_2 primers, Lane 3: Colony 2 with ECLO_1 and ECLO_2 primers, Lane 4: Colony 3 with ECLO_1 and ECLO_2 primers, Lane 5: Colony 4 with ECLO_1 and ECLO_2 primers, Lane 6: Colony 5 with ECLO_1 and ECLO_2 primers, Lane 7: Colony 6 with ECLO_1 and ECLO_2 primers.

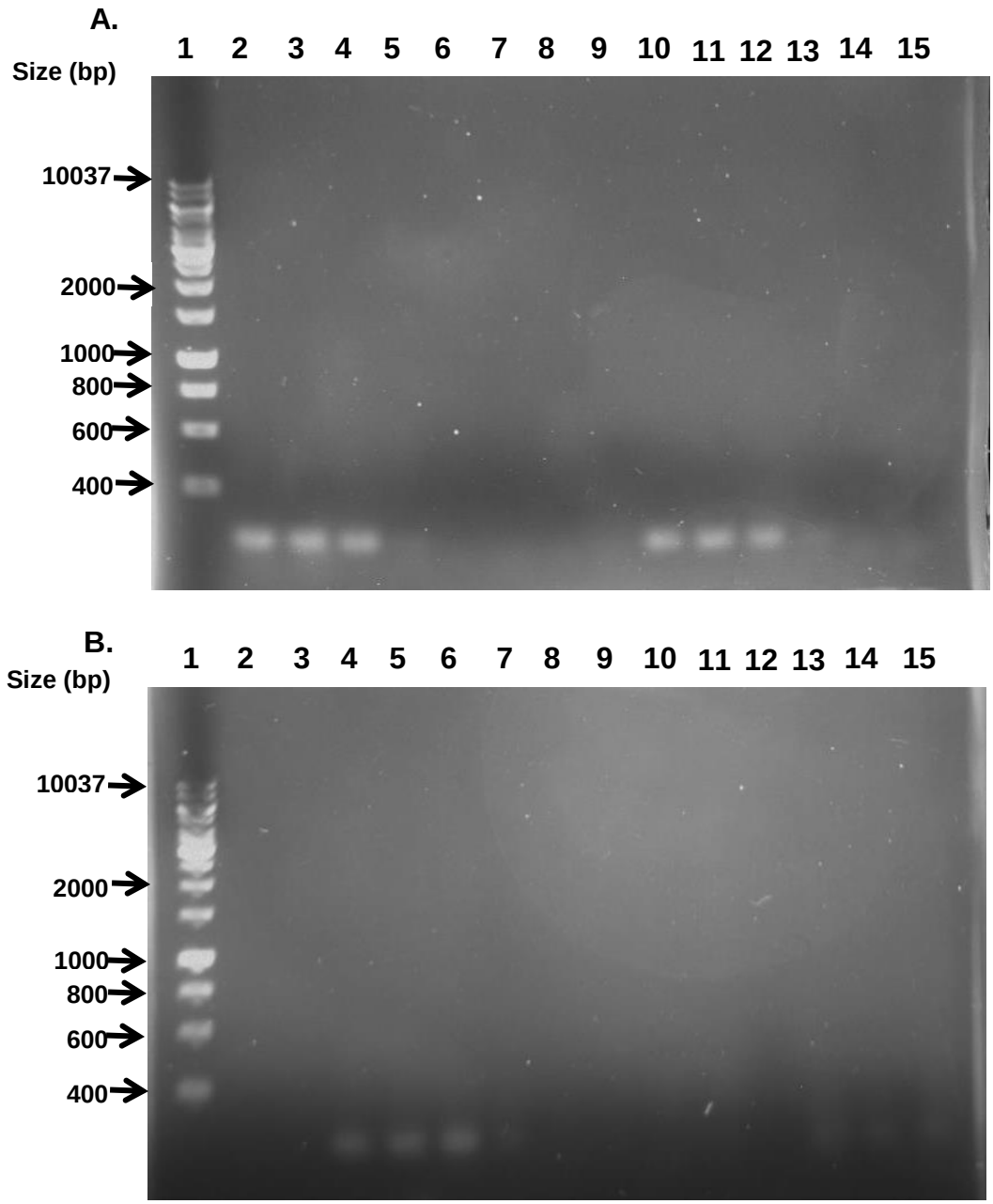

Figure 5.5: Agarose gel analysis showing PCR products from 3 different colonies taken from the contaminated *T. selenatis/E. cloacae* sample using SerCfwd and SerCrev primers using PCR conditions A. as described in the appendix A6. (A) Lane 1: HyperLadder™ 1kb, Lanes 2-9: Colony 1 with a temperature gradient for the annealing temperature during PCR. Temperatures increase with each lane as follows: 63 ^{o}C, 63.7 ^{o}C, 64.8 ^{o}C, 66.4 ^{o}C, 68.4 ^{o}C, 70.3 ^{o}C, 71.4 ^{o}C, 72 ^{o}C. Lanes 10-15: Colony 2 with a temperature gradient for the annealing temperature during PCR. Temperatures increase with each lane as follows: 63 ^{o}C, 63.7 ^{o}C, 64.8 ^{o}C, 66.4 ^{o}C, 68.4 ^{o}C, 70.3 ^{o}C. (B) Lane 1: HyperLadder™ 1kb, Lanes 2-3: Colony 2 continued from (A) with annealing temperatures of 71.4 ^{o}C and 72 ^{o}C. Lanes 4-11: Colony 3 with a temperature gradient for the annealing temperature during PCR. Temperatures increase with each lane as follows: 63 ^{o}C, 63.7 ^{o}C, 64.8 ^{o}C, 66.4 ^{o}C, 68.4 ^{o}C, 70.3 ^{o}C.

5.5 Discussion

The identification of the samples used being contaminated with either *E. cloacae* or something very similar means that the mRNA sequencing results cannot be used to form conclusions about differential expression in selenite-exposed *T. selenatis*. The attempts to isolate a pure *T. selenatis* sample also proved unsuccessful, as no positive results were obtained for the presence of the SefA, SerA, SerB, SerC, or SerD proteins using PCR experiments. Therefore, the *T. selenatis* genome was not able to be resequenced during this study.

However, the differentially expressed genes in the *T. selenatis*/*E. cloacae* bacterial sample grown with or without selenite still show some interesting results. The superoxide dismutase (Fe) gene sodB_1 was found to be the third most downregulated gene in the *T. selenatis*/*E. cloacae* sample when selenite was present in the growth medium. Superoxide dismutases are responsible for catalysing the reaction: $2\ O_2^- + 2H^+ \rightarrow H_2O_2 + O_2$. These enzymes are metalloproteins and in *E. coli* are dimeric with a single Fe coordinated to each protomer, which are 21 kDa in size (Fee, 1991). This superoxide dismutase employs iron to carry out the dismutation of superoxide and the following two half reactions demonstrates this process (where SOD represents the iron superoxide dismutase) (Miller, 2012) :

$$O_2^- + H^+ + SOD \cdot Fe^{3+} \cdot OH^- \rightarrow O_2 + SOD \cdot Fe^{2+} \cdot OH_2$$

$$O_2^- + H^+ + SOD \cdot Fe^{2+} \cdot OH_2 \rightarrow H_2O_2 + SOD \cdot Fe^{3+} \cdot OH^-$$

The iron superoxide dismutase gene, sodB_1 had a log2(foldchange) value of -5.62996. This is an unexpected result considering selenite reduction results in the production of superoxide and therefore causes oxidative stress. *E. coli* has been shown to induce the production of enzymes with antioxidant properties, including the SodB protein, in the presence of selenite (Bébien *et al*., 2002). However, another protein that is employed by cells during oxidative stress is the Dps protein. This protein was identified in chapter 1 as potentially interacting

with the N-terminal of SefA and was searched for in the list of differentially regulated genes. The Dps protein was identified and was found to be downregulated with a log2(fold change) value of -1.64157. The downregulation of this protein normally occurs during the exponential phase of growth when cells are not being subjected to oxidative stress. Translational downregulation of Dps is controlled in *E. coli* by the nucleoid-assocated proteins, Fis and N-HS (Azam *et al*., 1999; Grainger *et al*., 2008). The fact that both the iron superoxide dismutase and Dps protein genes are downregulated when selenite is present in the growth medium and therefore selenite reduction is being carried out, is unusual. Selenite reduction results in the production of superoxide anions and these two proteins are normally upregulated in these conditions. The fact that they are both downregulated suggests that another form of superoxide removal is being carried out in the cell. The cyt*c*-Ts7 c-type cytochrome has been identified in *T. selenatis* and has been found to be upregulated during selenate respiration. This c-type cytochrome does not play a role in the transfer of electrons to SerABC (Lowe *et al*., 2010). It has been suggested that its function is in fact to detoxify O_2^- (Debieux *et al*., 2011). This could provide an explanation for reduced expression of the genes encoding the Dps and iron superoxide dismutase proteins when selenite reduction is occurring within the cell. The genes encoding the glucosamine-fructose-6 phosphate aminotransferase and threonyl-tRNA synthetase proteins, also identified in chapter 1 as potentially interacting with the N-terminal of SefA, were not found to be differentially expressed. Therefore these two proteins may be upregulated during selenate respiration in *T. selenatis* but not during selenite reduction.

Only 3 out of the top 20 upregulated genes were known genes with known gene products. These hypothetical protein products from unknown upregulated genes could originate from the *T. selenatis* bacterial cells within the contaminated sample. If the *T. selenatis* genome is sequenced in future work, these upregulated genes and their products could be identified and provide more information about the behaviour of *T. selenatis* cells during selenite reduction in aerobic conditions. These proteins could be isolated and their effects on selenite reduction by GSH could be investigated *in vitro*. If the isolated proteins have a significant effect on GSH-mediated selenite reduction, it could give

further insight into the mechanism involved in selenite reduction in *T. selenatis* cells. Some of these hypothetical proteins could also be proteins that aid in the assembly of the selenium nanospheres and function similarly to SefA. Identification of these proteins would provide a greater understanding of SeNP formation and secretion from the cell and could help in providing optimised selenium nanoparticle protein coronas for use in medical treatments.

Although the sample was contaminated, the presence of *T. selenatis* in the sample is highly likely due to the identification of the downregulation of the gene encoding the SerB protein. The log2(fold change) for this gene was -0.36923. The SerB protein is an iron-sulfur protein which forms part of the SerABC selenate reductase that has been isolated from *T. selenatis,* and the genes encoding this have been sequenced (Schroder *et al*., 1997; Krafft *et al*., 2000). This slight downregulation in *T. selenatis* cells grown in selenite is not surprising due to the fact that SerB is involved in selenate reduction and not thought to be involved in selenite reduction.

Three respiratory nitrate reductase genes narG_1, narI_1, and narH_1 as well as the nitrate reductase molybdenum cofactor assembly chaperone protein gene narJ_1 were found to be upregulated when the *T. selenatis*/*E. cloacae* cells were grown in selenite. The respiratory nitrate reductases (NAR) in both *T. selenatis* and *E. cloacae* SLD1a-1 enable nitrate to be used as a terminal electron acceptor during anaerobic growth (Watts *et al*., 2003; Rech *et al*., 1992). The heterotrimeric NAR nitrate reductase is membrane-bound and is composed of three subunits, NarG, NarH, and NarI. NarI receives electrons from the quinol pool which are then transferred through the iron-sulfur clusters of NarH, to NarG which is the catalytic subunit (Bertero *et al*., 2003). NarJ is a chaperone that is necessary for molybdenum cofactor insertion into the apo-NarG subunit as well as the final assembly of the NarGHI complex (Vergnes *et al.,* 2006). The gene encoding the catalytic NarG subunit of the nitrate reductase was upregulated the most in the *T. selenatis*/*E. cloacae* cells with a log2(fold change) of 4.312444. The NarH, NarI, and NarJ were upregulated with a log2(fold change) of 2.957347, 1.738608, and 3.318653 respectively. The upregulation of these genes is interesting because of the association of nitrate

reductases with selenate reductases, as well as the fact that selenate reducers are also able to reduce nitrate. Despite nitrate reductases being poor reducers of selenate, the ability of membrane-bound nitrate reductases to reduce selenate has been demonstrated, for example in *Paracoccus denitrificans* and *Paracoccus pantotrophus* (Sabaty *et al*., 2001).

The genes encoding the DMSO reductase anchor and iron-sulfur subunits, dmsB_1 and dmsC_1, as well as the gene encoding the DMSO reductase DmsA precursor, dmsA_2, were also upregulated in the *T. selenatis*/*E. cloacae* bacteria in the presence of selenite. The log2(fold change) values for the dmsB_1, dmsC_1, and dmsA_2 genes are 1.060354, 0.251167, and 0.706652 respectively. The genes for the sulfite reductase hemoprotein beta-component (cysI) and flavoprotein alpha-component (cysJ_3) were also upregulated in the *T. selenatis*/*E. cloacae* bacteria with log2(fold change) values of 1.081889 and 1.47425 respectively. DMSO reductase is an enzyme that enables anaerobic respiratory growth of bacteria, for example in *E. coli*, using DMSO as an electron acceptor. (Weiner *et al*., 1992) **The sulfite reductase enzyme catalyzes the 6-electron reduction of sulfite to sulfide. This reduction is the central energy conserving step of sulfate respiration and allows bacteria to use sulfate as a terminal electron acceptor during anaerobic respiration (Odom et al., 1984). The upregulation of protein subunits that form the DMSO reductase and the sulfite reductase enzymes could indicate that these two proteins play a role in selenite reduction in T. selenatis/E. cloacae. Further investigations into how these two proteins interact with selenite and the proteins involved in selenite reduction in T. selenatis/E. cloacae could provide more information on the mechanisms used to carry out selenite reduction in these bacteria.**

After identifying that the previously sequenced *Thauera selenatis* AX genome is in fact likely a mixture of both the *T. selenatis* and *E. cloacae* genomes but definitely not just the *T. selenatis* genome, attempts were made to isolate a pure sample of *T. selenatis* with the aim of sequencing the *T. selenatis* genome. Although multiple primers and multiple conditions were used to try to identify the presence of, and isolate *T. selenatis* colonies, no successful PCR reactions were carried out.

6 Concluding comments and future work

6.1 Concluding comments

Three proteins thought to interact with the N-terminal of SefA have been identified in this study. They are thought to interact specifically with the N-terminal of SefA due to their absence in the elution samples from nickel columns investigating protein-protein interactions with His-SefA-His. A search of the peptide sequences against BLASTp revealed the closest matches of the three proteins to be a threonyl-tRNA synthetase protein, a glucosamine-fructose-6 phosphate aminotransferase protein, and a DNA starvation/stationary phase protection protein Dps/ferritin. These are interesting proteins to potentially be interacting with the N-terminal of SefA. Both the threonyl-tRNA synthetase protein and the glucosamine-fructose-6 phosphate aminotransferase protein could be interacting with SefA due to their interaction with Thr residues as part of their functions in the cell, as SefA is very rich in threonine (Ibba *et al.*, 2000; Bond *et al.*, 2015; Hart *et al*., 2007; Debieux *et al*., 2011). The Dps protein has twelve catalytic ferroxidase sites that catalyse the oxidation of ferrous ions to form a ferrihydrite mineral core that is saturated with Fe^{3+} ions (Nair *et al*., 2004). The interaction between SefA and Dps could be related to function: SefA could have a spherical hollow cavity, similar to that seen in Dps, which stabilises selenium particles and allows them to form the selenium nanospheres seen both intracellularly and extracellularly in *T. selenatis* cells (Debieux *et al*., 2011). It was discovered in the final part of this work that the '*T. selenatis*' cultures were actually a mixed culture that included *T. selenatis* and *E. cloacae* bacteria. Therefore these proteins identified as interacting with SefA could have originated from *E. cloacae* instead of *T. selenatis*.

Crystals of the His-SefA-His protein were not able to be successfully grown in this work. However the oligomeric state of the His-SefA-His protein was found to be a tetramer and differential scanning fluorimetry experiments resulted in the identification of stabilising buffers which could be used in future experiments. It seems that the SefA protein in this form is very difficult to successfully

crystallise. Other S-layer proteins have also proven to be difficult to crystallise due to their tendency to spontaneously form 2D structures *in vitro* (Fagan *et al*., 2014). The presence of the glycine rich repeat in SefA that in S-layer proteins usually binds calcium ions and stabilises the folding of the protein (Baumann *et al*., 1993; Delepelaire, 2004), along with the absence of extra calcium ions in the conditions used to prepare SefA for crystallisation trials, could have also affected the protein's ability to fold and form a stable structure needed for successful crystallisation.

A transcriptome analysis of *T. selenatis* was carried out and differential expression investigated when the bacteria were grown with or without sodium selenite. This led to the identification that the glycerol stocks of '*T. selenatis*' were actually a mixture of bacterial species thought to include *T. selenatis* and *E. cloacae*, as well as the fact that the original draft *T. selenatis* AX genome was also that of a mixture of bacterial species thought to most likely be *T. selenatis* and *E. cloacae*. Out of the top 20 upregulated gene products in the transcriptome analysis, 17 were hypothetical or unidentified proteins. These proteins could originate from *T. selenatis* and some may be involved with selenium nanosphere assembly and exportation. Two proteins which are normally upregulated during times of oxidative stress, were in fact found to be downregulated when the bacterial culture was grown in selenite and therefore in conditions that result in oxidative stress in the cell. This was an interesting result and suggests there may be something else involved that removes superoxide anions produced during selenite reduction. The Cyt*c* Ts7 c-type cytochrome could fill this role in *T. selenatis* as it does not play a part in electron transfer to SerABC during selenate reduction, and has previously been suggested to play a role in superoxide anion detoxification in *T. selenatis* (Debieux *et al*., 2011). Subunits of the nitrate reductase protein, the DMSO reductase protein, and the sulfite reductase protein were found to be upregulated during selenite conditions, therefore suggesting that these proteins could play a role in selenite reduction in *T. selenatis*/*E. cloacae*. Attempts to isolate a pure culture of *T. selenatis* proved unsuccessful. Despite testing multiple colonies and PCR conditions, there was no positive result for the presence of *T. selenatis*. Multiple colonies were found to be *E. cloacae* but not all gave a positive result for this

bacteria. It is unusual that *E. cloacae* was found in cultures that had previously been grown anaerobically in selenate as previous work found that *E. cloacae* does not grow under these conditions (Losi *et al*., 1997). The *E. cloacae* bacteria could therefore have been present in the anaerobically grown with selenate cultures, and whilst not actively growing, they could have survived and then started growing when the cultures were transferred to favourable conditions. Also the difficulty in isolating *T. selenatis* and the ability of *T. selenatis* and *E. cloacae* to grow together could suggest a co-dependence between the two bacteria. Could it be that these two bacteria have evolved to grow together in order to make harsh conditions more favourable for growth for both the bacteria?

6.2 Future work

To continue on with the work described here, successful isolation of pure *T. selenatis* cells would be required. Upon confirmation that the *T. selenatis* was in a pure culture, genomic DNA could be extracted from the *T. selenatis* cells and the genome could be sequenced. Further investigations into the three proteins identified here that are thought to interact with the N-terminal of SefA could be undertaken. The three proteins could be isolated and experiments to confirm an interaction between each of the proteins and SefA could be run. Differential scanning fluorimetry could also be used to test whether the three proteins stabilise the SefA protein by quantifying the melting temperature of SefA in the presence of each of the three proteins. Further attempts to crystallise the SefA protein could be undertaken with alterations to the protocol during expression of the His-SefA-His protein including: lowering the concentration of IPTG and the temperature at which the *E. coli* cells are incubated to increase the quality and concentration of SefA expressed, refrigeration of the *E. coli* overnight after expression of the SefA protein to aid with protein folding, and use of autoinduction media for higher yields of SefA. A different approach to crystallising the SefA protein could also be adopted that has proved successful with other S-layer proteins. Instead of trying to crystallise SefA as a whole, recombinant or proteolytically derived fragments of SefA could be formed and

crystallisation trials could be undertaken to see if SefA fragments could be successfully crystallised (Fagan *et al*., 2014). A number of interesting proteins were identified as being differentially regulated in the *T. selenatis*/*E. cloacae* cells when grown in selenite. These proteins could be isolated and their effects on selenite reduction by GSH could be investigated *in vitro*. If the isolated proteins have a significant effect on GSH-mediated selenite reduction, it could give further insight into the mechanism involved in selenite reduction in *T. selenatis* cells.

Appendix

A1. SefA homologues sequence alignment

```
DespoDRAFT_01458      -----MAVTREQVAQIYVATFNRAPLDAGLDYWAGSGF------TI----EQIATSFFDQ
CAMSH0001_1621        -----MAVTQAQVAQLYVALFNRAPEGAGLNAWVSAGAA----KTQ----AQIADDMLKA
SPICUR_08450          --MAITEEMQEQISELYVGLIGRAPDNDGLSFWVQALDARRAELDEPAALKSVAQDMFE-
Selin_0231            -----MSVTTAEIIELYVASFGRAPRKSELEALETASA----GKTK----SEVAADMIES
Nitro_communis        --MAISSQQKEDILALTVATFNAAPSAKIMQELASAVE---SGMTN----QQL-ADILVA
Nit79A3_0436          --MAITSTQKTEILKIVAGLFNAAPGGSNLTELANLVS---GGMTT----SQL-ADALAA
NAL212_3002           --MAITAEQQTSILEVAIGLFNAAPGKIYMTELANMVDANGGNLSI----EQL-ADFLDD
Nitro_ureae           --MAISKEQETEVLKVTAGLFNAAPGGDYLTEMANMVE---GGMTI----PQL-ADFLAA
Com_aquatica_CJG      -------------------MFDAAPGAQYLEEFTSAFLA--LGNDY----AAL-ATALGN
SefA                  --MAITATQRTEIVKVVVGLFNAAPGATYLDSFTAYA-D-----NI----DGL-VNDLVA
P._spirulinae         MANNITNEVQDQLISMVVGMHGAAPGKKILSDLAALY-N--ADNSL----AAI-AATLGE
                                        . **    :                     :    :

DespoDRAFT_01458      PEAQAIYTDDGEPISSEEFVTRIFDNLFNR-------EPAEAGLEYWSTALDEGTVSQAE
CAMSH0001_1621        -PAVQS-YFNGSIDTDKGYIENIYKNILGKD-----YSQDPAGIDAWVRHLQAGHTRGET
SPICUR_08450          -SASSN-GYYPGFQTNEQIVRSFYENVLGR----GEGEQDQEGIDFWTSAMDSREP-GDV
Selin_0231            SGSFAS-ADNTAFL-N----EAYQAFFGRV--------ADAEGLAFWGAALEAGLSRADL
Nitro_communis        TDEFKE-GVLKGAVTNEEITANLLKNFGLAAGNTDAASPDAQAEAFFMNRLESGASIGSI
Nit79A3_0436          NTLFTN-GIMGGKVTVEDQAAVLAHNFGLAADS-DPASAGSQAEAYFTQLINDGVGFGNI
NAL212_3002           TAVFKD-NILVGKVTIEEQASILLNNFGLAADD-DPASAGSQAKAFFEGELAAGKGLGEI
Nitro_ureae           HPLFTN-GIMGGRVTTEDQVEALMNNFGLVADG-VEGSAATQAEDFFTGQIDSGVGFGAI
Com_aquatica_CJG      TSAFK--SQYPSSLTVEETANKFLGSLG-L-------ANNTEAQDFVQSKLNAGEGIASV
SefA                  DPAFT--AIYPTFLTNEEFADKYIDALVGDA---AATADKDWAKDWLAGLLNAGMSRADA
P._spirulinae         GDLFT--GIYPTFLTNQQFATNFVNNVVGSL---VSQEEKDWAVGVLTADLNAGASRGEV
                                          .              .      :

DespoDRAFT_01458      MILAVA-----------NGATGVDAAILANKTKVGLYYADQGGEET----T--------Y
CAMSH0001_1621        LTKLFEVAASAEAK----AADPRAAKIFENKSAVAAYMAEKIGDIGKDGSGNFDYAPFQE
SPICUR_08450          IVDMISSLLDSEGG---SELTQQSRDLLQNKVAVANYYGTDVSEPGEPSQE--DVNVSEA
Selin_0231            IAELVAGADNYPAEGANAAEAAKDKAIAANKKAVATYFAESGI-------E--DEAQASE
Nitro_communis        LLEASAYLTGTPA-----EEFKPTADLFQNKVTVADVYSRE------GKGE--TLDAMQN
Nit79A3_0436          VVQAVTYLSGTPA-----TEFTEAATLLDNKVLVSDAYSKA------ASAS--DLDTLQK
NAL212_3002           VIEGINYLNGSPA-----EEFAATKTLLDNKVLVAKAYSAT------GSSQ--DIALLQT
Nitro_ureae           IVEAVTFLSQDPATL--PAEFADTAALLSNKALVAELYSKE------HSSA--DLAKLQS
Com_aquatica_CJG      VFQALQALVDYAGD---DAELQAAQTQLANKAAVAEYYSVTLG----ASSD--QLAVLQG
SefA                  VTLAVTEL-QAAAD---NPKWAAAATQFANKVTVAEYYSVDML----GTAT--DVGVLQG
P._spirulinae         AYSAILALREVAST---EPNWGDASAAFANKMEVATYYTVTKQ----LDAG--TLAELQE
                                             **  *.

DespoDRAFT_01458      YLIDIDETDESV----EAAKDEIDHILDPDVEKSFTAGTDDITGGAGDDTFEAPIVQNPW
CAMSH0001_1621        IIRTTNESN----LEAQ--KAKIDELASKGVEKSLTDGLDNITGTAGNDVFNGVYYTG--
SPICUR_08450          LIDSVTADTDTSTPEAVKSFVDAEVEADSGETFTLTTSINDFTGTADDDKFEQTKD----
Selin_0231            VLDGVTEDPATVDSAK-DVID--EATQVPGETFTLVSGAEVVEGTAGNDTIIAVTDNL-A
Nitro_communis        VLIGVTPTFPTTEAEAEGFVAGKGTG--PDNTFHLTTGVDNPRTTTGSDEINGVVDTA-A
Nit79A3_0436          VLSNVTGTAPYTDADVEAILKDSGTA--GGKTFTLTNTTDAFTGTSGDDIFIGDNVSA-S
NAL212_3002           VLSKVTGDAPYTEADVQQALADSGVPTGSGSGFALIVGEDSLTGTSGDDVFTALAIQD-N
Nitro_ureae           ILGGVTASTPTTEEDAMAYLDSIGEGANVGGTLALTFGADILTGGAGNDTFIASIVND-G
Com_aquatica_CJG      VVANVTADPASVE------AAKEASNGSNGQTYMLTKGLDNPAATSGNDTFIGAIDNV-A
SefA                  VIADVTATTDVSTPEAIEAVIDATPAGTTGQTFTLTVGVDAVAGTSGNDTITGSYDPI--
P._spirulinae         VIADVDNTEQSV----TDAKAEADGTSSKGQTYSLTTGVDTLVGTSANDTFNAAN-----
                       :                           .    :    :     : .* :

DespoDRAFT_01458      AGGVSNSLSTADSLDGGAGTDSLYAELVPEYYGVT--GDNTMDIQPHIQNVEDIQFESMD
CAMSH0001_1621        NGTQKSTLSPLDKIDGGAGKDTLNLTVFKNDAPQNLTTTELQNIFKGVSNVENLNLISET
SPICUR_08450          -----GQLSIDDTLDGGAGDDTLFVRDQDGGTGKF--------T---ATNIETIDVRASE
Selin_0231            SK---RTLDQGDQIDGGEGNDVLKVALGANFNGFT--------GDGYLKNVETIELTNES
Nitro_communis        NGG---TLTNGDNVNGGAGFDTANLVVASSA--WP--------AGATIKDVEKIVFKNVN
Nit79A3_0436          AG---------DTLVGGTGTDTLKV--YGTN------------TVPNISGIEQVYYNA--
NAL212_3002           VGGVVNSLESIDRLDGGTGTDTLTATLIANA------------A-PSLTSVENIIARF--
Nitro_ureae           AGTLVNSLENLDILDGAAGRDTLNATLDGDT------------ISPAISNLEVINVRA--
Com_aquatica_CJG      NS-ELNTLSSQDIINGGAGTDTLKIAHGGTAAT-T--------TLGNLSNVEIVEIESSS
SefA                  -N-KLHTLSGLDNIDGGAGTDTLTVTDAAGGNIDF--------TGVTIKNVEVLNVQAAG
P._spirulinae         -----TTFTALDSIDGGAGADVLNVNDVAGATAIP--------GGIKLSNVETLNWASAG
                                * : *. * *                           .:* :

DespoDRAFT_01458      VLDGHTTITVDAKNI----TDVDHIGSAYS--------------------DGDLVIENLT
CAMSH0001_1621        E--------FDAGGV-KFNFGLENLNISTIGDVSISETDATNKVSVNTTGKVSLNAKNAQ
SPICUR_08450          DN-----ADIELDNV----TGYTALVANALTTDGTNAD-DLEFTEIENSADLTLEVKNIA
Selin_0231            NF----ARTFNANGI----EGVTEYVVNAT--------------------TKDVKVTNIK
```

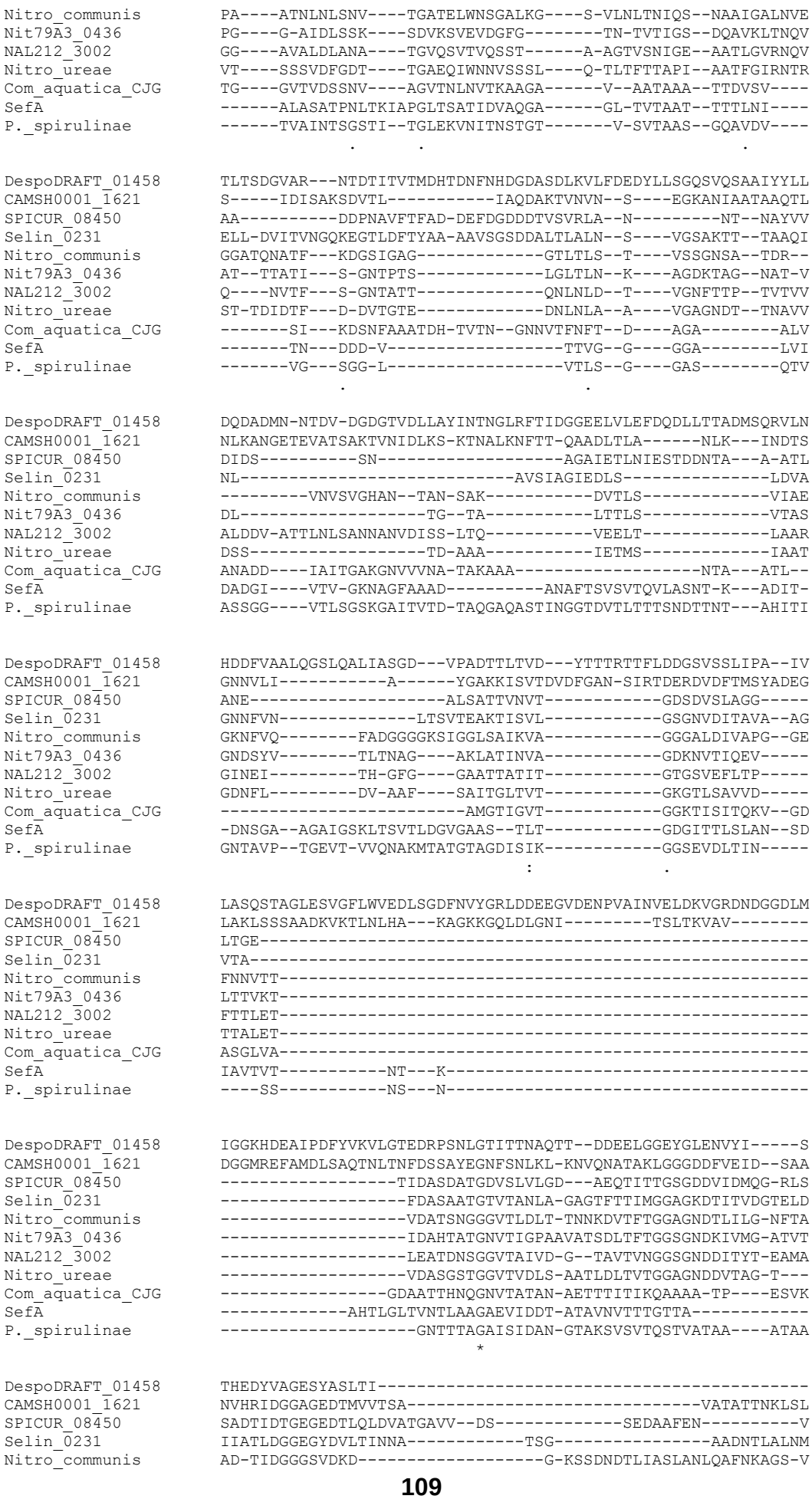
Nitro_communis PA----ATNLNLSNV----TGATELWNSGALKG----S-VLNLTNIQS--NAAIGALNVE
Nit79A3_0436 PG----G-AIDLSSK----SDVKSVEVDGFG--------TN-TVTIGS--DQAVKLTNQV
NAL212_3002 GG----AVALDLANA----TGVQSVTVQSST------A-AGTVSNIGE--AATLGVRNQV
Nitro_ureae VT----SSSVDFGDT----TGAEQIWNNVSSSL----Q-TLTFTTAPI--AATFGIRNTR
Com_aquatica_CJG TG----GVTVDSSNV----AGVTNLNVTKAAGA------V--AATAAA--TTDVSV----
SefA ------ALASATPNLTKIAPGLTSATIDVAQGA------GL-TVTAAT--TTTLNI----
P._spirulinae ------TVAINTSGSTI--TGLEKVNITNSTGT-------V-SVTAAS--GQAVDV----
DespoDRAFT_01458 TLTSDGVAR---NTDTITVTMDHTDNFNHDGDASDLKVLFDEDYLLSGQSVQSAAIYYLL
CAMSH0001_1621 S-----IDISAKSDVTL-----------IAQDAKTVNVN--S----EGKANIAATAAQTL
SPICUR_08450 AA----------DDPNAVFTFAD-DEFDGDDDTVSVRLA--N---------NT--NAYVV
Selin_0231 ELL-DVITVNGQKEGTLDFTYAA-AAVSGSDDALTLALN--S----VGSAKTT--TAAQI
Nitro_communis GGATQNATF---KDGSIGAG-------------GTLTLS--T----VSSGNSA--TDR--
Nit79A3_0436 AT--TTATI---S-GNTPTS-------------LGLTLN--K----AGDKTAG--NAT-V
NAL212_3002 Q----NVTF---S-GNTATT-------------QNLNLD--T----VGNFTTP--TVTVV
Nitro_ureae ST-TDIDTF---D-DVTGTE-------------DNLNLA--A----VGAGNDT--TNAVV
Com_aquatica_CJG -------SI---KDSNFAAATDH-TVTN--GNNVTFNFT--D----AGA--------ALV
SefA -------TN---DDD-V------------------TTVG--G----GGA--------LVI
P._spirulinae -------VG---SGG-L------------------VTLS--G----GAS--------QTV
DespoDRAFT_01458 DQDADMN-NTDV-DGDGTVDLLAYINTNGLRFTIDGGEELVLEFDQDLLTTADMSQRVLN
CAMSH0001_1621 NLKANGETEVATSAKTVNIDLKS-KTNALKNFTT-QAADLTLA------NLK---INDTS
SPICUR_08450 DIDS----------SN------------------AGAIETLNIESTDDNTA---A-ATL
Selin_0231 NL----------------------------AVSIAGIEDLS---------------LDVA
Nitro_communis ---------VNVSVGHAN--TAN-SAK-----------DVTLS-------------VIAE
Nit79A3_0436 DL-------------------TG--TA-----------LTTLS-------------VTAS
NAL212_3002 ALDDV-ATTLNLSANNANVDISS-LTQ-----------VEELT-------------LAAR
Nitro_ureae DSS------------------TD-AAA-----------IETMS-------------IAAT
Com_aquatica_CJG ANADD----IAITGAKGNVVVNA-TAKAAA--------------------NTA---ATL--
SefA DADGI----VTV-GKNAGFAAAD----------ANAFTSVSVTQVLASNT-K---ADIT-
P._spirulinae ASSGG----VTLSGSKGAITVTD-TAQGAQASTINGGTDVTLTTTSNDTTNT---AHITI
DespoDRAFT_01458 HDDFVAALQGSLQALIASGD---VPADTTLTVD---YTTTRTTFLDDGSVSSLIPA--IV
CAMSH0001_1621 GNNVLI-----------A------YGAKKISVTDVDFGAN-SIRTDERDVDFTMSYADEG
SPICUR_08450 ANE--------------------ALSATTVNVT-------------GDSDVSLAGG-----
Selin_0231 GNNFVN--------------LTSVTEAKTISVL------------GSGNVDITAVA--AG
Nitro_communis GKNFVQ--------FADGGGGKSIGGLSAIKVA------------GGGALDIVAPG--GE
Nit79A3_0436 GNDSYV--------TLTNAG----AKLATINVA------------GDKNVTIQEV-----
NAL212_3002 GINEI---------TH-GFG----GAATTATIT------------GTGSVEFLTP-----
Nitro_ureae GDNFL---------DV-AAF----SAITGLTVT------------GKGTLSAVVD-----
Com_aquatica_CJG -------------------------AMGTIGVT------------GGKTISITQKV--GD
SefA -DNSGA--AGAIGSKLTSVTLDGVGAAS--TLT------------GDGITTLSLAN--SD
P._spirulinae GNTAVP--TGEVT-VVQNAKMTATGTAGDISIK------------GGSEVDLTIN-----
DespoDRAFT_01458 LASQSTAGLESVGFLWVEDLSGDFNVYGRLDDEEGVDENPVAINVELDKVGRDNDGGDLM
CAMSH0001_1621 LAKLSSSAADKVKTLNLHA---KAGKKGQLDLGNI---------TSLTKVAV--------
SPICUR_08450 LTGE--
Selin_0231 VTA--
Nitro_communis FNNVTT--
Nit79A3_0436 LTTVKT--
NAL212_3002 FTTLET--
Nitro_ureae TTALET--
Com_aquatica_CJG ASGLVA--
SefA IAVTVT----------NT---K---------------------------------------
P._spirulinae ----SS----------NS---N---------------------------------------
DespoDRAFT_01458 IGGKHDEAIPDFYVKVLGTEDRPSNLGTITTNAQTT--DDEELGGEYGLENVYI-----S
CAMSH0001_1621 DGGMREFAMDLSAQTNLTNFDSSAYEGNFSNLKL-KNVQNATAKLGGGDDFVEID--SAA
SPICUR_08450 ----------TIDASDATGDVSLVLGD---AEQTITTGSGDDVIDMQG-RLS
Selin_0231 ----------FDASAATGTVTANLA-GAGTFTTIMGGAGKDTITVDGTELD
Nitro_communis ----------VDATSNGGGVTLDLT-TNNKDVTFTGGAGNDTLILG-NFTA
Nit79A3_0436 ----------IDAHTATGNVTIGPAAVATSDLTFTGGSGNDKIVMG-ATVT
NAL212_3002 ----------LEATDNSGGVTAIVD-G--TAVTVNGGSGNDDITYT-EAMA
Nitro_ureae ----------VDASGSTGGVTVDLS-AATLDLTVTGGAGNDDVTAG-T---
Com_aquatica_CJG ----------GDAATTHNQGNVTATAN-AETTTITIKQAAAA-TP----ESVK
SefA ----------AHTLGLTVNTLAAGAEVIDDT-ATAVNVTTTGTTA----------
P._spirulinae ----------GNTTTAGAISIDAN-GTAKSVSVTQSTVATAA----ATAA
DespoDRAFT_01458 THEDYVAGESYASLTI----------
CAMSH0001_1621 NVHRIDGGAGEDTMVVTSA----------VATATTNKLSL
SPICUR_08450 SADTIDTGEGEDTLQLDVATGAVV--DS----------SEDAAFEN----------V
Selin_0231 IIATLDGGEGYDVLTINNA----------TSG----------AADNTLALNM
Nitro_communis AD-TIDGGGSVDKD----------G-KSSDNDTLIASLANLQAFNKAGS-V

```
Nit79A3_0436          ALDVLKGGTGTDTLSV---------------------------SDADTIDTAAEVIG-I
NAL212_3002           ATAAVALGAGDDTFTIT-----VAAVDGAT-ADG-GDGNDALGVVDGALLDAAAQT-V-Y
Nitro_ureae           GDDTIDLGAGDDRVAFA-----TGTIDGNDTVEG-GDEGEDTLAIDGDDVASLDGT-V-Q
Com_aquatica_CJG      AVAKVDEVATVTFTKLTSG--QSVTVSGLTFTAS-KDLTAEQVAAAFANLSATAPTPANL
SefA                  -------DGENSTVIIDAGKAATITVDGA------GDVTLAAAGADYAALTTFN------
P._spirulinae         AVAAVTETASAKFVALAAG--DTLVVDGLTFTAGASGTTAAQTAAAFANLSATATQG---


DespoDRAFT_01458      -------------------------------RNGFDGQWSVDLVDADDFLGDLILGTGTA
CAMSH0001_1621        LNFENLKITDALSGAVDMTKW------ANLSSITLAGGAGAGA-----KIDNLANNS---
SPICUR_08450          SNVEVVENT---ETALT-----------GTITVDFS-----------------ELDGMTG
Selin_0231            QNFEELRINGAATQELTFAA----ASVSGLEKVVL-GTMGVGG-S--VVLAQMQAENMTL
Nitro_communis        KNVETLGINLGAPLAANATV---NGELFGISNITFNDALNLNGKS--LILSNLANNT-NV
Nit79A3_0436          TEFETFEAAGVDATAYNLSIIGAKNTLSGLVVSA------TGG-A--ATISNLNAAT-TG
NAL212_3002           TNFETLEIGGGTG-TYDME-----NLPG-LVAVTIGAALT--G-A--AIIDNAVADT-TV
Nitro_ureae           TGFEVLELTTATG-AVTFD-----NADFGVTKVVLSGDVTSAG-D--LTIDNFEAGT---
Com_aquatica_CJG      TNV-----TAAAPNPATGDTNGGNALANGVFTGTLLAKWSSAA----------ASGN-TV
SefA                  -------------------------------YTGS--GSAT--A----------DLKG-AA
P._spirulinae         ------------------------NSTLGTYQGTFGGNWTTGA----------ASTD-TV


DespoDRAFT_01458      VNDLIVLEARGGGDVTFMGLVDGTTAGIDDVLANDDRAYSYTTGSGNDTFVV------TL
CAMSH0001_1621        ---------------------------------------T----------------------
SPICUR_08450          YTQGAG----DNEGLTLTNVTNN---------------ATITLGDAAN----------DF
Selin_0231            QLQTATAGSATVGKATYDGYGEL---------------T-ITTGDAANDKTAPRE-----
Nitro_communis        TFKGSA-G-AGGGTIGVD--------------------------V--K------------
Nit79A3_0436          NITING-A--APTTITLT--------------------------A-AD------------
NAL212_3002           TVN--A-E--EGTDLALG--------------------------QTVD------------
Nitro_ureae           ------------LEIQAT--------------------------QTAN------------
Com_aquatica_CJG      TFTASG-AM--GTDLAVSGTGAT---------------V-VTTTQGVN------------
SefA                  LLTKVV-AGSATGDLNVTVDGAI---------------TSVTTGSGDDTVTIDGTTTTDF
P._spirulinae         VFTS-T-AAGNVGDLTFAGTGTA---------------PTLTITQ--------GV-----


DespoDRAFT_01458      DGDAVDAAGVGPESF---------------AIITGGGDDTVDIISVDG-------VSQRT
CAMSH0001_1621        --------------IVVENVAIANDIAVNIKDAASGADDTLIL-KINP--KANTTGL---
SPICUR_08450          ----------------------------------------DDI-SIGMA---ENTGTQTV
Selin_0231            -TEI--EVIS--NNASIVNVNVAARTALN-SDILLTAADQ--L-TLNVA-----------
Nitro_communis        ------------G--------------------AVAGADNTATL-TFG-------------
Nit79A3_0436          ------------F--------------------VSGGTSDTATI-SLDNSVTKSGTGIDVT
NAL212_3002           ------------FALA-----------------TATGTADNVDL-TLN-------------
Nitro_ureae           ------------NILV-----------------TSVGAEDNLAV-LIN-------------
Com_aquatica_CJG      -------AITGKNTLGVTNGTVT----------IAGAA------ALK-------------
SefA                  DGTL--TLGAGSDTVGVASGGVITAT-----AVVDAGDDSDTL-ALS-------------
P._spirulinae         ------AASAAAGRAGVVNG-----A-----VTITDGAATDVL---E-------------


DespoDRAFT_01458      MFILDNL----SIETGDGADRVTINGYERFDIQTGAGDDYVEITSVDPADGSTDVWTFGA
CAMSH0001_1621        ------------------------------------DN-----------------------
SPICUR_08450          NFVLNGADVLNGNT------LSTS-------------------------------------
Selin_0231            --------------TGKASEAIGVTHVKGDE-LTSFGG----------------------
Nitro_communis        ----------KDANLGT---------------------------------------------
Nit79A3_0436          SLVFANADVINLKSIGDGSSTKTVGGAEENSVIL----------------------------
NAL212_3002           ------ALDGNDDSTANG--LITVDSF-----------------------------------
Nitro_ureae           ------ADA-----------AVAVNGL-----------------------------------
Com_aquatica_CJG      --------------------TVTVDGYAASTNTAGITG----------------------
SefA                  --------------------IVGVANVGAFKNFE--------------------------
P._spirulinae         --------------------SVSVNEYGANASVT--------------------------


DespoDRAFT_01458      TTGVQPFVDRVLYKSELTVTFAGFESTVTVDTDAA---GNFVAD----------------
CAMSH0001_1621        TGNFVI---------------DG-IENVRIVSNADTAKT---------------------
SPICUR_08450          ---------------------NGFLDEANLETAEA---ASFLEN----------------
Selin_0231            SINAQVATS-------VIIDAKGLLDGATIEANQ---AESVVADVAA-------------
Nitro_communis        --------------NKVTVNAGG-VETITIATDAT-SGA---------------GA----
Nit79A3_0436          -------TAS----DAEKVVITG-DEALSFATAAG-TNP---------------TEVDAS
NAL212_3002           -------------------TANA-IETFTIASNVT-VID---------------PDLANT
Nitro_ureae           -------------------DVTG-VETVSVTTTA----------------------DTDD-
Com_aquatica_CJG      ATNTALDTIS------L----AN-GGNFEIDS-AAATLGLTLANVNGTVD--------VQ
SefA                  --NFDVAGLTTNFDQAVLNTKNS-VENFI--GTDDTGAAITIQNMGAGVGFIVKGDMDSN
P._spirulinae         --SDALKTLS------LAN--SG-AGTFSVTNTKQTTLDLTVNDVDAGVN--------IG


DespoDRAFT_01458      -----------------QVIIN-----AAIIEAIE----------QSTVLSELLDYNLGS
CAMSH0001_1621        -----A-------AAKNVINLNASDATKCALSGVYVSGDGNTELKLGENIVKIK------
SPICUR_08450          --------------------LG-----SFDVNKLTISGDQDINL---------SAEQASN
Selin_0231            ----------------GDLTLI-----TGKVESIEMKATGAFQINDDS--------DLSA
Nitro_communis        ---Q-------------LFKLA-----DTALTTLKVTGSDGIGI------GDLTASK---
Nit79A3_0436          GLTNDAA---------VTIDTD-----ASAITSLLAKGTGKNDT------IDIDNAA---
```

```
NAL212_3002          DYTNTIS----------ALIG-------DAVQTLNISGNANLEV------TALTAAD---
Nitro_ureae          ---TTFT----------AIET-------DGVTGLTFAGAGDVII------TDITDAD---
Com_aquatica_CJG     AGTKTLNAAVSHAKATETSTLV-----SASAETVNVTGTGNVAGNTATG-----------
SefA                 GTFGTVTAA-------DVVTLT-----QATAGALNIT--VDVDGEEGDGVIETDA-----
P._spirulinae        GTYTTVNATATGTN--SVFSLT-----AGGVTTLN------VAG---DKLMNLSGAALGA
                                                          :

DespoDRAFT_01458     SDQ--------FLVITSDFDGANELAVDL--------FQPT---------LVAADAVAGE
CAMSH0001_1621       ----------------------------------------------------GVDASSLTGK
SPICUR_08450         ADHA-------I-----------------------------------SSATTTVDASELTGD
Selin_0231           LNSLVLTTGKVFTFEDANVNGLAELAYVQVDGNGSMTFGNNAIGADQEGVTVAATELLGG
Nitro_communis       ----------NITTID---------------------ATGV---------VKDAVGAVGG
Nit79A3_0436         ----------TVTSTL---------------------YLGG---------GSDTVTVDGG
NAL212_3002          ------------------------------------VN---------KIDASTMTGG
Nitro_ureae          ----------NTNNGA---------------------TKIG---------AIDLIGQTGG
Com_aquatica_CJG     -----------L-------------------------------------------T----
SefA                 --SFVASNATSLTV-T---------------------FDNQ---------NVDAVA----
P._spirulinae        LKTVAVSESASLTL-------------------------NAG---------EA---G----

DespoDRAFT_01458     VVLSSGDLTAIRR--GIINTTVLTSADLENEAEVIAEFNDGTTANLGD-GSLSQTGNDIS
CAMSH0001_1621       FTFDAGNHV-----------------------ERGGVVKGGSGDDT--------------
SPICUR_08450         LDVLAS----------G-TSTDI------TGGDGNDEIVGGSGSDV--------------
Selin_0231           ITVIVDDAASVAGSTAAVYGSTIGKNTIEIGARAEVELTGGVSADV--------------
Nitro_communis       VFVSVA--------QND-KSVTFTGG------EGGDAYIASAKGDI--------------
Nit79A3_0436         -GTDAH--------TLIYTATALNAGDIKAGDSSTLALTGVAAGDT--------------
NAL212_3002          LTIDAS---------TSGASGVEFV----GGAASDT--YTGTDGGDT--------------
Nitro_ureae          VQMAAN---------SLGY-GTTFTLANLGETAAGTFDFDDVNGGDE--------------
Com_aquatica_CJG     AATAIN---------TSGMTA---GKATFTIADGTKTSYTGGAGVDT--------------
SefA                 NLAEVN---------LTGTKATTLAIVSGGSEVSNKVDYTGANDGTNDLLTSVTVTGDQ--
P._spirulinae        TLTSVN---------SSATTGTVTA-----TIDSTKATYTGGAGVDN--------------

DespoDRAFT_01458     TDQFDYQFLAA-----NADAT----------ANATIEQNYSVINTSTGNDIVVLHSNEASA
CAMSH0001_1621       --------------------------LSF---GSVA-GLKITGGAGNDVFKVGKLGAEA
SPICUR_08450         ------------------------------------LSGGAGDDSLTFQPSSSST
Selin_0231           ---------------FTVDL-----------NVNVDQ-NITITGGAGNDKFVIGSTYQNK
Nitro_communis       ----------------------------------------VTGGLGSDVITLGAG--AD
Nit79A3_0436         ----------------------------------------VTINFSSALEALLKS----
NAL212_3002          ----------------------------------------ITGNGGGDLITLGA-GSVD
Nitro_ureae          ---------------------------------------AS-----EL--FGATGFRD
Com_aquatica_CJG     --------------------------VTVQSANIAI-TKAIDLGAGDDKLTLEGSGSTT
SefA                 ALTFDYTSGGKTLKLATVDASGQTDGGLTFSLDDLTA-TGTVKLGGGDDVISFDT----A
P._spirulinae        --------------------------VTFSN-TTAA-SKAVSLGGGNDKLTLAT----G
                                                                          .

DespoDRAFT_01458     NTLVFD-------SEFNYLTVVNFFDD-AA------R------TVTGNHILDFTYYLDNQ
CAMSH0001_1621       NSPFGT-DKLSSITDFSKGDKLY---TGGA----AAESNSIAKYDS-DASLDFANNLRE-
SPICUR_08450         D-------------TLTGGDGDDTFVQGTANSDSVNA-ATITDFSIDDDDLDLELTTLEN
Selin_0231           NIVTI--------TDFNSGDA---FHIDGT--DKIAASTVADTYDLND-AVAF--LLDAG
Nitro_communis       KLIYNAAAESDGQPAPNGSVDVIGNNT-----------AT-GDFDVAADSIQFAAALQTG
Nit79A3_0436         ------------------------------------------------------------
NAL212_3002          TLILNAVTDSQLNTDLDGHDQITGFGI------------A-GQL----DVIDL------G
Nitro_ureae          R--------FEFTTEFTGDVAISDIEV------------G-GDV--TDDKIDL------S
Com_aquatica_CJG     VAVPTA--------NLNGGAGTNTIAMSGA--SAAALSAN-GDF--AAKIDNFQKLEITD
SefA                 ITTTAA--------------------------------------------------------
P._spirulinae        TAIPTA--------TLNGGEGTDTLSMTAS--DAVTQSGS-TAF--STKVIGFEVLEVTG

DespoDRAFT_01458     QDP------SDAPAGNAQ--------SVVDIGITYDGPETAAAGDDLVGNEFTIVKPTFD
CAMSH0001_1621       ------------------------------------------------------------
SPICUR_08450         LQPGASADDVDLVDGNANTITAATDLTTVEVDGDGDNPTLAAGDQ---------------
Selin_0231           MSGATTN-----------------NVSV----------------------------------
Nitro_communis       TASFIGNAAFTNTG--------ATQVSFTN----------VADA----------------
Nit79A3_0436         --------GSTLLS--------ATGANINV------------HGT----------------
NAL212_3002          VLGFTGQQASALAN--------KGGAAIAS----------IADGS----------------
Nitro_ureae          AFGLASDDDLT-----------------ITD----------VAAGV----------------
Com_aquatica_CJG     TANAAT--TINMAN--------MDGIKYVV----------SKG-----------------
SefA                 ------------------------------------------------------------
P._spirulinae        AAGAQ---AIDLEA--------LGNYNSVS----------SA------------------

DespoDRAFT_01458     DDDTFNGLTASNFLAAINDDDGTADYADIDNDTLDAADSPFGDNFVGTVQDHIVFVENND
CAMSH0001_1621       ----------------------------------------------AE----KVAAQ-HA
SPICUR_08450         --------------------------------MIVLTEETFADSS--A----VEAAL-AS
Selin_0231           -------------------------------------Q-EFDAA--AE----DVTAI-YY
Nitro_communis       ----------------------------------NPFAVGN-------------QA
Nit79A3_0436         -------------------------------TISA-T---------T----NIAAA-EV
NAL212_3002          -------------------------------ATSI-TDFFASGGVDR----GVAIG-VS
```

```
Nitro_ureae           --------------------------------LIE--NDAFGGG---R----ILLVG-VT
Com_aquatica_CJG      -------------------------------------------------G----NAVAG-VT
SefA                  ------------------------------------------------------------
P._spirulinae         ------------------------------------------------------------

DespoDRAFT_01458      NRGEYKVFYLTSELDADG---NVDNADGDFETATLLG-T----------------------
CAMSH0001_1621        SKSAYFT-YQSNTYI--------VTSDGVQGVGQ--------------------------
SPICUR_08450          GKSHEFQ-FDTAPADNDGILIGYETTDGDFRVAVA--------------QMNANSDNSDD
Selin_0231            GGDTYFV---------I------GNSDGNFDAGEVLLKLQGV-TTVTAAQVTAL------
Nitro_communis        GG--AVK--------VD------LNGDGTSDMT----------------------------
Nit79A3_0436          GGTMTLQ--------ID------VNGDGAYAAA----------------------------
NAL212_3002           GGSTWVV--------ID------ANKDGNFTSG----------------------------
Nitro_ureae           GAD------------------------------------------------------------
Com_aquatica_CJG      GSKQVFV-FDIAGLAMD------NSGSGSLKAGDATLFTATAGTAVTDAQIATAIGTTAT
SefA                  ------------------------------------------------------------
P._spirulinae         ------------------------------------------------------------

DespoDRAFT_01458      ---IDFGAEITGDPISMANL--------------------------------------------
CAMSH0001_1621        ------------------------------------------------------------
SPICUR_08450          I-----------------------------------------------DGV--------
Selin_0231            -----FDLTV-------------------------------------------------
Nitro_communis        ------------------------------------------------------------
Nit79A3_0436          ------------------------------------------------------------
NAL212_3002           ------------------------------------------------------------
Nitro_ureae           ------------------------------------------------------------
Com_aquatica_CJG      VNGVVYNITKSGTTITLTSAANVAPQAGIAVVAAGAGTVPPTSAAVTTTPGVADVTAGTS
SefA                  ------------------------------------------------------------
P._spirulinae         ----------------------------------------------------------GTAG

DespoDRAFT_01458      ------------------LG-------SDDPTGDG--TTSWYEYYMND----VLLGEGSP
CAMSH0001_1621        ------------------------------------------------------------
SPICUR_08450          ---------GDVVTLTGLSAEDA--------------L--------NSANFDLIDA----
Selin_0231            ------------------------------------------------------------
Nitro_communis        ------------INLVGVTE----------------------GEFGASNFSFA--------
Nit79A3_0436          --------DDYQLTITGTGTDDT----------------LIYNAAADTLVFTVV------
NAL212_3002           --------DDAVVELATTVG------------------------VTLANFGF---------
Nitro_ureae           ---------------------------------------------VNASDFIFS--------
Com_aquatica_CJG      YLTIDKMANDGTLELVAASSGAV--VKMADATGSADSFNIVTKVDASPLTFGTVEVAGVE
SefA                  -------TSSSVVTINGLEKGA------EAGLGAQDGFDVLVFSG-A------V-------
P._spirulinae         TLTLNKMASGGTLTITGATTGGHTVAIKDAATGTADVLNVVVSSA-ASLAGGTVTAANVE

DespoDRAFT_01458      TDPTDPTDPTDPTDPTDPTDPTDPTNET--VSVNAT-------------------------
CAMSH0001_1621        ------------------------------------------------------------
SPICUR_08450          ------------------------------------------------------------
Selin_0231            ------------------------------------------------------------
Nitro_communis        ------------------------------------------------------------
Nit79A3_0436          ------------------------------------------------------------
NAL212_3002           ------------------------------------------------------------
Nitro_ureae           ------------------------------------------------------------
Com_aquatica_CJG      TLKLNAVDTAPVVDAT--ATPLVPSIQTASLTVKADKATSLTIEGNSNVTLTLDATTTKL
SefA                  ------------------------------------------------------------
P._spirulinae         TINITSTDTTTPFN------------AAHTLTLVATKATTVDLAGNAALTLTNTGNT-AQ

DespoDRAFT_01458      ---------------------------------------------TATDGALDADGAD---
CAMSH0001_1621        ------------------------------------------------------------
SPICUR_08450          ------------------------------------------------------------
Selin_0231            ------------------------------------------------------------
Nitro_communis        ------------------------------------------------------------
Nit79A3_0436          ------------------------------------------------------------
NAL212_3002           ------------------------------------------------------------
Nitro_ureae           ------------------------------------------------------------
Com_aquatica_CJG      ATIDAGTLTGNLIAGNSHAGVNTIAMTITGGKGADQLKASVGTNAKADVLNGGDGNDTLY
SefA                  ---QAADVTGAAAT---------------------------------------------
P._spirulinae         TAIDASDMTGALTV----TAAGTTATTITGGSGNDNLTASTGT--VADTLIGGAGNDTLT

DespoDRAFT_01458      --------------VTFEIAG--------FATYTQEIINFKPGDVLDFPADNTPTVINSS
CAMSH0001_1621        ------------------------------------------------------------
SPICUR_08450          ------------------------------------------------------------
Selin_0231            ------------------------------------------------------------
Nitro_communis        ------------------------------------------------------------
Nit79A3_0436          ------------------------------------------------------------
NAL212_3002           ------------------------------------------------------------
Nitro_ureae           ------------------------------------------------------------
```

```
Com_aquatica_CJG      AGSNGAKLTGGEGNDLFIVTATGTGNGNKESNTYSDILDFKAGDLLQLQYSNSGTTADVT
SefA                  -AAG---FSVADGAVTWLGAG------PANIAAAVALLDATL------------------
P._spirulinae         SNQGLTTLTGGAGADTFVIVA------PANLNSYSTITDASAGDKIQLPNQGTET-----

DespoDRAFT_01458      -FTDGI---VDVQYAFGGFVTTVELTGLDAALDQTLLGVQSFEDVFGAGTIV--------
CAMSH0001_1621        ------------------------------------------------------------
SPICUR_08450          ------------------------------------------------------------
Selin_0231            ------------------------------------------------------------
Nitro_communis        ------------------------------------------------------------
Nit79A3_0436          ------------------------------------------------------------
NAL212_3002           ------------------------------------------------------------
Nitro_ureae           ------------------------------------------------------------
Com_aquatica_CJG      NFAKLAATLNENTAVFSDFVNAAIKE--------ANLGQAVYFNYKGDAYVVVDSQAQSA
SefA                  ----------------------------------DDDEAVVFDFAGTYYIYGAGASAAG
P._spirulinae         -FQKSAVT-LAATAVFQDYANAAVNAGGDA----STNGYIAWFQFGGDTYIVQSNTDKTT

DespoDRAFT_01458      ------------------------------------
CAMSH0001_1621        -------DDYVTKLAGTVDLSGARVDSDHNIVL--
SPICUR_08450          ------------------------------------
Selin_0231            ------------------------------------
Nitro_communis        ------------------------------------
Nit79A3_0436          ------------------------------------
NAL212_3002           ------------------------------------
Nitro_ureae           ------------------------------------
Com_aquatica_CJG      GDVFINGEDLVVKLTGINGDNLSWNSDYATVALV-
SefA                  GSGTDLTDDLLVKLAGVTDVTGLDVAGAGNIYLF-
P._spirulinae         TPDFQNGTDVIVKLSGLVDLSSASLNTGTPTLLLG
```

A2. Hungates Media:

1.2 g l^{-1} NaCl, 0.3 g l^{-1} KCl, 0.3 g l^{-1} NH_4Cl, 0.2 g l^{-1} KH_2PO_4, 0.3 g l^{-1} Na_2SO_4, 0.6 g l^{-1} $NaHCO_3$, 4 g l^{-1} yeast extract

A3. SL8 Trace Elements:

5.2 g l^{-1} EDTA-2Na, 1.5 g l^{-1} $FeCl_3.H_2O$, 70 mg l^{-1} $ZnCl_3$, 100 mg l^{-1} $MnCl_2.4H_2O$, 62 mg l^{-1} H_3BO_3, 190 mg l^{-1} $CaCl_2.6H_2O$, 36 mg l^{-1} Na_2MoO_4, 17 mg l^{-1} $CuCl_2.2H_2O$, 24 mg l^{-1} $NiCl_2.6H_2O$

A4. Vitamin Solution:

2 mg l^{-1} folic acid, 5 mg l^{-1} riboflavin, 5 mg l^{-1} thiamine hydrochloride, 5 mg l^{-1} pantothenate, 5 mg l^{-1} nicotinamide, 0.1 mg l^{-1} vitamin B12, 5 mg l^{-1} biotin, 2 mg l^{-1} pyridoxine hydrochloride, 5 mg l^{-1} P-aminobenzoate

A5. Buffers used in differential scanning fluorimetry:

1. 400 mM pyridine-HCl & 600 mM NaCl
2. 400 mM etherdiamine-NaOH pH 9.5 & 600 mM NaCl
3. 400 mM TRIS-HCl pH 8.1 & 600 mM NaCl
4. 400 mM tricine-NaOH pH 8 & 600 mM NaCl

5. 400 mM PIPES/ NaOH pH 7 & 600 mM NaCl
6. 400 mM MES/ NaOH pH 6 & 600 mM NaCl
7. 400 mM MOPS/ NaOH pH 7.2 & 600 mM NaCl
8. 400 mM HEPES-NaOH pH 7.5 & 600 mM NaCl (2)
9. 400 mM (x4) sodium acetate p H5 & 600 mM NaCl
10. 400 mM borical NaOH p H9 & 600 mM NaCl
11. 400 mM HEPES-NaOH pH 7.5 & 600 mM NaCl & 40% glycerol
12. 400 mM HEPES-NaOH pH 7.5 & 2 M NaCl
13. 400 mM CHES-NaOH pH 9.5 & 600 mM NaCl
14. 400 mM HEPES-NaOH pH 7.5 & 2 M NaCl & 20% glycerol
15. 400 mM bicne pH 8.3 & 600 mM NaCl
16. 400 mM HEPES-NaOH pH 7.5 & 600 mM NaCl
17. 400 mM HEPES-NaOH pH 7.5
18. 400 mM BIS-TRIS/ HCl pH 6 HCl & 600 mM NaCl
19. 400 mM CAPS-NaOH pH 10 & 600 mM NaCl
20. 400 mM HEPES-NaOH pH 7.5 & 600 mM NaCl & 20% glycerol
21. 400 mM glycine NaOH pH 8.3 & 600 mM NaCl
22. 400 mM imidazole/ HCl pH 7 & 600 mM NaCl
23. 400 mM HEPES-NaOH & 200 mM NaCl
24. 400 mM HEPES-NaOH pH 7.5 & 600 mM NaCl (3)

A6. Primers and conditions used in PCR reactions

***E. cloacae* SLD1a-1 primers:**

ECLO_1: TGCTGGGGATTCTGAAGAGT

ECLO_2: CTGCCCAGGTTTGCTACTTT

PCR Mix:
0.5 µM ECLO_1 primer
0.5 µM ECLO_1 primer
5 µl ReadyMix™ Taq PCR Reaction Mix with $MgCl_2$ (Sigma Aldrich)

4µl PCR grade water

Single colony of *T. selenatis/E. cloacae* added in to the mixture

PCR conditions:

1 cycle	5 mins	95 ºC
35 cycles	1 min	95 ºC
	30 secs	57.3 ºC
	1 min	72 ºC
1 cycle	5 mins	72 ºC

***T. selenatis* primers:**

SEF_s: GTTCATATGGCTATCACTGCGACTCAACGC

SEF_as: GGACTCGAGTTAGAACAGGTAGATGTTGCC (Debeiux, 2011)

PCR mixes	PCR conditions		
A. 5 µl ReadyMix™ Taq PCR Reaction Mix with $MgCl_2$ (Sigma Aldrich) 0.5 µM SEF_s primer 0.5 µM SEF_as primer 4µl PCR grade water Single colony of *T. selenatis/E. cloacae* added in to the mixture	A. 1 cycle 35 cycles ºC 1 cycle 18 different colonies tested	5 mins 1 min 30 secs 3 mins 5 mins	95 ºC 95 ºC 60-73.8 72 ºC 72 ºC
B. 0.1 µl Phusion Hot Start II DNA Polymerase (2 U/µL) (ThermoFisher Scientific) 2 µl 5 x Phusion HF Buffer (ThermoFisher Scientific) 0.2 µl 10 mM dNTPs (ThermoFisher	B. 1 cycle 35 cycles 1 cycle	30 secs 10 secs 30 secs 1.5 mins 5 mins	98 ºC 98 ºC 60-72 ºC 72 ºC 72 ºC

Scientific) 0.5 µM SEF_s primer 0.5 µM SEF_as primer 2.65 µl PCR grade water 0.3 µl DMSO 3.75 µl of PCR grade water containing a single colony of *T. selenatis/E. cloacae* heated to 99 ºC for 10 minutes	3 different colonies tested
C. As in B. with: 1. 0.3 µM of each primer instead of 0.5 µM	C. As in B.

SerCfwd: ACTGGGAGAATTCATATGAGAACATCCAGC

SerCrev: AGCCCGGTTCTCGAGTCAGAAGTTCAGCTG (Lowe, 2008)

PCR mixes	PCR conditions		
A. 5 µl ReadyMix™ Taq PCR Reaction Mix with $MgCl_2$ (Sigma Aldrich) 0.5 µM SerC_fwd primer 0.5 µM SerC_rev primer 4µl PCR grade water Single colony of *T. selenatis/E. cloacae* added in to the mixture	A. 1 cycle 35 cycles 3 different colonies tested	 5 mins 1 min 30 secs 1 min 5 mins	 95 ºC 95 ºC 63-72 ºC 72 ºC 72 ºC
B. 0.1 µl Phusion Hot Start II DNA Polymerase (2 U/µL) (ThermoFisher Scientific)	B. 1 cycle 35 cycles	 30 secs 10 secs 30 secs	 98 ºC 98 ºC 60-72 ºC

2 µl 5 x Phusion HF Buffer (ThermoFisher Scientific) 0.2 µl 10 mM dNTPs (ThermoFisher Scientific) 0.5 µM SerC_fwd primer 0.5 µM SerC_rev primer 2.65 µl PCR grade water 0.3 µl DMSO 3.75 µl of PCR grade water containing a single colony of *T. selenatis/E. cloacae* heated to 99 ºC for 10 minutes.		30 secs 5 mins 3 different colonies tested	72 ºC 72 ºC
C. As in A.	C. 1 cycle 35 cycles 1 cycle 3 different colonies tested	5 mins 1 min 30 secs 1 min 5 mins	95 ºC 95 ºC 52-64 ºC 72 ºC 72 ºC
D. 5 µl DreamTaq Green PCR Master Mix (2X) (ThermoFisher Scientific) 0.2 µl SerC_fwd primer 0.2 µl SerC_rev primer 4.6 µl PCR grade water Single colony of *T. selenatis/E. cloacae* added in to the mixture	D. 1 cycle 35 cycles 1 cycle	5 mins 30 secs 30 secs 1 min 5 mins	95 ºC 95 ºC 52-64 ºC 72 ºC 72 ºC

SefAAfwd: GAACACCAAGAACTCCGTCG

SefAArev: CCCTTCTCCAGACCGTTGAT

PCR mixtures	PCR conditions		
A. 5 µl ReadyMix™ Taq PCR Reaction Mix with $MgCl_2$ (Sigma Aldrich) 0.5 µM SefAAfwd primer 0.5 µM SefAArev primer 4µl PCR grade water Single colony of *T. selenatis/E. cloacae* added in to the mixture	A. 1 cycle 35 cycles 3 different colonies tested	5 mins 1 min 30 secs 1 min 5 mins	95 ºC 95 ºC 52-63 ºC 72 ºC 72 ºC
B. As in A. with: 1. 2 µl of PCR grade water containing a single colony of *T. selenatis/E. cloacae* heated to 99 ºC for 10 minutes instead of adding a single colony straight in to the mixture 2. 2 µl of PCR grade water instead of 4 µl	B. As in A.		
C. 5 µl DreamTaq Green PCR Master Mix (2X) (ThermoFisher Scientific) 0.2 µl SefAAfwd primer 0.2 µl SefAArev primer 2.6 µl PCR grade water 2 µl of PCR grade water containing a single colony of *T. selenatis/E. cloacae* heated to 99 ºC for 10 minutes.	C. 1 cycle 35 cycles 3 different colonies tested	5 mins 1 min 30 secs 1 min 5 mins	95 ºC 95 ºC 52-63 ºC 72 ºC 72 ºC
D. 5 µl DreamTaq Green PCR Master Mix (2X) (ThermoFisher Scientific)	D. 1 cycle 35 cycles	5 mins 1 min	95 ºC 95 ºC

0.2 µl SefAAfwd 0.2 µl SefAArev 2.3 µl PCR grade water 2 µl of PCR grade water containing a single colony of *T. selenatis/E. cloacae* heated to 99 ºC for 10 minutes. 0.3 µl DMSO		30 secs 1 min 5 mins 3 different colonies tested	50-62 ºC 72 ºC 72 ºC
E. 5 µl DreamTaq Green PCR Master Mix (2X) (ThermoFisher Scientific) 0.2 µl SefAAfwd primer 0.2 µl SefAArev primer 1.7 µl PCR grade water 2 µl of PCR grade water containing a single colony of *T. selenatis/E. cloacae* heated to 99 ºC for 10 minutes. 0.6 µl DMSO	E. As in D.		

SerAAfwd: AACATCTCGCCCGACTACAA

SerAArev: CTTGTTGCCTTCCAGAACCC

PCR mixtures	PCR conditions		
A. 5 µl ReadyMix™ Taq PCR Reaction Mix with $MgCl_2$ (Sigma Aldrich) 0.5 µM SerAAfwd primer 0.5 µM SerAArev primer 4µl PCR grade water Single colony of *T. selenatis/E. cloacae* added in to the mixture	A. 1 cycle 35 cycles 1 cycle 3 different colonies tested	 5 mins 1 min 30 secs 1 min 5 mins	 95 ºC 95 ºC 52-63 ºC 72 ºC 72 ºC

B. As in A. with: 1. 2 µl of PCR grade water containing a single colony of *T. selenatis/E. cloacae* heated to 99 ºC for 10 minutes instead of adding a single colony straight in to the mixture	B. As in A.
C. 5 µl DreamTaq Green PCR Master Mix (2X) (ThermoFisher Scientific) 0.2 µl SerAAfwd primer 0.2 µl SerAArev primer 2.6 µl PCR grade water 2 µl of PCR grade water containing a single colony of *T. selenatis/E. cloacae* heated to 99 ºC for 10 minutes.	C. As in A.
D. As in C.	D. 1 cycle 5 mins 95 ºC 35 cycles 30 secs 95 ºC 30 secs 52-63 ºC 1 min 72 ºC 1 cycle 5 mins 72 ºC 3 different colonies tested
E. 0.1 µl Phusion Hot Start II DNA Polymerase (2 U/µL) (ThermoFisher Scientific) 2 µl 5 x Phusion HF Buffer	E. 1 cycle 30 secs 98 ºC 35 cycles 10 secs 98 ºC 15 secs 60-70 ºC 15 secs 72 ºC

(ThermoFisher Scientific) 0.2 µl 10 mM dNTPs (ThermoFisher Scientific) 0.5 µM SerAAfwd primer 0.5 µM SerAArev primer 2.95 µl PCR grade water 3.75 µl of PCR grade water containing a single colony of *T. selenatis/E. cloacae* heated to 99 ºC for 10 minutes.	1 cycle 3 different colonies tested	5 mins	72 ºC
F. 5 µl DreamTaq Green PCR Master Mix (2X) (ThermoFisher Scientific) 0.2 µl SerAAfwd primer 0.2 µl SerAArev primer 2.3 µl PCR grade water 2 µl of PCR grade water containing a single colony of *T. selenatis/E. cloacae* heated to 99 ºC for 10 minutes. 0.3 µl DMSO	F. 1 cycle 35 cycles 1 cycle 3 different colonies tested	 5 mins 30 secs 30 secs 1 min 5 mins	 95 ºC 95 ºC 50-62 ºC 72 ºC 72 ºC
G. As in F. with: 1. 0.6 µl DMSO instead of 0.3 µl 2. 2.0 µl PCR grade water instead of 2.3 µl	G. As in F.		

SerBBfwd: AAGAACTGGGAGCAGAAGGG

SerBBrev: CTTCTCCGACGTGCCTTTCT

PCR mixtures	PCR conditions		
A. 5 µl ReadyMix™ Taq PCR Reaction Mix with $MgCl_2$ (Sigma Aldrich) 0.5 µM SerBBfwd primer 0.5 µM SerBBrev primer 4µl PCR grade water Single colony of *T. selenatis/E. cloacae* added in to the mixture	A. 1 cycle 35 cycles 3 different colonies tested	 5 mins 1 min 30 secs 30 secs 5 mins	 95 ºC 95 ºC 52-63 ºC 72 ºC 72 ºC
B. As in A. with: 2 µl of PCR grade water containing a single colony of *T. selenatis/E. cloacae* heated to 99 ºC for 10 minutes instead of adding a single colony straight in to the mixture	B. As in A.		
C. 0.1 µl Phusion Hot Start II DNA Polymerase (2 U/µL) (ThermoFisher Scientific) 2 µl 5 x Phusion HF Buffer (ThermoFisher Scientific) 0.2 µl 10 mM dNTPs (ThermoFisher Scientific) 0.5 µM SerAAfwd primer 0.5 µM SerAArev primer 2.95 µl PCR grade water 3.75 µl of PCR grade water containing a single colony of *T. selenatis/E. cloacae* heated to 99 ºC for 10 minutes.	C. 1 cycle 35 cycles 1 cycle 3 different colonies tested	 30 secs 10 secs 15 secs 15 secs 5 mins	 98 ºC 98 ºC 60-70 ºC 72 ºC 72 ºC
D. 5 µl DreamTaq Green PCR Master Mix (2X) (ThermoFisher Scientific)	D. 1 cycle 35 cycles	 3 mins 30 secs	 95 ºC 95 ºC

0.2 µl SerBBfwd primer 0.2 µl SerBBrev primer 2.6 µl PCR grade water 2 µl of PCR grade water containing a single colony of *T. selenatis/E. cloacae* heated to 99 ºC for 10 minutes.		30 secs 45 secs 5 mins 3 different colonies tested	51-62 ºC 72 ºC 72 ºC
E. 5 µl DreamTaq Green PCR Master Mix (2X) (ThermoFisher Scientific) 0.2 µl SerBBfwd primer 0.2 µl SerBBrev primer 2.3 µl PCR grade water 2 µl of PCR grade water containing a single colony of *T. selenatis/E. cloacae* heated to 99 ºC for 10 minutes. 0.3 µl DMSO	E. 1 cycle 35 cycles 1 cycle 3 different colonies tested	 3 mins 30 secs 30 secs 45 secs 5 mins	 95 ºC 95 ºC 50-62 ºC 72 ºC 72 ºC
F. As in E. with: 1. 0.6 µl DMSO instead of 0.3 µl 2. 2.0 µl PCR grade water instead of 2.3 µl	F. As in E.		

SerDDfwd: AAGGCTACGGTCTCCCTCTA

SerDDrev: CAATTCTCCCAGTTGCGGTG

PCR mixtures	PCR conditions		
A. 5 µl ReadyMix™ Taq PCR Reaction Mix with $MgCl_2$ (Sigma Aldrich) 0.5 µM SerDDfwd primer 0.5 µM SerDDrev primer 4µl PCR grade water Single colony of *T. selenatis/E. cloacae* added in to the mixture	A. 1 cycle 35 cycles 3 different colonies tested	5 mins 1 min 30 secs 30 secs 5 mins	95 ºC 95 ºC 52-63 ºC 72 ºC 72 ºC
B. As in A. with: 2 µl of PCR grade water containing a single colony of *T. selenatis/E. cloacae* heated to 99 ºC for 10 minutes instead of adding a single colony straight in to the mixture	B. As in A.		
C. 5 µl DreamTaq Green PCR Master Mix (2X) (ThermoFisher Scientific) 0.2 µl SerDDfwd primer 0.2 µl SerDDrev primer 2.6 µl PCR grade water 2 µl of PCR grade water containing a single colony of *T. selenatis/E. cloacae* heated to 99 ºC for 10 minutes.	C. 1 cycle 35 cycles 1 cycle 3 different colonies tested	3 mins 30 secs 30 secs 45 secs 5 mins	95 ºC 95 ºC 51-62 ºC 72 ºC 72 ºC
D. 5 µl DreamTaq Green PCR Master Mix (2X) (ThermoFisher Scientific) 0.2 µl SerDDfwd primer 0.2 µl SerDDrev primer 2.3 µl PCR grade water 2 µl of PCR grade water containing a single colony of *T. selenatis/E. cloacae*	D. 1 cycle 35 cycles 1 cycle	3 mins 30 secs 30 secs 45 secs 5 mins	95 ºC 95 ºC 50-62 ºC 72 ºC 72 ºC

heated to 99 ºC for 10 minutes. 0.3 µl DMSO	 3 different colonies tested
E. As in D. with: 1. 0.6 µl DMSO instead of 0.3 µl 2. 2.0 µl PCR grade water instead of 2.3 µl	E. As in D.

References

Agapakis, C. M., Boyle, P. M., Silver, P. A., 2012, Natural strategies for the spatial optimization of metabolism in synthetic biology, Nature Chemical Biology **8**:527-535

Ali, E. N., El-Sonbaty, S. M., 2013, Evaluation of selenium nanoparticles as a potential chemopreventative agent against lung carcinoma, International Journal of Pharma and Biosciences, **2**:38-46

Almiron, M., Link, A. J., Furlong, D., Kolter, R. 1992, A novel DNA-binding protein with regulatory and protective roles in starved *Escherichia coli*, Genes and Development, **6**:2646–2654

Altuvia, S., Almiron, M., Huisman, G., Kolter, R. and Storz, G, 1994, The dps promoter is activated by OxyR during growth and by IHF and σs in stationary phase, Molecular Microbiology **13**:265–272

Azam, A., T., Iwata, A., Nishimura, A., Ueda, S., Ishihama, A., 1999, Growth phase-dependent variation in protein composition of the *Escherichia coli* nucleoid, Journal of Bacteriology, **181**:6361–6370.

Baumann, U., Wu, S., Flaherty, K. M., McKay, D. B., 1993, Three-dimensional structure of the alkaline protease of *Psuedomonas aeruginosa*: A two-domain protein with a calcium binding parallel beta roll motif, The EMBO Journal, **12**:3357-64

Bébien, M., Lagniel, G., Garin, J., Touati, D., Verméglio, A., Labarre, J., 2002, Involvement of Superoxide Dismutases in the Response of *Escherichia coli* to Selenium Oxides, Journal of Bacteriology, **184**:1556-1564

Bellapadrona, G., Ardini, M., Ceci, P., Stefanini, S.,Chiancone, E., 2010, Dps proteins prevent Fenton-mediated oxidative damage by trapping hydroxyl

radicals within the protein shell, Free Radical Biology and Medicine, **48**:292–297

Berg, J. M., Tymoczko, J. L., Stryer, L., 2012, Biochemistry, seventh edition, W. H. Freeman and Company, Basingstoke, England, 927-930

Bertero, M. G., Rothery, R. A., Palak, M., Hou, C., Lim, D., Blasco, F., Weiner, J.H., Strynadka, N.C., 2003, Insights into the respiratory electron transfer pathway from the structure of nitrate reductase A, Nature Structural and Molecular Biology, **10**:681–687

Bond, M. R., Hanover, J. A., 2015, A little sugar goes a long way: the cell biology of O-GlcNAc. The Journal of Cell Biology, **208**:869–880

Boyd, R., 2011, Selenium stories, Nature Chemistry, **3**:570

Buchs, B., Evangelou, M. W., Winkel, L. H., Lenz, M., 2013, Colloidal properties of nanoparticular biogenic selenium govern environmental fate and bioremediation effectiveness, Environmental Science and Technology, **47**:2401-2407

Bücking, W., Massadeh, S., Merkulov, A., Xu, S., Nann, T., 2010, Electrophoretic properties of BSA-coated quantum dots, Analytical and Bioanalytical Chemistry, **396**: 1087. doi:10.1007/s00216-009-3107-z

Butler, C. S., 2012, The complexity of bacterial selenate respiration: Metals, non-metals and minerals, Biochemical Society, 23-27

Calhoun, L. N., Kwon, Y. N., 2010, Structure, function and regulation of the DNA-binding protein Dps and its role in acid and oxidative stress resistance in *Escherichia coli*: a review, Journal of Applied Microbiology, **110**:375-386

Choi, S. H., Baumler, D. J., Kaspar, C. W., 2000, Contribution of dps to acid stress tolerance and oxidative stress tolerance in *Escherichia coli* O157:H7, Applied and Environmental Microbiology, **66:**3911–3916

Chudobova, D., Cihalova, K., Dostalova, S., Ruttkay-Nedecky, B., Rodrigo, M. A. M., Tmejova, K., Kopel, P., Nejdl, L., Kudr, J., Gumulec, J., Krizkova, S., Kynicky, J., Kizek, R., Adam, V., 2014, Comparison of the effects of silver phosphate and selenium nanoparticles on *Staphylococcus aureus* growth reveals potential for selenium particles to prevent infection, FEMS Microbiology Letters, **351**:195-201

Cuicui, G., Jian, T., Zhao, Y., Chen, C., Zhou, R., Chai, Z., 2015, Towards understanding of nanoparticle–protein corona, Archives of Toxicology, **89**:519-539

Debieux, C. M., Dridge, E. J., Mueller, C. M., Splatt, P., Paszkiewicz, K., Knight, I., Florance, H., Love, J., Titball, R. W., Lewis, R. J., Richardson, D. J., Butler, C. S., 2011, A bacterial process for selenium nanosphere assembly, Proceedings of the National Academy of Sciences of the United States of America, **108**:13480-13485

Delepelaire, P., 2004, Type I secretion in gram-negative bacteria, Biochimica et Biophysica Acta, **1694**:149-161

Del Pino, P., Pelaz, B., Zhang, Q., Maffre, P., Nienhaus, G. U., Parak, W. J., 2013, Protein corona formation around nanoparticles – from the past to the future, Materials Horizons, **1**:301-313

DeMoll-Decker, H., Macy, J., 1993, The periplasmic nitrite reductase of *Thauera selenatis* may catalyze the reduction of selenite to elemental Selenium, Archives of Microbiology, **160**: 241-247

Dittrich, C., Burckhardt, C. J., Danuser, G., 2012, Delivery of membrane impermeable cargo into CHO cells by peptide nanoparticles targeted by a protein corona, Biomaterials, **33**:2746-2753

Dobias, J., Suvorova, E. I., **Bernier-Latmani, R.,** 2011, Role of proteins in controlling selenium nanoparticle size, Nanotechnology, **22**:195605

Dock-Bregeon, A-C., Sankaranarayanan, R., Romby, P., Caillet, J., Springer, M., Rees, B., Francklyn, C. S., Ehresmann, C., Moras, D., 2000, Transfer RNA-mediated editing in threonyl-tRNA synthetase: The class II solution to the double discrimination problem, Cell, **103**:877–884

Dridge, C. L., 2014, Developing self-assembling nanocages with naturally occurring bacterial peptides, University of Exeter

Dridge, E. J., Butler, C. S., 2010, Thermostable properties of the periplasmic selenate reductase from *Thauera selenatis*, Biochimie, **92**:1268–1273

Dridge, E. J., Watts, C. A., Jepson, B. J. N., Line, K., Santini, J. M., Richardson, D. J., Butler, C. S., 2007, Investigation of the redox centres of periplasmic selenate reductase from *Thauera selenatis*, Journal of Biological Chemistry, **408**:19-28

Dupeux, F., Röwer, M., Seroul, G., Blot, D., Márquez, J. A., 2011, A thermal stability assay can help to estimate the crystallization likelihood of biological samples, Acta Crystallographica Section D, **67**:915–919

Fagan, R. P., Fairweather, N. F., 2014, Biogenesis and functions of bacterial S‐layers, Nature Reviews Microbiology, **12**:211-222

Fee, J. A., 1991, Regulation of sod genes in *Escherichia coli*: relevance to superoxide dismutase function, Molecular Microbiology, **5**:2599-2610

Fersht, A. R.,1977, Editing mechanisms in protein synthesis, Rejection of valine by the isoleucyl-tRNA synthetase, Biochemistry, **16**:1025–1030

Fleischer, C. C., Christine, K. P., 2014, Nanoparticle–cell interactions: molecular structure of the protein corona and cellular outcomes, Accounts of Chemical Research, **47**: 2651-2659

Fordyce, F. M., 2013, Selenium deficiency and toxicity in the environment, Essentials of Medical Geology, **16**:375-416

Forootanfara, H., Mahboubeh, A., Maryam N., Mitra, M., Bagher, A., Ahmad, S., 2013, Antioxidant and cytotoxic effect of biologically synthesized selenium nanoparticles in comparison to selenium dioxide, Journal of Trace Elements in Medicine and Biology, **28**:27-29

Fujita, M., Ike, M., Nishimoto, S., Takahashi, K., Kashiwa, M., 1997, Isolation and characterization of a novel selenate-reducing bacterium, *Bacillus sp.* SF-1, Journal of Fermentation and Bioengineering, **83**:517–522

Gao, X., Kong, L., 2011, Treatment of cancer with selenium nanoparticles, US20110262564 A1

Gebauer, J. S., Malissek, M., Simon, S., Knauer, S. K., Maskos, M., Stauber, R. H., Peukert, W., Treuel, L., 2012, Impact of the Nanoparticle–Protein Corona on Colloidal Stability and Protein Structure, Langmuir, **28**:9673-9679

Grabski, A., Mehler, M., Drott, D., 2003, Unattended high-density cell growth and induction of protein expression with the Overnight Express Autoinduction System, Innovations, **17**:3

Grainger, D. C., Goldberg, M. D., Lee, D. J., Busby, S. J., 2008, Selective repression by Fis and H-NS at the *Escherichia coli* dps promoter, Molecular Microbiology, **68**:1366–1377

Grant, R. A., Filman, D. J., Finkel, S. E., Kolter, R., Hogle, J. M., 1998, The crystal structure of Dps, a ferritin homolog that binds and protects DNA, Nature Structural and Molecular Biology, **5**:294–303

Guth, E. C., Francklyn, C. S., 2007, Kinetic discrimination of tRNA identity by the conserved motif 2 loop of a class II aminoacyl-tRNA synthetase, Molecular Cell, **25**:531–542

Guymer, D., Maillard, J., Sargent, F., 2009, A genetic analysis of *in vivo* selenate reduction by *Salmonella enterica* serovar Typhimurium LT2 and *Escherichia coli* K12, Archives of Microbiology, **191**: 519-528

Haikarainen, T., Papageorgiou, A. C., 2010, Dps-like proteins: structural and functional insights into a versatile protein family, Cellular and Molecular Life Sciences, **67**:341–351

Hariharan, H., Al-harbi, N., Karuppiah, P., Rajaram, S., 2012, Microbial synthesis of selenium nanocomposite using *Saccharomyces cerevisiae* and its antimicrobial activity against pathogens causing nosocomial infection, Chalcogenide Letters, **9**:509-515

Hart, G. W., Housley, M. P., Slawson, C., 2007, Cycling of O-linked β-N-acetylglucosamine on nucleocytoplasmic proteins, Nature, **446**:1017–1022

Ibba, M., Söll, D., 2000, Aminoacyl-tRNA synthesis, Annual Review of Biochemistry, **69**:617–650

Ilari, A., Ceci, P., Ferrari, D., Rossi, G. L., Chiancone, E., 2002, Iron Incorporation into *Escherichia coli* Dps Gives Rise to a Ferritin-like Microcrystalline Core, Journal of Biological Chemistry, **277**:37619-37623

Iranifam, M., Fathinia, M , Sadeghi Rad, T., Hanifehpour, Y., Khataee, A. R., Joo, S. W., 2013, A novel selenium nanoparticles-enhanced

chemiluminescence system for determination of dinitrobutylphenol, Talanta, **107**:263-269

Kato, N., Dasgupta, R., Smartt, C. T., Christensen, B. M., 2002, Glucosamine:fructose-6-phosphate aminotransferase: gene characterization, chitin biosynthesis and peritrophic matrix formation in *Aedes aegypti*, Insect Molecular Biology, **3**:207-216

Kessi, J., Hanselmann, K. W., 2004, Similarities between the abiotic reduction of selenite with glutathione and the dissimilatory reaction mediated by *Rhodospirillum rubrum* and *Escherichia coli*, Journal of Bological Chemistry, **279**:50662-50669

Krafft, T., Bowen, A., Theis, F. Macy, J. M., 2000, Cloning and sequencing of the genes encoding the periplasmic cytochrome B-containing selenate reductase of *Thauera selenatis*, DNA Sequence, **10**:365-377

Kuroda, M., Yamashita, M., Miwa, E., Imao, K., Fujimoto, N., Ono, H., Nagano, K., Sei, K., Ike, M., 2011, Molecular cloning and characterization of the srdBCA operon, encoding the respiratory selenate reductase complex, from the selenate-reducing bacterium *Bacillus selenatarsenatis* SF-1, Journal of Bacteriology, **193**:2141–2148

Lenz, M., Kolvenbach, B., Gygax, B., Moes, S., Corvini, P. F. X., 2011, Shedding light on selenium biomineralization: proteins associated with bionanominerals, Applied and Environmental Microbiology, doi: 10.1128/AEM.01713-10

Liang, X. J., Chen, C., Zhao, Y., Jia, L., Wang, P. C., 2008, Biopharmaceutics and therapeutic potential of engineered nanomaterials, Current Drug Metabolism, **9**:697–709.

Li, D. B., Cheng, Y. Y., Wu, C., Li, W. W., Li, N., Yang, Z. C., Tong, Z. H., Yu, H. Q., 2014, Selenite reduction by *Shewanella oneidensis* MR-1 is mediated by fumarate reductase in periplasm, Scientific Reports, **4**:3755

Ling, J., Reynolds, N., Ibba, M., 2009, Aminoacyl-tRNA synthesis and translational quality control, Annual Review of Microbiology, **63**:61–78

Liochev, S. I., Fridovich, I., 1994, The role of O_2^- in the production of $HO^{\cdot}$: in vitro and in vivo, Free Radical Biology and Medicine, **16**:29-33

Losi, M. E., Frankenberger W. T., 1997, Reduction of Selenium Oxyanions by *Enterobacter cloacae* SLD1a-1: Isolation and Growth of the Bacterium and Its Expulsion of Selenium Particles, Applied and Environmentl Microbiology, **63**:3079-3084

Lowe, E. C., 2008, Resolving electron transport pathways in the selenate respiring bacteria *Thauera selenatis*, University of Exeter

Lowe, E. C., Bydder, S., Hartshorne, R. S., Tape, H. L. U., Dridge, E. J., Debieux, C. M., Paszkiewicz, K., Singleton, I., Lewis, R. J., Santini, J. M., Richardson, D. J., Butler, C. S., 2010, Quinol-cytochrome *c* Oxidoreductase and Cytochrome c_4 Mediate Electron Transfer during Selenate Respiration in *Thauera selenatis*, Journal of Biological Chemistry, **285**:18433-18442

Macy, J. M., Michel, T. A., Kirsch, D. G., 1989, Selenate reduction by a *Pseudomonas* species: a new mode of anaerobic respiration, FEMS Microbiology Letters, **61**:195-198

Macy, J. M., Rech, S., Auling, G., Dorsch, M., Stackebrandt, E., Sly, L. I., 1993, *Thauera selenatis* gen. nov., sp. nov., a Member of the Beta Subclass of *Proteobacteria* with a Novel Type of Anaerobic Respiration, International Journal of Systematic Bacteriology, **43**:135-142

Ma, J., Kobayashi, D. Y., Yee, N., 2007, Chemical kinetic and molecular genetic study of selenium oxyanion reduction by *Enterobacter cloacae* SLD1a-1, Environmental Science and Technology, **41**:7795-7801

Ma, J., Kobayashi, D. Y., Yee, N., 2009, Role of menaquinone biosynthesis genes in selenate reduction by *Enterobacter cloacae* SLD1a-1 and *Escherichia coli* K12, Environmental microbiology, **11**:149-58

Miller, A-F., 2012, Superoxide dismutases: ancient enzymes and new insights, FEBS Letters, **586**:585-595

Minaev, V. S., Timoshenkov, S. P., Kalugin, V. V., 2005, Structural and phase transformations in condensed selenium, Journal of Optoelectronics and Advanced Materials, **7**:1717-1741

Myers, T., 2013, Remediation scenarios for selenium contamination, Blackfoot watershed, southeast Idaho, USA, Hydrogeology Journal, **104**:309-339

Nair, S., Finkel, S. E., 2004, Dps protects cells against multiple stresses during stationary phase, Journal of Bacteriology **186**:4192-4198

Nancharaiah, Y. V., Lens, P. N. L., 2015, Ecology and Biotechnology of Selenium-Respiring Bacteria, Microbiology and Molecular Biology Reviews, **79**:61-80

Nureki, O., Vassylyev, D. G., Tateno, M., Shimada, A., Nakama, T., Fukai, S., Konno, M., Hendrickson, T. L., Schimmel, P., Yokoyama, S., 1998, Enzyme structure with two catalytic sites for double-sieve selection of substrate, Science, **280**:578–582

Odom, J. M., Peck, H. D. Jr., 1984, Hydrogenase, electron transfer proteins, and energy coupling in the sulfate-reducing bacteria *Desulfovibrio*, Annual Review of Microbiology, **38**:551–592

Ohlendorf, H. M., Hoffman, D. J., 1986, Embryonic mortality and abnormalities of aquatic birds: Apparent impacts of selenium from irrigation drainwater, The Science of the Total Environment, **52**:49-63

Oremland, R. S., Herbel, M. J., Blum, J. S., Langley, S., Beveridge, T. J., Ajayan, P. M., Sutto, T., Ellis, A. V., Curran, S., 2004, Structural and Spectral Features of Selenium Nanospheres Produced by Se-Respiring Bacteria, Applied and Environmental Microbiology, **70**:52-62

Overschelde, O., Guisbiers, G., Snyders, R., 2013, Green synthesis of selenium nanoparticles by excimer pulsed laser ablation in water, Applied Materials, **1**:042114

Papp, L. V., Lu, J., Holmgren, A., Khanna, K. K., 2007, From selenium to selenoproteins: synthesis, identity, and their role in human health, Antioxidants and Redox Signalling, **9**:775-806

Pearce, C. I., Coker, V. S., Charnock, J. M., Pattrick, R. A. D., Mosselmans, J. F. W., Law, N., Beveridge, T. J., Lloyd, J. R., 2008, Microbial manufacture of chalcogenide-based nanoparticles via the reduction of selenite using *Veillonella atypica*: an in situ EXAFS study, Nanotechnology, **19**:155603

Prapainop, K., Witter, D. P., Wentworth, P. Jr., 2012, A Chemical Approach for Cell-Specific Targeting of Nanomaterials: Small-Molecule-Initiated Misfolding of Nanoparticle Corona Proteins, Journal of the American Chemical Society, **134**:4100-4103

Presser, T. S., Ohlendorf, H. M.,1987, Biogeochemical Cycling of Selenium in the San Joaquin Valley, California, Environmental Management, **11**:805-821

Ramamurthy, C., Sampath, K., Arunkumar, P., Suresh Kumar, M., Sujatha, V., Premkumar, K., Thirunavukkarasu, C., 2013, Green synthesis and characterization of selenium nanoparticles and its augmented cytotoxicity with

doxorubicin on cancer cells, Bioprocess and Biosystems Engineering, **36**:1131-1139

Rech, S. A., Macy, J. M., 1992, The Terminal Reductases for Selenate and Nitrate Respiration in *Thauera selenatis* Are Two Distinct Enzymes, Journal of Bacteriology, **174**:7316-7320

Ridley, H., Watts, C. A., Richardson, D. J., Butler, C. S., 2006, Resolution of distinct membrane-bound enzymes from *Enterobacter cloacae* SLD1a-1 that are responsible for selective reduction of nitrate and selenate oxyanions, Applied and Environmental Microbiology, **72**:5173-5180

Sabaty, M., Avazéri, C., Turner, R. J., Pignol, D., Verméglio, A., 2001, Characterization of the Reduction of Selenate and Tellurite by Nitrate Reductases, Applied and Environmental Microbiology, **67**:5122–5126

Saiki, M. K., Lowe, P. T., 1987, Selenium in Aquatic Organisms From Subsurface Agricultural Drainage Water, San Joaquin Valley, California, Archives of Environmental Contamination and Toxicology, **16**:657-670

Saptarshi, S. R., Duschl, A., Lopata, A. L., 2013, Interaction of nanoparticles with proteins: relation to bio-reactivity of the nanoparticle, Journal of Nanobiotechnology, **11**:26

Schmidt, E., Schimmel, P., 1994, Mutational isolation of a sieve for editing in a transfer RNA synthetase, Science, **264**:265–267

Schroder. I., Rech. S., Krafft. T., Macy. J. M., 1997, Purification and Characterization of the Selenate Reductase from *Thauera selenatis*, The Journal of Biological Chermistry, **272**:23765-23768

Shakibaie, M., Khorramizadeh, M., Faramarzi, M., Sabzevari, O., Shahverdi, A., 2010, Biosynthesis and recovery of selenium nanoparticles and the effects on

matrix metalloproteinase-2 expression, Biotechnology and Applied Biochemistry, **15**:7-15

Singh, R., Ray, P., Das, A., Sharma, M., 2009, Role of persisters and small-colony variants in antibiotic resistance of planktonic and biofilm-associated *Staphylococcus aureus*: an in vitro study. Journal of Medical Microbiology, **58**:1067–1073.

Sonkusre, P., Cameotra, S. S., 2015, Biogenic selenium nanoparticles inhibit *Staphylococcus aureus* adherance on different surfaces, Colloids and Surfaces B:Biointerfaces, **136**:1051-1057

Stolz, J. F., Basu, P., Oremland, R. S., 2002, Microbial transformation of elements: the case of arsenic and selenium, International Microbiology, **5**:201-207

Stolz, J. F., Basu, P., Santini, J. M., Oremland, R. S., 2006, Arsenic and selenium in microbial metabolism, Annual Review of Microbiology, **60**:107-130

Stolz, J. F., Oremland, R. S., 1999, Bacterial respiration of arsenic and selenate, FEMS Microbiology Reviews, **23**:615-627

Storz, G., Tartaglia, L. A., Farr, S. B., Ames, B. N., 1990, Bacterial defenses against oxidative stress, Trends in Genetics **6**:363–368

Suwa, Y., Imamura, Y., Suzuki, T., Tashiro, T., Urushigawa, Y., 1994, Ammonia-oxidising bacteria with different sensitivities to $(NH_4)SO_4$ in activated sludges, Water Research, **28**:1523-1532

Suwa, Y., Sumino, T., Noto, K., 1997, Phylogenetic relationships of activated sludge isolates of ammonia oxidisers with different sensitivities to ammonia sulphate, Journal of Applied Microbiology, **43**:373-379

Tartaglia, L. A., Storz, G., Ames, B. N., 1989, Identification and molecular analysis of oxyR-regulated promoters important for the bacterial adaptation to oxidative stress. Journal of Molecular Biology, **210**:709–719

Tran, P. A., Webster, T. J., 2011, Selenium nanoparticles inhibit *Staphylococcus aureus* growth, International Journal of Nanomedicine, **6**:1553-1558

Turner, R. J., Weiner, J. H., Taylor, D. E., 1998, Selenium metabolism in *Escherichia coli*, Biometals, **11**:223-227

Velayudhan, J., Castor, M., Richardson, A., Main-Hester, K. L., Fang, F. C., 2007, The role of ferritins in the physiology of *Salmonella enterica* sv. Typhimurium: a unique role for ferritin B in iron-sulphur cluster repair and virulence, Molecular Microbiology, **63**:1495–1507

Vekariya, K. K., Kaur, J., Tikoo, K., 2013, Alleviating anastrozole induced bone toxicity by selenium nanoparticles in SD rats, Toxicology and Applied Pharmacology, **268**:212-220

Vergnes, A., Pommier, J., Toci, R., Blasco, F., Giordano, G., Magalon, A., 2006, NarJ chaperone binds on two distinct sites of the aponitrate reductase of *Escherichia coli* to coordinate molybdenum cofactor insertion and assembly, Journal of Biological Chemistry, **281:**2170-2176

Wadhwani, S. A., Shedbalkar, U. U., Singh, R., Chopade, B. A., 2016, Biogenic selenium nanoparticles: current status and future prospects, Applied Microbiology and Biotechnology, **100**:2555-2566

Watts, C. A., Ridley, H., Condie, K. L., Leaver, J. T., Richardson, D. J., Butler, C. S., 2003, Selenate reduction by *Enterobacter cloacae* SLD1a-1 is catalysed by a molybdenum-dependent membrane-bound enzyme that is distinct from the membrane-bound nitrate reductase, FEMS Microbiology Letters, **228**:273-279

Weiner, J. H., Rothery, R. A.,Sambasivarao, D., Trieber, C. A., 1992, Molecular analysis of dimethylsulfoxide reductase: a complex iron-sulfur molybdoenzyme of *Escherichia coli*, Biochimica Biophysica Acta, **1102**:1– 18

Weres, O., Jaouni, A.-R., Tsao, L., 1989, The distribution, speciation and geochemical cycling of selenium in a sedimentary environment, Kesterson Reservoir, California, U.S.A., Applied Geochemistry, **4**:543-563

Wolfram, J., Yang, Y., Shen, J., Moten, A., Chen, C., Shen, H., Ferrari, M., Zhao, Y., 2014, The nano-plasma interface: Implications of the protein Corona, Colloids and Surfaces B: Biointerfaces, **124**:17-24

Wolf, S. G., Frenkiel, D., Arad, T., Finkel, S. E., Kolter, R., Minsky, A., 1999, DNA protection by stress-induced biocrystallization, Nature, **400**:83–85

Yamamura, S., Yamashita, M., Fujimoto, N., Kuroda, M., Kashiwa, M., Sei, K., Fujita, M., Ike, M., 2007, *Bacillus selenatarsenatis sp*. nov., a selenate- and arsenate-reducing bacterium isolated from the effluent drain of a glass-manufacturing plant, International Journal of Systematic and Evolutionary Microbiology, **57**:1060–1064

Yang, F., Tang, Q., Zhong, X., Bai, Y., Chen, T., Zhang, Y., Li, Y., Zhang, X., 2012, Surface decoration by *Spirulina* polysaccharide enhances the cellular uptake and anticancer efficacy of selenium nanoparticles, International Journal of Nanomedicine, **7**:835-844

Yazdi, M., Mahdavi, M., Setayesh, N., Esfandyar, M., Shahverdi, A., 2013, Selenium nanoparticle-enriched *Lactobacillus brevis* causes more efficient immune responses in vivo and reduces the liver metastasis in metastatic form of mouse breast cancer, DARU Journal of Pharmaceutical Sciences, **21**:33

Yu, M. J., Ren, J., Zeng, Y. L., Zhou, S. N., Lu, Y. J., 2009, The *Legionella pneumophila* Dps homolog is regulated by iron and involved in multiple stress tolerance, Journal of Basic Microbiology, **49**:79–86

Zhang, J., Spallholz, J., 2011, Toxicity of selenium compounds and nano-selenium particles, General, Applied, and Systems Toxicology, DOI: 10.1002/9780470744307

Zhao, G., Ceci, P., Ilari, A., Giangiacomo, L., Laue, T. M., Chiancone, E., Chasteen, N. D. 2002, Iron and hydrogen peroxide detoxification properties of DNA-binding protein from starved cells, Journal of Biological Chemistry, **277**:27689–27696